University of Alberta

An Examination of Horizontal Advection and the Causes of Mixed Layer Variability in the Northeast Pacific Ocean from 2001-05 using Argo Data and the General Ocean Turbulence Model

by

Jennifer Martine Jackson ©

A thesis submitted to the Faculty of Graduate Studies and Research in partial fulfillment of the requirements for the degree of Master of Science

Department of Earth and Atmospheric Sciences

Edmonton, Alberta

Spring 2006

Canada

Abstract

For unknown reasons, the mixed layer depth (MLD) in the Gulf of Alaska (GOA) has been shoaling over the past 50 years with the shallowest winter MLD from 2002-03. The 1-D General Ocean Turbulence Model (GOTM) was used to calculate the MLD at in the northeast Pacific Ocean from 2001-05 and sensitivity experiments were run to determine how atmospheric processes affect the MLD. To determine whether the 1-D assumption was realistic, a proxy to calculate advection was established based on changes to the observed heat content.

It was found that GOTM produced the most realistic MLD in the subtropical gyre despite significant advection because the method that GOTM used to calculate the MLD was more accurate in warmer water. In addition, although changes to the wind speed and heat fluxes can explain some MLD variability, the occurrence of anomalous atmospheric and oceanographic events also significantly impact the MLD.

Acknowledgements

I would first of all like to offer sincere gratitude to my supervisor, Paul Myers, first of all for his belief that I could do physical oceanographic project and secondly for his endless support throughout the past 2 years. I would like to thank Debby Ianson for arranging my passage on the incredible trip to Queen Charlotte Sound (complete with a swim in 'sub-arctic' waters), for the interesting talks and ideas, and for the endless help with the many revisions and drafts. Howard Freeland saved me a huge amount of time by interpolating the Argo data for me, without which I might still be working on the project. I was lucky to run into Bill Crawford one morning and am thankful for his insight on the Gulf of Alaska, especially the cold water anomaly. I would like to thank John Postma, Elizabeth Shadwick, Nilgun Cetin and Daniel Decau for helping me to maintain my sanity (oh and for the computer and math help). My lab mates (Duo Yang, Michelle Li, Sanjay Rattan, Yan Tsehtik, Mike Pritchard and Samir Douik) and my office mates (Blythe McLennan, Kim Deschamps, Will Hobbs, Lidia Zabcic and Britta Jensen (you too Berto)) were a comfort to have around. The support staff at U of A were very helpful, often going out of their way to offer assistance.

I would like to thank my mom and dad and sister for their many forms of emotional, intellectual and drop everything-at-the-last minute Jen needs our help because she wants to get married during her masters support. Mom and Dad, thank you for telling Kathryn and I that we could do anything that we put our minds to. Above all, I could not have done this without my partner, Simon Winfield, and I am endlessly grateful for his infinite support.

Table of Contents

List of Tables

List of Figures

List of Symbols and Abbreviations

AG	Alaska Gyre
CAG	Station in the center of the Alaska gyre (55°N, 145°W)
C_D	Drag Coefficient
C_P	Specific Heat Capacity ($Jkg^{-1}°C^{-1}$)
D_S	Transport of salt (psu)
E	Evaporation (Volume time^{-1} area^{-1})
ENSO	El Nino Southern Oscillation
GOTM	General Ocean Turbulence Model
HZ	Halocline zone
LH	Latent heat flux (W m^{-2})
LW	Longwave radiation (W m^{-2})
LZ	Lower zone
ML	Mixed layer
MLD	Mixed layer depth (m)
NPC	North Pacific Current
NSG	Station on the northern edge of the subtropical gyre (40°N,145°W)
Q_{AD}	Advection (Δ°C)
Q_{AVG}	Average Q_{SF} over winter or summer season (W m^{-2})
Q_{HC}	Heat Content (°C)
Q_{HCobs1}	Observed heat content at the beginning of the month (°C)
Q_{HCobs2}	Observed heat content at the end of the month (°C)
Q_{SF}	Total surface heat fluxes (W m^{-2})
OSP	Ocean Station Papa (50°N, 145°W)
P	Precipitation (Volume time^{-1} area^{-1})
PDO	Pacific Decadal Oscillation
S	Salinity (psu)
S16	Station 16 along Line P (49°17N, 134°40W)
SH	Sensible heat flux (W m^{-2})
SLP	Sea level pressure (db)
SST	Sea surface temperature (°C)
SW	Shortwave radiation (W m^{-2})
T	Temperature (°C)
T_a	Air Temperature (°C)
$\bar{U}$	Average U_{10} over winter or summer season (ms^{-1})
U_{10}	Net wind speed at 10 m (ms^{-1})
UZ	Upper Zone
c_u	Parameterized stability function to calculate the diffusivity of momentum
c_u'	Parameterized stability function to calculate the diffusivity of heat

k	Turbulent kinetic energy (m^2s^{-2})
l	Typical length scale to calculate diffusivity
q	Velocity scale of turbulence (ms^{-1})
u	Zonal wind speed
u'	Zonal turbulent flux
v	Meridional wind speed (ms^{-1})
v'	Meridional turbulent flux
v^S	Turbulent diffusivity of salt
v_t	Turbulent diffusivity of momentum
v'_t	Turbulent diffusivity of heat
w'	Vertical turbulent flux
z	Depth (m)
δ	SST $- T_a$ (°C)
θ	Potential Temperature (°C)
ρ	Density (kgm^{-3})
ρ_o	Reference Density (kgm^{-3})
τ_{ox}	Zonal wind stress ($N\ m^{-2}$)
τ_{oy}	Meridional wind stress ($N\ m^{-2}$)

Chapter 1

Introduction

1.1 Introduction

At the surface of the ocean lies the mixed layer (ML), a region with a relatively homogeneous density that is in direct contact with the atmosphere. The depth of this layer is strongly influenced by atmospheric forces – wind and buoyancy, which result from variations in radiation, evaporation and precipitation (Mellor, 1996). The depth of the ML undergoes regional as well as diurnal, seasonal, interannual and interdecadal variations, and can range from a few meters in subtropical regions during the summer to over a kilometre in the Labrador Sea in winter (de Boyer Montegut, et al., 2004). The base of the ML is defined where the water properties undergo an abrupt change. For example, previous studies have classified the base of the ML as a temperature change from the surface of at least 0.2°C (in the North Pacific Ocean, Thompson, 1976) or as a change of at least 0.8°C (in the global ocean, Kara, et al., 2000a). These examples illustrate the regional differences among mixed layer depths (MLD) and emphasize the need for local studies. In addition, since the MLD is strongly influenced by atmospheric conditions (for example Tabata, 1961, Denman and Miyake, 1973) we would expect climate change to

1

affect it. Since the MLD affects biological productivity in the oceans because the factors

that limit productivity, light and nutrients, change with the MLD (Polovina, et al 1995),

we would expect that climate change would thus affect biological productivity. How

climate change will affect ocean productivity is not known, however a greater

understanding of how different atmospheric processes affect the MLD is necessary to

predict future trends.

1.2 Study Area

1.2.1. Meteorology

The northeast Pacific Ocean (Figure 1-1), which we classify as the region north

of 40°N and east of 160°W, lies on the storm track of the Aleutian Low and in winter

experiences strong storms that are characterized by winds speeds of up to 60 knots and a

central pressure as low as 950mb (Cardone and Overland, 1980) as well as up to 800cm

of annual precipitation and waves as high as 30m (Wilson and Overland, 1987). From

June to August, the Pacific high-pressure system, with an average central pressure of

1024mb, is dominant and is characterized by reduced winds, decreased cloud cover and

smaller waves (Wilson and Overland, 1987). The spring (fall) is a transition period and is

typified by increasing (decreasing) shortwave radiation (SW) and decreasing (increasing)

latent heat (LH), sensible heat (SH), longwave radiation (LW) and wind speeds (Tabata,

1961).

The annual average net heat flux (SW+SH+LH+LW) in the northeast Pacific is

10-30 ± 10 Wm^{-2}, indicating a net heat gain in the ocean, particularly to the southern

region (Moisan and Niiler, 1998). The mean winter wind stress, or the work done on the

ocean surface by the horizontal force of wind, is 0.167 Nm^{-2} to the NNE, the mean spring

2

wind stress is 0.156 Nm^{-2} to the NE, the mean summer wind stress is 0.083 Nm^{-2} to the

NE and the mean fall wind stress is 0.15 Nm^{-2} to the NE (Trenberth, et al., 1990).

Overall, the northeast Pacific Ocean has an annual average value of evaporation –

precipitation (E-P) of –1 mm/day in the open ocean and –2 mm/day in the coastal ocean,

indicating that there is more precipitation than evaporation, particularly near the coast

(Kara, et al., 2000b).

1.2.2. General Circulation

Large-scale ocean currents influence the northeast Pacific (Figure 1-1). The

Kuroshio and Oyashio Currents are strong western boundary currents that separate near

the coast of Japan between 35-40°N (Thomson, 1981) and travel eastward as the

Kuroshio Extension, transporting 80-90 Sv (1Sv = 1x10^6 m^3/s) from the surface to the

bottom, reaching depths of 6000m across 152°E (Roemmich and McCallister, 1989) into

the central North Pacific. The Kuroshio Extension can be separated into a northern

section, the Subarctic Current that is mainly fed by the Oyashio Current and the southern

section, the North Pacific Current that is mainly fed by the Kuroshio Current (Thomson,

1981). These currents are separated by the subarctic front that normally resides along

40°N and divides warm, salty water to the south from cold, fresh water to the north

(Thomson, 1981). Yuan and Talley (1996) found that the temperature and salinity

differences across the front in the northeast Pacific is about 5°C and 1.5 psu and that the

strength of the temperature gradient varies seasonally, with a maximum in spring, while

the salinity gradient has little annual variability. Henceforth, both the Subarctic and North

Pacific Current will be considered the same and be called the North Pacific Current.

3

As it travels across the North Pacific Ocean, the North Pacific Current weakens and shoals, transporting 28.0 Sv from the surface to a depth of 2000m across 175°W (Roemmich and McCallister, 1989). In the region between 45-50°N and 130-150°W (Thomson, 1981), the North Pacific Current bifurcates to form the northward flowing Alaska Current that transports about 10 Sv from the surface to a depth of 1500m and the southward flowing California Current that transports up to 8.7 Sv from the surface to a depth of 1000m (Myers and Weaver, 1997). The Alaska Current travels counterclockwise to the head of the Gulf of Alaska at which time it turns westward as the Alaska Stream and strengthens to transport 12 Sv from the surface to 1000m (Myers and Weaver, 1997).

1.2.3. The History of Line P

Line P (Figure 1-2, 47°N to 50°N, 125°W to 145°W) is a series of 26 oceanographic sampling stations that stretches from just offshore of Vancouver Island, British Columbia, to 1500 km offshore, in the Gulf of Alaska. It is one of the best-studied oceanic regions in the world, with data collection dating back to 1956 (Whitney and Freeland, 1999). Line P originally started at Ocean Weather Station 'Papa' (henceforth known as OSP; 50°N, 145°W), a meteorological station that was first occupied by the United States in 1949, then taken over as a Canadian weather station in 1950. In 1959, Line P was created with the addition of 5 stations east of OSP, and in 1964, 8 more stations were added. Line P was sampled every six weeks from 1964 to 1981 and from 1981 to present has been sampled every 2-6 months when 13 more stations were added to increase the amount of data collected per trip (Whitney and Freeland, 1999). OSP became Station P26, with the station numbers decreasing along the line with P1 at the mouth of the Juan de Fuca Strait. Currently, Line P is sampled three times per year - in February,

4

June and August. This wealth of data has allowed Line P to be used to represent

oceanographic conditions and long-term variability in the Gulf of Alaska.

1.3. The MLD in the northeast Pacific

1.3.1. Vertical Structure of Upper Ocean

The change in density over the change in temperature ($\delta\rho/\delta T$) is greater in warm

waters so in cold regions the water temperature in the summer has a larger impact on the

density than in the winter (Carmack, 2000). Conversely, salinity has a similar impact on

density year-round since the change in density over the change in salinity ($\delta\rho/\delta S$) is

constant throughout the oceans (Carmack, 2000). This leads to the definition of two

different types of oceans – alpha oceans that are located south of the subarctic front and

beta oceans that are found north of the subarctic front where the density equation is

dominated by salinity (Carmack, 2000). In alpha oceans, the density equation is

dominated by temperature whereas in beta oceans, the density equation is dominated by

salinity. Thus, changes to the salinity in the northeast Pacific would potentially have a

greater impact on the MLD than changes to the temperature.

An initial classification of the vertical structure of the water at OSP by Tabata

(1961) found that there are three main layers in the upper waters – the upper zone, the

halocline and the lower zone. The upper zone, which includes the MLD, extends from the

surface to 100m and is characterized by a relatively fresh, homogenous salinity of 32.7

psu. The halocline normally lies between100-200m and is discernible by a change in

salinity of up to 1.0 psu over its depth. The lower zone begins at a depth of 200m and is

classified with a gradually increasing salinity with depth. A seasonal thermocline also

exists in the northeast Pacific that is strongest and shallowest in the summer, normally

5

residing around 50-100m, and is weaker and deeper in the winter, often found below the

halocline if at all (Tabata, 1961; Kara, et al., 2000b). Thus, the thermocline is always

deeper than the MLD. The presence of a permanent halocline can be explained by the fact

that generally, precipitation is greater than evaporation in the northeast Pacific so there is

always a fresher layer overtop of the bottom waters, forming a salinity gradient. The

thermocline in the northeast Pacific is present in the summer when strong SW warms the

surface waters and creates a vertical temperature gradient that then disperses in winter

when the surface layer cools.

1.3.2. The Observed MLD

Several studies have examined the average MLD at OSP and along Line P.

Thomson (1981) reported that the summer minimum MLD is approximately 20m while

the winter maximum MLD is greater than 100m. When investigating the MLD at OSP

from 1953-1967, McClain et al. (1996) found that based on a temperature difference

criterion of 0.1°C, the MLD varied from less than 10m in the summer to more than 250m

in the winter. Whitney and Freeland (1999) calculated the monthly average MLD at OSP

from the observed 1956-1997 data and found that it reached a maximum depth of 120m

from February – April and reached a minimum depth of 40m in August. Kara, et al

(2000b) used monthly climatologies of temperature and salinity to calculate the average

MLD throughout the North Pacific with a temperature difference criterion of 0.8°C and

found that in February, the average MLD north of 40°N and west of about 135°W in the

northeast Pacific was less than 100m and in August was close to 0m. Recently, Li, et al.

(2005a), using a temperature difference of 0.8°C to calculate the MLD (as is outlined in

Kara, et al., 2000a) from observed Line P data, examined the historical monthly MLD

6

along Line P and found that in the winter the MLD increases as you move westward from a maximum of just under 100m at station 16 to 120m at OSP.

In addition to the historical averages of MLD, several studies have discussed MLD variability in the northeast Pacific, whose maximum values can vary by as much as 70m in different winters (Freeland and Cummins, 2005). When comparing the periods of 1977-88 to 1960-76, Polovina et al (1995) found that winter and spring MLD in the subarctic North Pacific was 20-30% shallower during the more recent period than the earlier one although Li et al (2000a) found that even through there was a large amount of MLD variability during this period, there was no definitive shoaling along Line P. Recent studies of the maximum winter MLD at OSP since 1956 have shown (despite much variability) a shoaling trend (Freeland, et al., 1997) at a rate of 56m per century (Freeland and Cummins, 2005). In addition, the shallowest winter MLDs ever recorded were in 2002-03 and 2003-04, with a maximum MLD of about 75m and 80m respectively (Freeland and Cummins, 2005; Li, et al., 2005b). Several hypotheses have been established to explain the observed MLD variability and shoaling trend at OSP and the northeast Pacific Ocean.

1.3.3. Studies to explain MLD variability in the northeast Pacific

Early observations at OSP found that the depth of the ML is dependent on the magnitude of mixing through wind and the buoyancy flux, which is the balance of evaporation and precipitation (Tabata, 1961). Essentially, wind causes mixing through the action of waves and the generation of currents that cause frictional stresses and vertical shear while evaporation and heat loss to the atmosphere causes mixing by making the surface water denser, thereby causing it to sink (Tabata, 1961). Since

7

precipitation is usually greater than evaporation at OSP, the density structure of the ML is normally stable, however strong evaporation in the fall can create a density inversion, significant mixing and ML deepening (Tabata, 1961).

Some of the earliest MLD numerical models, several of which were validated by comparing their results to OSP observations, discovered that while wind and buoyancy flux control the MLD in the winter, SW controls the MLD in summer (Kraus and Turner, 1967; Adamec and Elsberry, 1984; Alexander and Penland, 1996) when there are low wind speeds that are less than 12.5m/s, a value that is anomalously high for summer (Denman, 1973). These early models were 1-D and based on calculations by Tabata (1965), who found that horizontal advection would cause a maximum temperature and salinity change at OSP of 0.26-0.78°C and 0.02-0.05 psu per month, a seemingly small change when compared to the seasonal cycle of MLD temperature that ranges from about 6°C in winter to 12°C in summer (Whitney and Freeland, 1999). It was assumed that it would take several weeks for advection to change the heat and salt content in the upper zone and therefore would not affect the monthly vertical calculation of the MLD (Denman and Miyake, 1973).

In an attempt to explain the generation of sea surface temperature (SST) anomalies at OSP, Elsberry and Garwood (1978) demonstrated that storms in the fall cause the surface layer to decrease by at least 1°C in 2 days whereas the same storms can cause water in a layer near 50m to increase in temperature by as much as 5°C in 2 days. In addition, a normal diurnal cycle in winter can cause the MLD to decrease from 100-150m at night to 10-40m during the day. Most importantly, the winter-summer MLD transition occurs when weak winds are accompanied by strong heating in the spring and

8

if an early transition occurs, the summer SST will be warmer than if there is a later transition (Elsberry and Garwood, 1978; Adamec and Elsberry, 1984). Alexander and Penland (1996) expanded on this idea by forcing a ML model with 30 years of atmospheric data from OSP and found that the SST anomalies can be partially explained by a re-emergence mechanism, where the same water from the MLD during one winter remains underneath the summer MLD and is re-entrained back into the MLD the following winter. Thus, a SST anomaly that was present during the first winter would persist into the following winter.

Several recent studies have suggested the Pacific Decadal Oscillation (PDO) is a dominant cause of MLD variability in the northeast Pacific Ocean (for example Miller, et al., 1994; Lagerloef, 1995; Polovina, et al., 1995; Miller and Schneider, 2000; Cummins and Lagerloef, 2002; Capotondi, et al., 2005). PDO can be described as a pattern of interdecadal climate variability that alternates between positive and negative regimes where during positive (negative) phases, the SST is anomalously warm (cold) and the sea level pressure (SLP) is anomalously low (high) in the northeast Pacific (Mantua and Hare, 2002). The last regime shift, from a negative to a positive phase, was in 1976-77 (Mantua and Hare, 2002) and currently the PDO is in a weakly positive phase (Crawford, et al., 2005). In addition to the SST and SLP changes, Lagerloef (1995) found that after the 1976-77 regime shift, the Aleutian Low intensified and shifted the center of the Alaskan Gyre, causing increased wind stress and Ekman pumping that resulted in a shallower pycnocline (Cummins and Lagerloef, 2002; Capotondi, et al., 2005). Contrary to these results, Li et al (2005a) found that there was no definitive MLD shoaling trend along Line P between 1957-1976 and 1977-1996, however since much regional MLD

9

variability was noted they suggest that the mechanism that caused the regime shift did not uniformly affect the MLD along Line P. In addition, although the PDO explains much of the interdecadal MLD variability, it cannot explain the MLD shoaling at OSP over the past 50 years.

Several studies have considered whether ENSO (El Nino Southern Oscillation) can explain some of the MLD variability in the northeast Pacific since anomalously high SSTs have been observed at the same time as ENSO events (for example Brown and Fu, 2000; Overland, et al., 2001). Mysak (1986) attributed interannual SST changes and variable surface currents primarily to alterations in the strength of the Aleutian Low, and suggested that some variability may be caused by ENSO. Satellite and ship-based data from the 1997-1998 ENSO were used to determine the cause for the abnormally high SST in the Gulf of Alaska and Freeland (2002) described two mechanisms that caused this change. The first is the meteorological phase, where ENSO affects atmospheric conditions in the northeast Pacific, bringing decreased LH and wind speeds (Brown and Fu, 2000) and decreased cloud cover (Overland, et al., 2001) and the second is the oceanographic phase where ENSO-induced Kelvin waves propagate along the coast, bringing warm water from the equator and reaching as far north as Vancouver Island (Whitney and Freeland, 1999) roughly 6 months after they leave South America (Strub and James, 2001). These Kelvin waves are often reflected back into the open ocean as Rossby waves that travel westward at a depth of roughly 200m (White and Tabata, 1987), and reach the western Pacific Ocean about 5-10 years after leaving the eastern Pacific (Miller and Schneider, 2000). Freeland and Cummins (2005) found that in the past 50 years, three of the four shallowest winter maximum MLDs at OSP (1982-83, 1997-98

10

and 2002-03) corresponded to ENSO years, indicating that ENSO explains some of the MLD shoaling. However, the 2002-03 ENSO was about one-third the strength of 1982-83 and 1997-98 on the Multi-variate ENSO Index (NOAA-CIRES Climate Diagnostic Center, 2005) and the shallow MLD in 2003-04 cannot be explained solely by ENSO.

A recent appraisal of historical temperature and salinity data from the Gulf of Alaska indicated that ML variability may be occurring on both longer and shorter scales than the PDO or ENSO can explain (Freeland, et al., 1997; Freeland and Cummins, 2005). In addition, significant changes of water column properties in the Gulf of Alaska are taking place that are likely related to changes to the MLD. In an assessment of data of coastal stations and OSP from 1935 – 1995, water in the upper layers is became warmer at a rate of up to 2 ($\pm$1)°C per century and fresher at a rate of up to 1 ($\pm$0.5) psu per century (Whitney and Freeland, 1999; Freeland, et al., 1997). Warmer, fresher properties would cause a greater density gradient between surface and lower waters and if atmospheric conditions were insufficient to cause mixing between the layers, we would expect the winter MLD to become shallower.

1.4. An Overview of this Study

There are two parts to this study. The first (chapter 2) examines the observed temperature data at four stations in the northeast Pacific (OSP, station 16 along Line P station (S16) on the south-eastern edge of the Alaska gyre, CAG in the centre of the Alaska gyre and station NSG on the northern edge of the subtropical gyre) and calculates the change in heat content once per month to quantify the horizontal advection of heat at each station. The motivation behind this study is to test the 1-D assumption to determine how and when increased horizontal advection may affect the results from a 1-D ML

11

model. In addition, this study will challenge the long-held assumption that horizontal advection is negligible in the Gulf of Alaska. The second part (chapter 3) of this study uses a 1-D ML model called the General Ocean Turbulence Model (GOTM; Burchard, et al., 2005) to calculate the MLD at the four stations from 2001-05. Several sensitivity studies that changed the atmospheric forcing were run to determine which processes have the greatest impact on the MLD. In addition, several recorded ocean and atmospheric events occurred during these study years and MLD behaviour was discussed in context with the timing of these events to understand how they affect it. The results of this study were used to explain why the MLD was so shallow in the winters of 2002-03 and 2003-04.

The ocean dataset was from Project Argo and was interpolated by Howard Freeland to each station as outlined in Freeland and Cummins (2005). The atmospheric input was from the NCEP/NCAR Reanalysis project (Kalnay, et al., 1996) and was downloaded and interpolated by Jennifer Jackson. The model, GOTM (Burchard, et al., 2005), was downloaded and set-up by Paul Myers and model experiments were run by Jennifer Jackson. Jennifer Jackson analyzed the results with input from Paul Myers and Debby Ianson. This manuscript was written by Jennifer Jackson and edited by Paul Myers and Debby Ianson.

This thesis was written in a paper format. Chapters 2 and 3 have been prepared as manuscripts and will be submitted to the journals *Geophysical Research Letters* and *Deep-Sea Research* respectively.
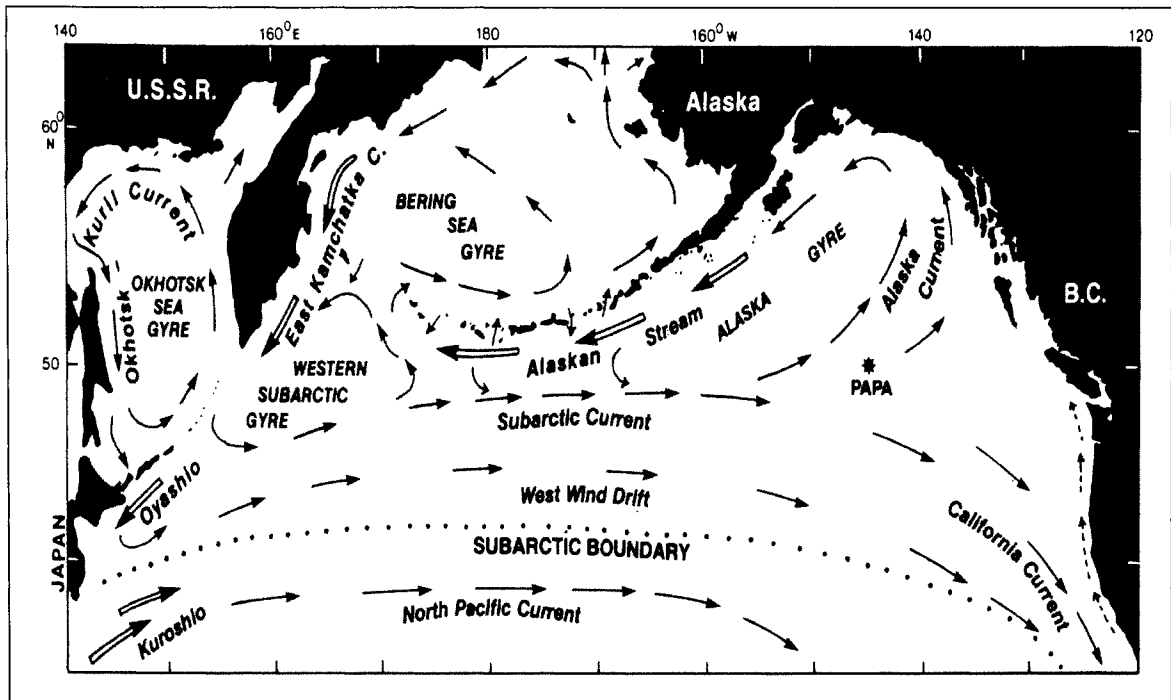
Figure 1-1: Map of the North Pacific Ocean with surface currents (used with permission from Thomson, 1981)
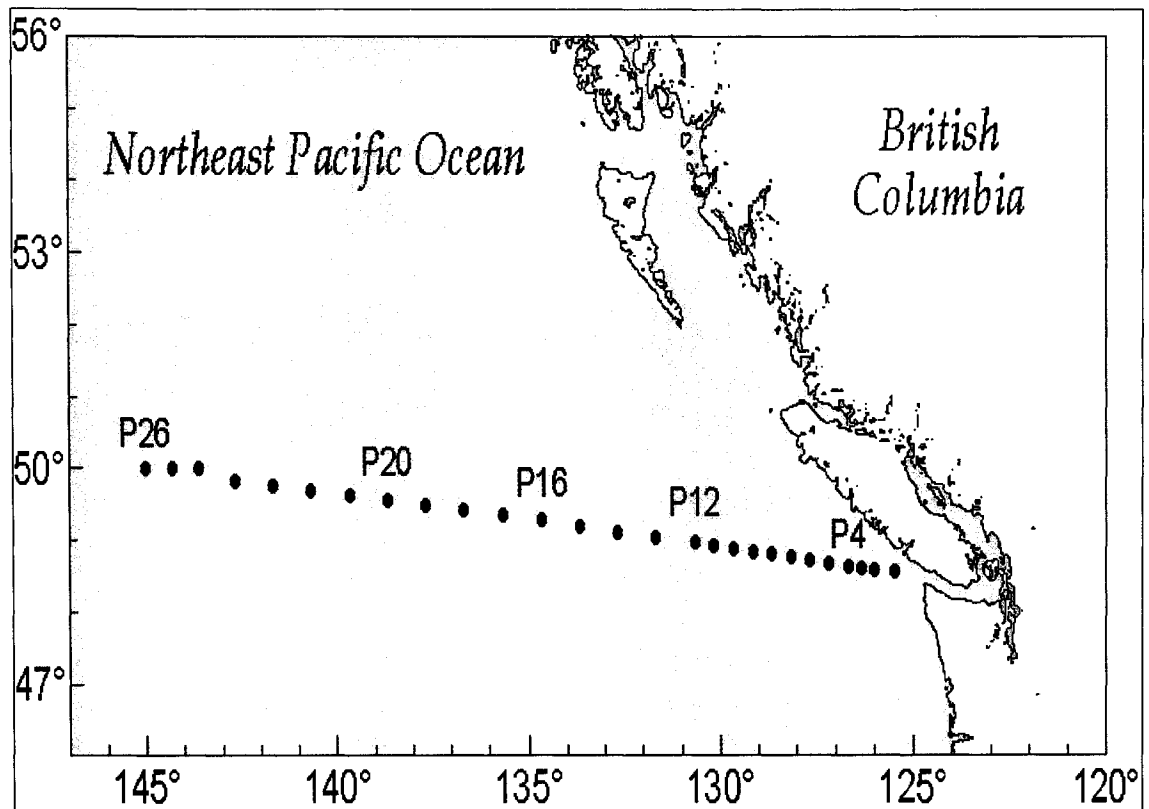
Figure 1-2: Map of Line P in the Gulf of Alaska. The stations are marked with dots, with the original stations in red. (Used with permission from http://www-sci.pac.dfo_mpo.gc.ca/osap/projects/linepdata/images/map-1.htm)

13

1.5. Bibliography

Adamec, D. and R.L. Elsberry. 1984. Sensitivity of Mixed Layer Predictions at Ocean

Station Papa to Atmospheric Forcing Parameters. *Journal of Physical Oceanography*,

14, 769-780.

Alexander, M.A. and C. Penland. 1996. Variability in a Mixed Layer Ocean Model

Driven by Stochastic Atmospheric Forcing. *Journal of Climate*, 9, 2424-2442.

Brown, R.G. and L.L. Fu. 2000. An Examination of the Spring 1997 Mid-Latitude East

Pacific Sea Surface Temperature Anomaly. *Atmosphere-Ocean,* 38(4), 577-599.

Burchard, H., K. Bolding and L. Umlauf. 2005. GOTM – The General Ocean Turbulence

Model. http://www.gotm.net

Capotondi, A., M.A. Alexander, C. Deser and A.J. Miller. 2005. Low-frequency

Variability in the Northeast Pacific. *Journal of Physical Oceanography,* 35, 1403-1420.

Cardone, V.J. and J.E. Overland. 1980. Case studies of four severe Gulf of Alaska

Storms. NOAA Technical Memorandum ERL PMEL-19, 68 pp.

Carmack, E.C. 2000. The Arctic Ocean's Freshwater Budget: Sources, Storage and

Export. In *The Freshwater Budget of the Arctic Ocean*, Kluwer Academic Publishers,

The Netherlands, 91-126.

Crawford, W., P. Sutherland and P. van Hardenberg. 2005. Cold Water Intrusion in the

Eastern Gulf of Alaska in 2002. *Atmosphere-Ocean*, 43(2), 119-128.

Cummins, P.F. and G.S.E. Lagerloef. 2002. Low-Frequency Pycnocline Depth

Variability at Ocean Weather Station P in the Northeast Pacific. *Journal of Physical*

Oceanography, 32, 3207-3215.

De Boyer Montegut, C., G. Madec, A.S. Fischer, A. Lazar and D. Iudicone. 2004. Mixed

layer depth over the global ocean: An examination of profile data and a profile-based

climatology. *Journal of Geophysical Research*, 109, C12003,

doi:10.1029/2004JC002378.

Denman, K.L. 1973. A Time-Dependent Model of the Upper Ocean. *Journal of Physical Oceanography*, 3, 173-184.

Denman, K.L. and M. Miyake. 1973. Upper Layer Modification at Ocean Station *Papa*:

Observations and Simulations, *Journal of Physical Oceanography*, 3, 185-196.

Elsberry, R.L. and R.W. Garwood, Jr. 1978. Sea-Surface Temperature Anomaly

Generation in Relation to Atmospheric Storms. *Bulletin of the American Meteorological Society*, 59(7), 786-789.

Freeland, H. 2002. The Heat Flux across Line-P 1996-1999. *Atmosphere-Ocean* 40(1),

81-89.

Freeland, H.J. and P.F. Cummins, 2005. Argo: A new tool for environmental monitoring

and assessment of the world's oceans, an example from the N.E. Pacific. *Progress in Oceanography*, 64, 31-44.

Freeland, H., K. Denman, C.S. Wong, F. Whitney and R. Jacques. 1997. Evidence of

change in the winter mixed layer in the Northeast Pacific Ocean. *Deep-Sea Research* I,

44(12), 2117-2129.

Kalnay, E., M. Kanamitsu, R. Kistler, W. Collins, D. Deaven, L. Gandin, M. Iredell, S.

Saha, G. White, J. Woollen, Y. Zhu, A. Leetmaa, B. Reynolds, M. Chelliah, W.

Ebisusaki, W. Higgins, J. Janowiak, K.C. Mo, C. Ropelewski, J. Wang, R. Jenne and

D. Joseph. 1996. The NCEP/NCAR 40-Year Reanalysis Project. *Bulletin of the American Meteorological Society*, 77(3), 437-471.

Kara, A.B., P.A. Rochford and H.E. Hurlburt. 2000a. An optimal definition for ocean mixed layer depth. *Journal of Geophysical Research*, 105, 16,803-16,821.

Kara, A.B. P.A. Rochford and H.E. Hurlburt. 2000b. Mixed layer depth variability and barrier layer formation over the North Pacific Ocean. *Journal of Geophysical Research*, 105, 16,783-16,801.

Kraus, E.B. and J.S. Turner. 1967. A one-dimensional model of the seasonal thermocline II. The general theory and its consequences. *Tellus*, XIX(1), 98-105.

Lagerloef, G.S.E. 1995. Interdecadal Variations in the Alaska Gyre. *Journal of Physical Oceanography*, 25, 2242-2258.

Li, M., P.G. Myers and H. Freeland. 2005a. An examination of historical mixed layer depths along Line P in the Gulf of Alaska. *Geophysical Research Letters*, 32, doi:10.1029/2004GL021911.

Li, M., H. Freeland and P.G. Myers. 2005b. An Examination of Mixed Layer Depth in the Gulf of Alaska using Argo Data. *Geophysical Research Letters,* submitted.

Mantua, N.J. and S.R. Hare. 2002. The Pacific Decadal Oscillation. *Journal of Oceanography*, 58, 35-44.

McClain, C.R., K. Arrigo, K-S. Tai and D. Turk. 1996. Observations and simulations of physical and biological processes at ocean weather station P, 1951-1980. *Journal of Geophysical Research*, 101, 3697-3713.

Mellor, G.L. 1996. *Introduction to Physical Oceanography*. Springer-Verlag, New York, 260 pp.

Miller, A.J., D.R. Cayan, T. P. Barnett, N.E. Graham and J.M. Oberhuber. 1994. Interdecadal variability of the Pacific Ocean: model response to observed heat flux and

wind stress anomalies. *Climate Dynamics*, 9, 287-302.

Miller, A.J. and N. Schneider. 2000. Interdecadal climate regime dynamics in the North

Pacific Ocean: theories, observations and ecosystem impacts. *Progress in*

Oceanography, 47, 355-379.

Moison, J.R. and P.P. Niiler. 1998. The Seasonal Heat Budget of the North Pacific: Net

Heat Flux and Heat Storage Rates (1950-1990). *Journal of Physical Oceanography*, 28,

401-421.

Myers, P.G. and A.J. Weaver. 1997. On the circulation of the North Pacific Ocean:

climatology, seasonal cycle and interpentadal variability. *Progress in Oceanography*,

38(1), 1-49.

Mysak, L.A. 1986. El Nino, interannual variability and fisheries in the northeast Pacific

Ocean. *Canadian Journal of Fisheries and Aquatic Sciences*, 43(2), 464-497.

NOAA-CIRES Climate Diagnostic Centre, University of Colorado at Boulder. 2005.

Multivariate ENSO Index, http://www.cdc.noaa.gov/people/klaus.wolter/MEI/

Overland, J.E., N.A. Bond and J.M. Adams. 2001. North Pacific Atmospheric and SST

Anomalies in 1997: Links to ENSO? *Fisheries Oceanography*, 10(1), 69-80.

Polovina, J.J., G.T. Mitchum and G. T. Evans. 1995. Decadal and basin-scale variation in

mixed layer depth and the impact on biological production in the Central and North

Pacific, 1960-88. *Deep-Sea Research*, 42(10), 1701-1716.

Roemmich, D. and T. McCallister. 1989. Large scale circulation in the North Pacific

Ocean. *Progress in Oceanography*, 22, 171-204.

Strub, P.T. and C. James. 2002. The 1997-98 oceanic El Nino signal along the southeast

and northeast Pacific boundaries – an altimetric view. *Progress in Oceanography*, 54,

17

439-458.

Tabata, S. 1961. Temporal Changes of Salinity, Temperature, and Dissolved Oxygen Content of the Water at Station "P" in the Northeast Pacific Ocean, and Some of Their Determining Factors. *Journal of the Fisheries Research Board of Canada*, 18(6), 1073-1124.

Tabata, S. 1965. Variability of oceanographic conditions at Ocean Station "P" in the northeast Pacific Ocean. *Transactions of the Royal Society of Canada, Series* 4, 3, Section 3, 367-418.

Thompson, R.O.R.Y. 1976. Climatological numerical models of the surface mixed layer of the ocean. *Journal of Physical Oceanography*, 6, 496-603.

Thomson, R.E. 1981. *Oceanography of the British Columbia Coast*. Canadian Special Publication of Fisheries and Aquatic Sciences, 56, 291pp.

Trenberth, K.E., W.G. Large and J.G. Olson. 1990. The Mean Annual Cycle in Global Ocean Wind Stress. *Journal of Physical Oceanography*, 20, 1742-1760.

White, W.B. and S. Tabata. 1987. Interannual Westward-Propagating Baroclinic Long-Wave Activity on Line P in the Eastern Midlatitude North Pacific. *Journal of Physical Oceanography*, 17, 385-395.

Whitney, F.A. and H.J. Freeland. 1999. Variability in upper-ocean water properties in the NE Pacific Ocean. *Deep-Sea Research* II, 46, 2351-2370.

Wilson, J.G. and J.E. Overland. 1987. Meteorology. In Eds. D.W. Hood and S.T. Zimmerman. *The Gulf of Alaska: Physical Environment and Biological Resources*, U.S. Department of Commerce, NOAA, Alaska, 31-54.

Yuan, X. and L.D. Talley. 1996. The subarctic frontal zone in the North Pacific:

characteristics of frontal structure from climatological data and synoptic surveys.

Journal of Geophysical Research, 101, 16,491-16,508.

Chapter 2

An Examination of Advection in the Northeast Pacific Ocean, 2001-05

2.1. Introduction

Ocean Station Papa (OSP, 50°N, 145°W) is a station that has almost 50 years of oceanographic data and has long been used to represent conditions in the Gulf of Alaska (figure 2-1; Whitney and Freeland, 1999). The vertical salinity structure at OSP shows three main surface features – an upper zone (UZ, 0-100m), a halocline zone (HZ, 100-200m) and a lower zone (LZ, >200m) (Tabata, 1961). The HZ is a permanent feature while the thermocline is a seasonal trait that only affects the vertical structure in summer

20

(Tabata, 1961) so the density north of the subarctic front is dominated by salinity (Freeland, et al., 1997). The interior of the Alaska Gyre has long been considered a region with minimal horizontal advection and an ideal location for 1-D mixed layer (ML) models (for example Denman and Mikaye, 1973). Thus, OSP has been a traditional test site for such models. However, recent processes that increase advection at OSP, such as the northward migration of the North Pacific Current (NPC; Freeland and Cummins, 2005) have been documented.

Previously, the change in heat content due to horizontal advection was assumed negligible at OSP, ranging from 0.26-0.78°C per month (Tabata, 1965; Denman and Miyake, 1973). We test this assumption at four stations – OSP, Station 16 (S16; 49°17N, 134°40W) along oceanographic Line P which is on the southeastern edge of the Alaskan Gyre, 55°N, 145°W in the center of the Alaskan Gyre (CAG) and 40°N, 145°W along the northern edge of the subtropical gyre (NSG) (figure 2-1). We use real-time, continuous temperature profiles from Argo floats (Gould, et al., 2004) and the NCEP/NCAR Reanalysis (Kalnay, et al., 1995) to calculate the monthly change of heat content. Current estimates of surface heat flux are more accurate than freshwater flux estimates (Taylor, 2002) so local changes in heat content were used as a proxy for advection.

2.2. Data and Methods

Temperature and salinity data from the Argo dataset (Gould, et al., 2004) was interpolated as per Freeland and Cummins (2005) to our 4 stations. We studied OSP, S16 and CAG from July 2001 –July 2005 and NSG from April 2002 – July 2005 at NSG because NSG was limited by the availability of Argo data prior to this period (Freeland and Cummins, 2005). Daily average surface heat fluxes from the NCEP/NCAR

21

Reanalysis (Kalnay, et al., 1995) were linearly interpolated to our 4 stations and then summed to calculate the total surface heat fluxes (Q_{SF}) at each station.

Heat content (Q_{HC}) was calculated as:

$$Q_{HC} = \rho_o \, C_p \int T \, dz \tag{2.2.1}$$

where ρ_o (reference density) is 1026.95 kg m^{-3}, C_p (specific heat of seawater) is 3986 Jkg^{-1}°C^{-1} and T is the temperature interpolated in 1m intervals. Advection is expected to affect the heat budget only after several weeks (Denman and Miyake, 1973). Thus, once a month, Q_{HC} was integrated over the three distinct depth ranges: UZ (0-100m), HZ (0-200m) and LZ (0-250m) (figure 2-2). The vertical flux through the bottom of each layer was assumed to be zero. It is possible that upwelling and downwelling could influence the heat content in the UZ because the wind stress curl influences temperatures in the Gulf of Alaska to 150m (Murphee, et al., 2003). However, a simple scaling argument suggests that vertical advection is one to two orders of magnitude smaller than horizontal in the Gulf of Alaska (based on a horizontal length scale of ~500 km, a vertical length scale of 100 m, typical horizontal velocities of 0.1 m/s, Ekman pumping velocities smaller than 1.5x10^{-5} m/s (Li et al., 2005) and observed temperature gradients), especially through the base of our deepest box, the LZ layer.

The observed heat content at the beginning of the month (Q_{HCobs1}) and the surface heat fluxes through that month (Q_{SF}) were subtracted from the observed heat content at the end of the month (Q_{HCobs2}) and the difference was classified as advection (Q_{AD}):

$$Q_{AD} = Q_{HCobs2} - (Q_{HCobs1} - Q_{SF}) \tag{2.2.2}$$

22

The advection was considered significant when the monthly change in heat content was greater than the maximum value of 0.78°C calculated by Tabata (1965). Our method can only detect advection where horizontal gradients in temperature are present.

2.3. Results and Discussion

Overall, all stations underwent a net heat loss due to horizontal advection throughout the study period (Table 1). OSP had the greatest heat loss, with a monthly average through the LZ of -0.09 ± 0.05°C while CAG had the smallest heat loss of -0.00 ± 0.03°C. Although NSG had a smaller average (-0.07 ± 0.06°C) than OSP, it had the largest standard error, suggesting that considerable monthly advection with heat gains and losses were occurring.

At OSP (figure 2-3a) there was no significant advection until December 2002. Although the northward migration of the NPC did not cause a significant change in the heat content from advection, we can see its signature in our results. The NPC traveled north through OSP in February 2002 to 51.5°N, where the main axis resided from March – May and then returned to its normal location in June 2002 (Freeland and Cummins, 2005). The largest advective heat loss was seen in March, with a maximum change in temperature of -0.48°C, -0.42°C and -0.41°C in the UZ, HZ and LZ. Constant heat loss with depth suggests that the main axis of the current was near OSP and that the NPC was transporting cold water. A heat gain would have implied that the subarctic front had migrated as far north as OSP. During this period, very little advection occurred at any of the other stations, suggesting that it was the NPC, and not a region wide process, that caused advection at OSP. It is possible that significant advection from the NPC would have been detected if the change in salt content had been calculated since the UZ became

23

0.1 psu saltier during the spring of 2002 (not shown). The arrival of the subsurface cold water anomaly (Crawford, et al., 2005) was not observed as there was no significant heat loss in the HZ at OSP and S16 during the summer of 2002. We suggest that the anomalous water mass was already present in the summer of 2002 and at OSP was likely a remnant of the cold water from the NPC. At OSP, there was a significant heat loss in December 2002 (-1.16°C) in the UZ. It is possible since this significant heat loss was restricted to the UZ, this temperature change was caused by upwelling from increased Ekman pumping. The average wind speed in January 2002 (10.8 ± 4.2 m/s) was much higher than in January 2003 (7.9 ± 3.4 m/s), January 2004 (8.5 ± 3.7 m/s) and January 2005 (7.9 ± 3.0 m/s) and the required time for the wind stress curl to affect the Ekman pumping velocity at OSP (8-12 months) (Lagerloef, 1995; Capotondi, et al., 2005; Li, et al., 2005) supports this idea. The affect of the 2002-03 El Nino (ENSO) event on the water column in the Northeast Pacific Ocean can be broken into two phases, the early meteorological phase that is characterized by decreased cloud cover and latent heat fluxes and a reversal in wind direction and the delayed oceanographic phase caused by the passage of a Rossby wave into the open ocean (Freeland, 2002 and references therein). Effects of the meteorological phase are accounted for by Q_{SF} (equation 2). The oceanographic phase may have affected our 2004-05 results. Starting in November 2004, Q_{AC} oscillated from heating to cooling until July 2005. Significant values occurred in November (1.26°C), February (-0.78°C), April (-1.17°C) and July (-1.19°C) with the largest heat gain was seen in the LZ.

S16 had similar changes to the heat content from advection as OSP (figure 2-3b), with sporadic periods of significant advection that were associated with a heat loss until

24

the winter of 2004-05. The first period of significant change in heat content was in February 2003, with a heat loss of -1.22°C. Increased southward flow into the California Current and decreased northward flow into the Alaska Current from the NPC may have caused this loss (Freeland, et al., 2003). Most of the advection was in the UZ so it is likely that the main axis of the Alaska Current did not travel through S16. Similarly in February 2004, there was a heat loss (-1.09°C) that was primarily in the UZ so we suggest that this was again caused by the close proximity of the Alaska Current to S16. Significant advection occurred in October 2004, March 2005 and June 2005 with values of 1.00°C, -0.79°C and -1.04°C, respectively. The heat gain occurred 1 month earlier at S16 than at OSP and was found primarily in the UZ instead of the LZ. Aside from the heat gain in October, there were no rapid temperature gains and losses through the winter of 2004-05 at S16.

At CAG (figure 2-3c), significant advection associated with a heat gain of 0.81°C, 0.74°C and 0.69°C in the UZ, HZ and LZ in September 2002 was followed by enhanced advection and heat loss in October. We suggest that the Haida Eddy 2000a caused this heat gain since it resided within the vicinity of CAG during the summer of 2002 and was near to the station on September 1, 2002 (Crawford and Whitney, 2005). The following September, there was a similar heat gain (0.94°C) principally in the UZ again followed by the heat loss (-0.75°C) in November 2003 and then a heat gain of 0.69°C in December 2003 consistent with passage of a warm-core eddy or some other anomalous water mass. However, there were no observed eddies in the region during these months (Crawford and Whitney, 2005). In November 2004 significant advection that was associated with a heat gain (0.84°C) was followed by a heat loss in February 2005 (-0.75 °C). Again, we

25

see a similar pattern at CAG as at OSP and S16, with a significant heat gain in November yet there were no observed eddies near CAG during this period.

NSG was more variable than stations in the Alaska gyre (figure 2-3d). The first period of significant advection was September, October and December 2002 with oscillatory monthly Q_{AD} (-1.02°C, 1.57°C and -0.80°C) in the UZ. We know that the NPC did not return to the region of NSG until much later (Freeland and Cummins, 2005) so another mechanism must have caused this event. Significant heat loss (-0.82°C) in May 2003 that was primarily in the UZ accompanied the return of the NPC. In December 2004 and February 2004 significant advection with a heat gain of 1.01°C was followed by a heat loss of -1.34°C. The reversal from the heat gain to heat loss in January is concurrent with the movement of the NPC (Freeland and Cummins, 2005). We suggest that the significant advection with a heat loss in June 2004 (-0.94°C) in the UZ was also caused by the NPC and since there was substantial advection through all layers, the main axis of the NPC was likely near NSG. More oscillatory heat gains and losses occurred in October 2004, December 2004, April 2005 and June 2005 with values of 1.47°C, 1.09°C, -0.83°C and -1.02°C, respectively.

Since there was a significant heat gain from horizontal advection at all observed stations in the northeast Pacific during the fall of 2004 followed by a period of a significant advective heat loss in the spring, it appears that a basin-scale process was responsible.

2.4. Summary and Implications

Horizontal advection is assumed to be negligible in the Gulf of Alaska so many 1-D ML models are used in that region. Recent events such as the northern migration of the

NPC show that atypical processes arise, thereby creating a need to verify the accuracy of this assumption. In this study, advection was estimated from the difference between the observed heat content and the expected heat content (based on surface heat fluxes). The timing and magnitude of heat content changes were assessed to determine which documented atmospheric and oceanographic events may have influenced advection. The change in heat content was usually within the same order of magnitude as the surface heat fluxes.

OSP, where previous calculations have shown that the maximum monthly heat change from advection was 0.78°C (Tabata, 1965), experienced 5 out of 48 months where the advection was greater than this value, with a maximum change of 1.26°C in November 2004. S16 also experienced 5 months where the change in heat content due to advection was greater than 0.78°C with a maximum of -1.22°C in February 2003. We suggest that aside from the heat gain seen in October 2004, the meandering of the AC caused the advection. At CAG, there were only 3 months where the change in heat content was greater than 0.78°C with a maximum of 0.94°C in September 2003. It is likely that the passage of eddies through the Alaska Gyre caused these changes. Overall, our proxy showed that NSG had the strongest advection and the most number of months, 11 out of 36, when the change in heat content from advection was greater than 0.78°C with a maximum of 1.57°C in October 2002. This advection was likely caused by its proximity to the NPC, a poor location for 1-D models. All stations experienced a significant amount of heat gain in the fall of 2004 followed by significant heat loss in early 2005. Although we are unsure what mechanisms caused these anomalies, it is probable that the process was region-wide

27

Thus, our results show that while stations in the Gulf of Alaska experienced negligible advection most of the time (consistent with the historical limits of Tabata, 1965), events occurred that increased the advection and would be expected to affect ML calculations and results of 1-D coupled models. Of the stations studied, CAG would be the best location to use a 1-D ML model as anticipated as it is in the center of the gyre away from boundary currents, however there were still several months when horizontal transport was significant. We suggest that heat budgets are estimated when 1-D models are used to ensure that the horizontal advection assumption is reasonable. The availability of CTD data from Argo floats makes such model checks possible.
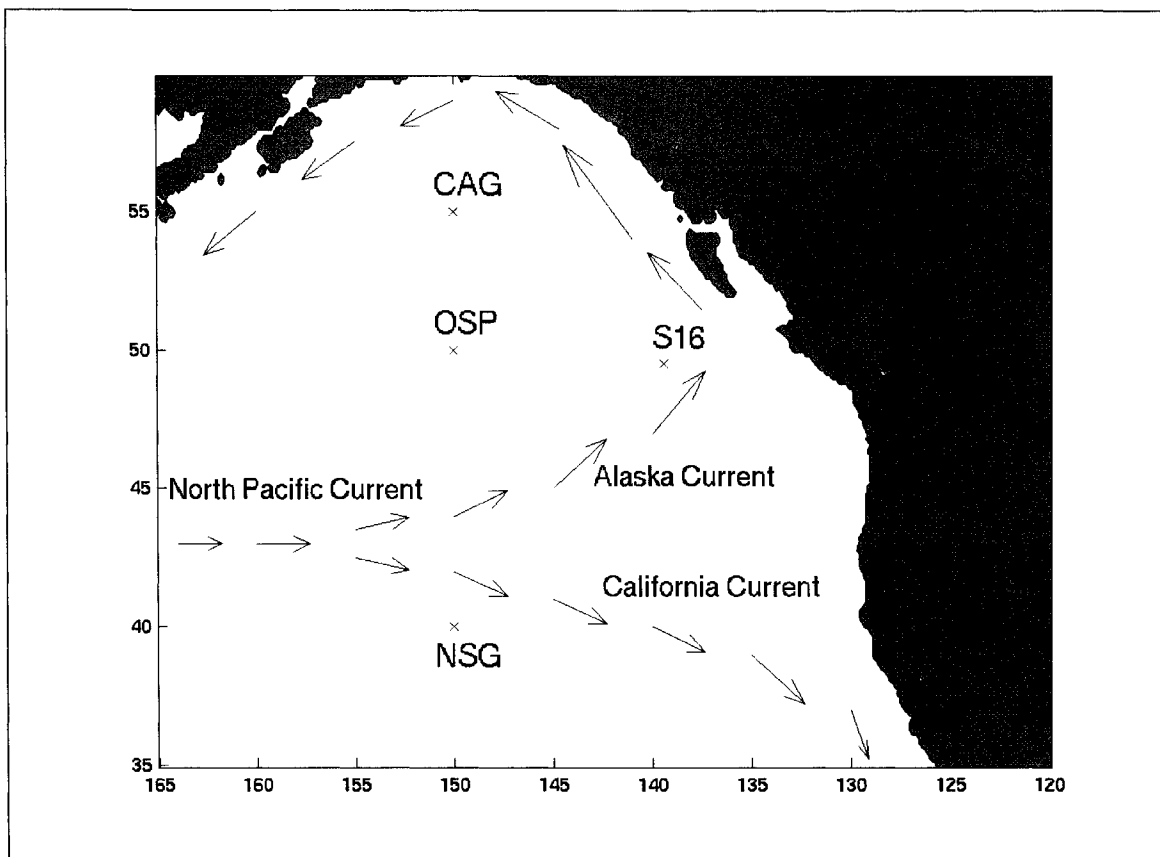
Figure 2-1: A map of the North Pacific Ocean with surface currents and stations used in this experiment. The NPC separates the Alaskan gyre (to the north) from the subtropical gyre (to the south).

28

Table 2-1: The average monthly temperature change (°C) and standard deviation (n=48 at OSP, S16 and CAG and n=36 at NSG) at each level from August 2001 – July 2005 at OSP, S16 and CAG and from August 2002 – July 2005 at NSG. Negative values indicate a heat loss.

	OSP	S16	CAG	NSG
100m	-0.22 ± 0.06	-0.17 ± 0.06	-0.02 ± 0.06	-0.16 ± 0.11
200m	-0.11 ± 0.04	-0.09 ± 0.03	-0.01 ± 0.04	-0.08 ± 0.07
250m	-0.09 ± 0.05	-0.08 ± 0.03	-0.003 ± 0.03	-0.07 ± 0.06
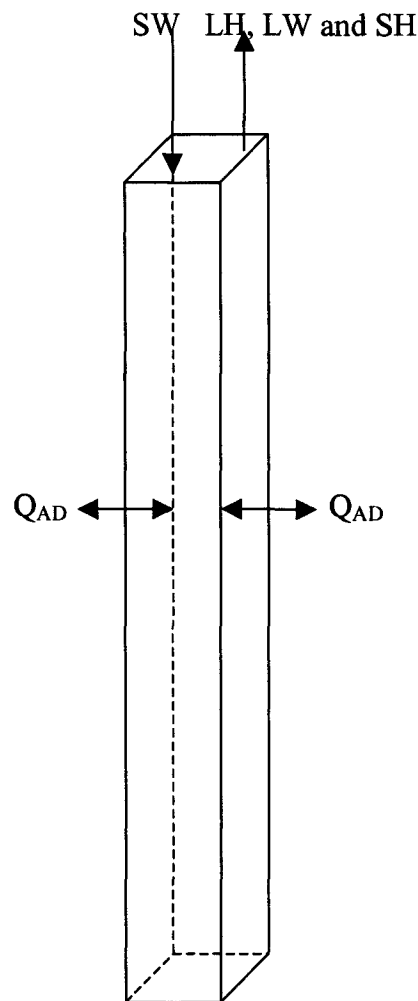
Figure 2-2: A schematic of model of the movement of heat in and out of model. Heat fluxes through bottom of vertical layer have been calculated to be negligible so are assumed to be zero.

29
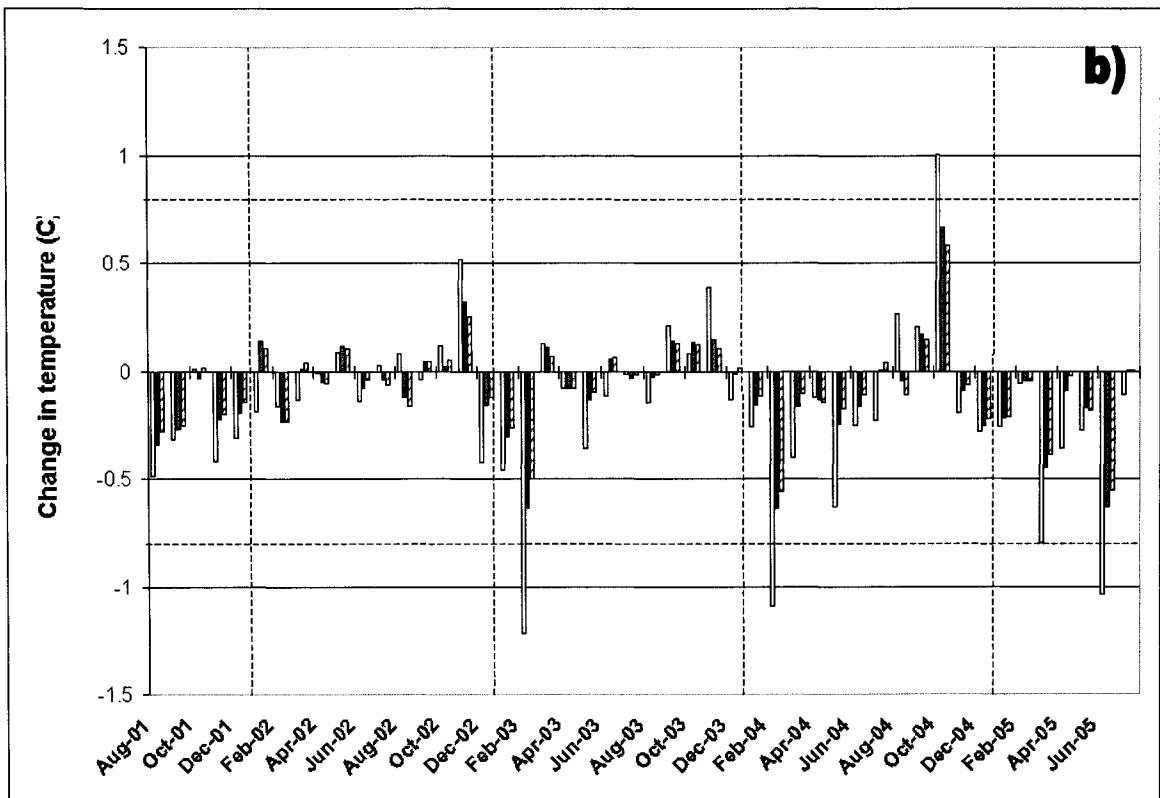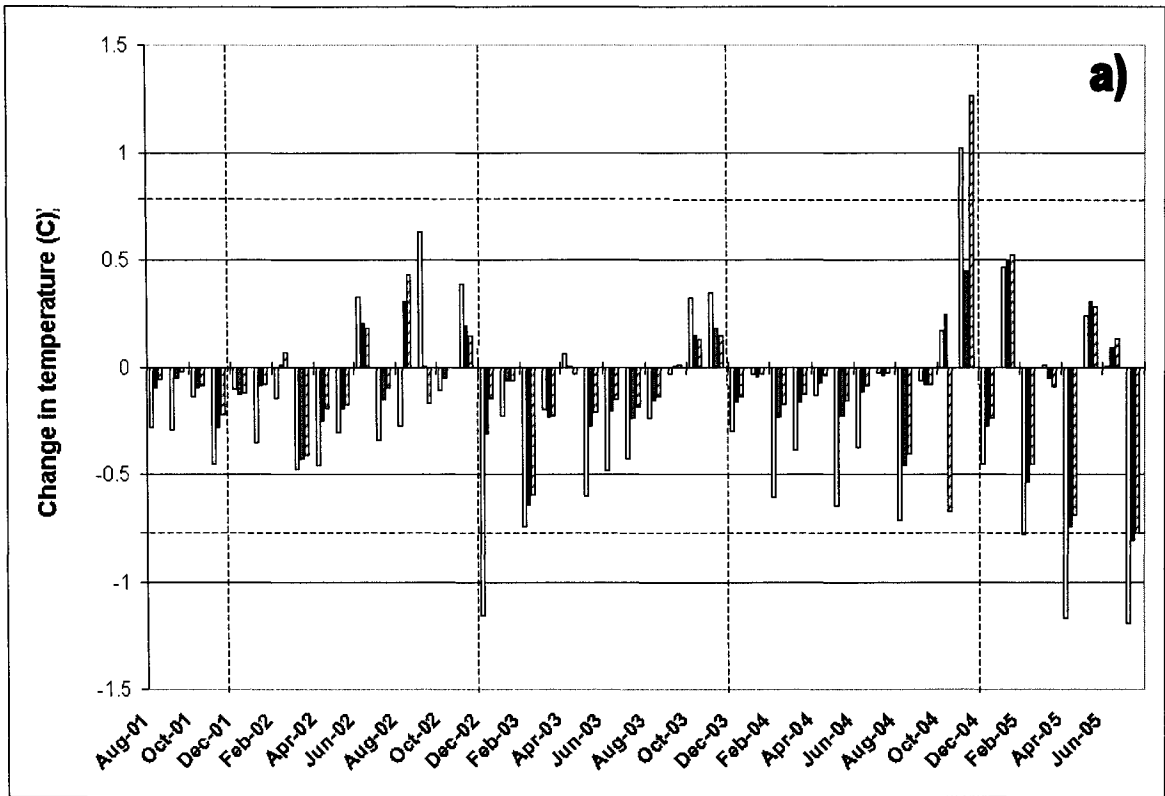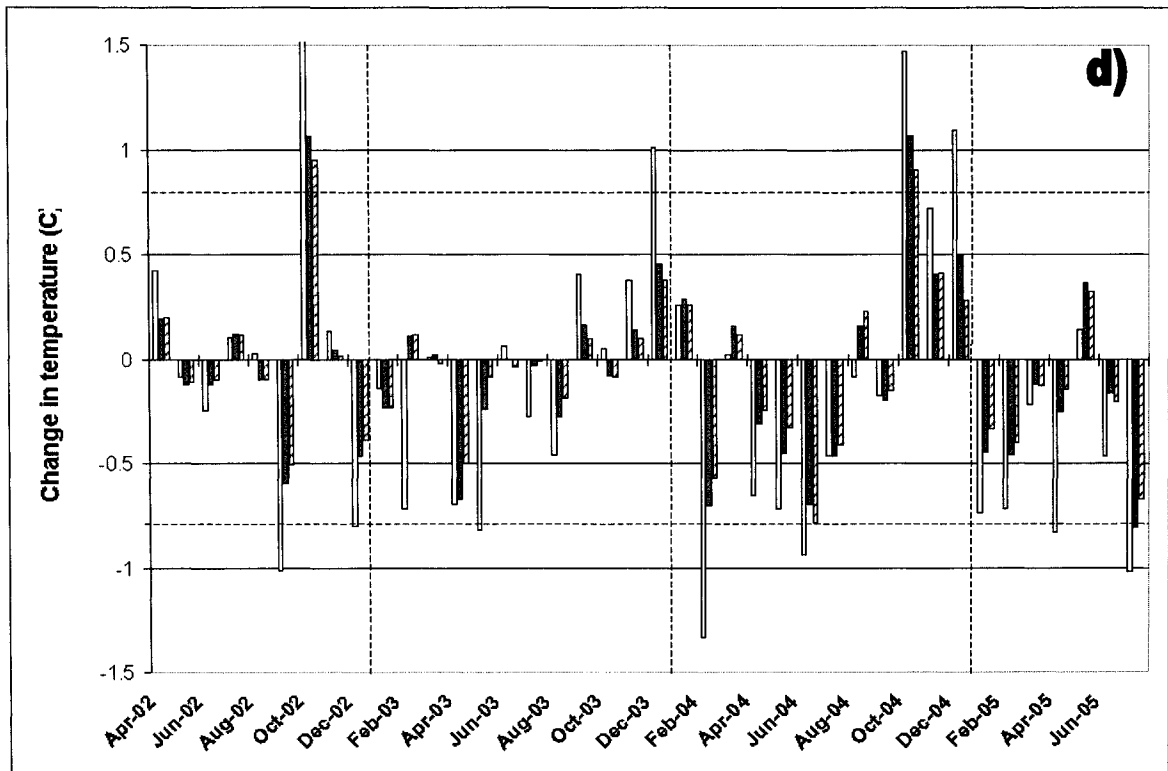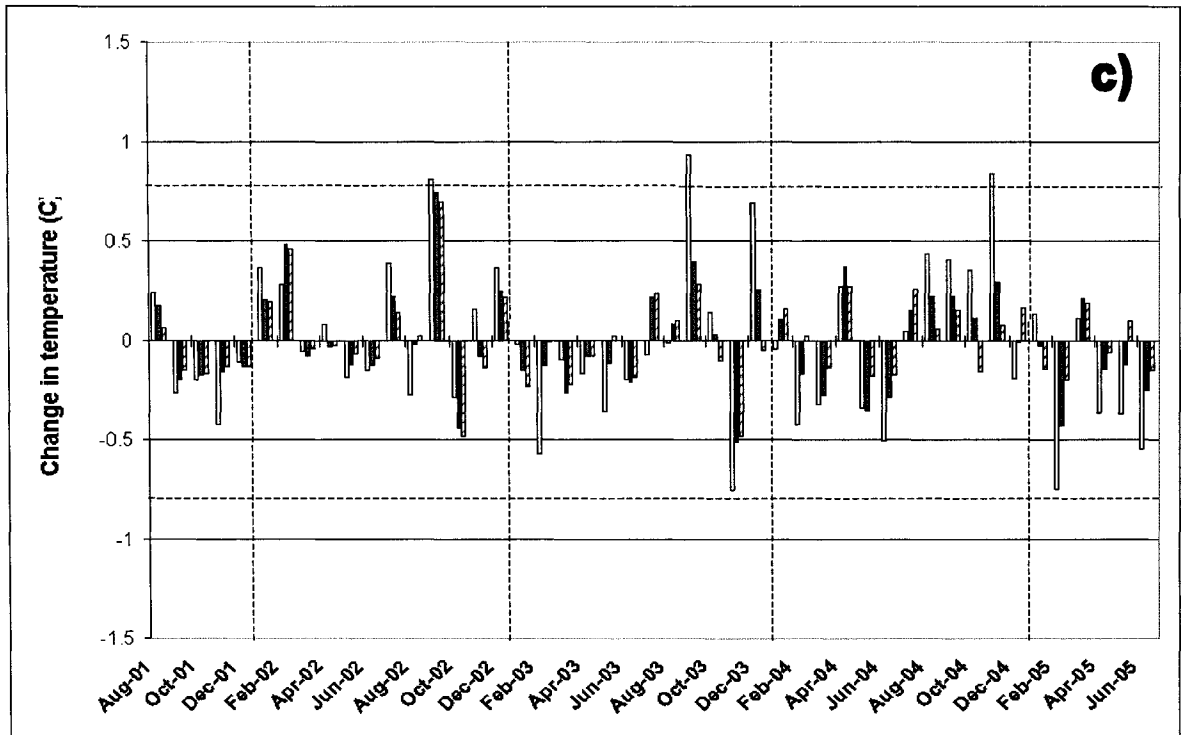
Figure 2-3: Calculated change in temperature from advection at a) OSP b) S16 c) CAG and d) NSG. White bars represent temperature change to 100m, gray bars represent temperature change to 200m and bars with gray diagonal lines represent temperature change to 250m. Vertical dashed lined intersect at January of each year. Horizontal dashed lines intersect at ± 0.78°C. Maximum value at NSG in October 2002 is 1.57°C.

31

2.5. Bibliography

Capotondi, A., M.A. Alexander, C. Deser, and A.J. Miller (2005), Low-frequency
Variability in the Northeast Pacific, *Journal of Physical Oceanography,* 35, 1403-1420.

Crawford, W.R (2005), Heat and fresh water transport by eddies into the Gulf of Alaska,
Deep-Sea Research II, 52, 893-908.

Crawford, W., and F. Whitney, (2005). *Graphic Images of the Haida Eddy,*
http://www.sci.pac.dfo-mpo.gc.ca/osap/projects/HaidaEddy

Crawford, W., P. Sutherland, and P. van Hardenberg (2005), Cold water intrusion in the
Eastern Gulf of Alaska in 2002, *Atmosphere-Ocean,* 43, 119-128.

Denman, K.L., and M. Miyake (1973), Upper Layer Modification at Ocean Station *Papa:*
Observations and Simulation, *Journal of Physical Oceanography,* 3, 185-196.

Freeland, H (2002), The Heat Flux across Line-P 1996-1999, *Atmosphere-Ocean,* 40,
81-89.

Freeland, H (2005), *Argo Status Globally and in the Gulf of Alaska,*
http://www-sci.pac.dfo-mpo.gc.ca/osap/projects/argo/status_e.htm

Freeland, H.J., and P.F. Cummins (2005), Argo: A new tool for environmental
monitoring and assessment of the world's oceans, an example from the N.E. Pacific,
Progress in Oceanography, 64, 31-44.

Freeland, H., K. Denman, C.S. Wong, F. Whitney, and R. Jacques (1997), Evidence of
Change in the winter mixed layer in the Northeast Pacific Ocean, *Deep-Sea Research I,*
44, 2117-2129.

Freeland, H.J., G. Gatien, A. Huyer, and R.L. Smith (2003), Cold halocline in the
Northern California Current: An invasion of subarctic water. *Geophysical Research*

Letters, 30(3), doi:10.1029/2002GL016663.

Gould, J., D. Roemmich, S. Wijffels, H. Freeland, M. Ignaszewsky, X. Jianping, S. Pouliquen, Y. Desaubies, U. Send, K. Radhakrishnan, K. Takeuchi, K. Kim, M. Danchenkov, P. Sutton, B. King, B. Owens, and S. Riser (2004), Argo Profiling Floats Bring New Era of In Situ Ocean Observations, *EOS Transactions, AGU*, 85, 185-190.

Kalnay, E., M. Kananitsu, R. Kistler, W. Collins, D. Deaven, L. Gandin, M. Iredell, S. Saha, G. White, J. Woollen, Y. Zhu, A. Leetmaa, B. Reynolds, M. Chelliah, W. Ebisuzaki, W. Higgins, J. Janowiak, K.C. Mo, C. Ropelewski, J. Wang, R. Jenne, and D. Joseph (1996), *Bulletin of the American Meteorological Society*, 77, 437-471.

Lagerloef, G.S.E (1995), Interdecadal Variations in the Alaska Gyre. *Journal of Physical Oceanography*, 25, 2242-2258.

Li, M., P.G. Myers, and H. Freeland (2005), An Examination of Mixed Layer Depth in the Gulf of Alaska using Argo Data, *Geophysical Research Letters*, submitted.

Murphee, T., P. Green-Jessen, F.B. Schwing, and S.J. Bograd (2003), The seasonal Cycle of wind stress curl and its relationship to subsurface ocean temperature in the North Pacific, *Geophysical Research Letters,* 30(9), 1469, doi:1029/2002GL016366.

Robert, M (2005), *Line-P Profiles*,

http://www-sci.pac.dfo-mpo.gc.ca/osap/data/linep/linepselectdata_e.htm

Tabata, S (1961), Temporal Changes of Salinity, Temperature and Dissolved Oxygen Content of the Water at Station "P" in the Northeast Pacific Ocean, and Some of Their Determining Factors, *Journal of the Fisheries Research Board of Canada,* 18, 1073-1124.

Tabata, S (1965), Variability of oceanographic conditions at Ocean Station "P" in the northeast Pacific Ocean. *Transactions of the Royal Society of Canada*, Series 4, 3, Section 3, 367-418.

Taylor, P.K (2002), Ocean exchanges with the atmosphere – did we learn anything during WOCE? *Paper presented at the conference*: "WOCE and Beyond", San Antonio, Texas, USA, 18-22 November, 2002.

Whitney, F.A., and H.J. Freeland (1999), Variability in upper-ocean water properties in the NE Pacific Ocean, *Deep-Sea Research II*, 46, 2351-2370.

Wong, A.P.S., G.C. Johnson, and W.B. Owens (2003), Delayed-Mode Calibration of Autonomous CTD Profiling Float Salinity Data by θ-S Climatology, *Journal of Atmospheric and Oceanic Technology*, 20, 308-318.

Chapter 3

An Examination of Mixed Layer Sensitivity in the Northeast Pacific Ocean from July 2001 – July 2005 using the General Ocean Turbulence Model and Argo data

3.1. Introduction

3.1.1 The Mixed Layer Depth in the Northeast Pacific Ocean.

The mixed layer (ML) lies at the surface of the ocean and has a homogenous temperature, salinity and density. Wind stress and outgoing heat fluxes (latent heat (LH), sensible heat (SH) and longwave radiation (LW)) add kinetic energy (a destabilizing effect) into the ML while freshwater and incoming heat fluxes (shortwave radiation (SW)) add potential energy (a stabilizing effect) into the ML (Thomson and Fine, 2003).

The depth of the ML is determined by the balance between kinetic and potential energy (Thomson and Fine, 2003). The mixed layer depth (MLD) varies regionally and can range from a few meters in the Gulf of Alaska in summer to more than 1000m in the Labrador Sea in winter (de Boyer Montegut, et al., 2004). The MLD also varies on a diurnal, seasonal and interannual basis (Thomson and Fine, 2003; de Boyer Montegut, et al., 2004) and much of the variability has been linked changes to atmospheric forcing (for example Tabata, 1961; Denman, 1973; Adamec and Elsberry, 1984; Large and Crawford, 1995; Alexander and Penland, 1996). Changes to the MLD affects biological productivity, for instance the subarctic region of the northeast Pacific Ocean (NEP) is light limited so a deeper ML would spread out the available light, thereby limiting primary productivity whereas the subtropical region is nutrient limited so a deeper ML would bring in new nutrients, thereby increasing primary productivity (Polovina, et al., 1995). The MLD in the NEP has undergone significant variability in recent years.

Ocean Station Papa (OSP, 50°N, 145°W; figure 3-1) is a station in the Gulf of Alaska along oceanographic Line P, a 1500 km line of 26 sampling stations that extends from the southern tip of Vancouver Island to OSP, where the temperature and salinity have been sampled at least twice per year since 1952. Since it has the longest dataset in the Gulf of Alaska, OSP has been used to represent oceanographic conditions for the region (Whitney and Freeland, 1999). An examination of the historical MLD at OSP to the mid-1990s showed that it varied from ~120m in the winter to ~40m in the summer (Whitney and Freeland, 1999) but in a later study (and using a different criterion to calculate the MLD), the average MLD ranged from 105m in the winter to 25m in the summer (Li, et al., 2005a). Other studies of the Gulf of Alaska have shown a MLD

36

shoaling trend (for example Polovina, et al., 1995; Freeland, et al., 1997; Freeland and Cummins, 2005; Li, et al., 2005b) over the past 50 years at a rate of 56 m per century (Freeland and Cummins, 2005) with the winters of 2002-03 and 2003-04 having the shallowest MLDs ever recorded (Freeland and Cummins, 2005). Conversely, the MLD in the subtropical gyre has been deepening (Polovina, et al., 1995). Several theories have emerged to explain this shoaling.

The first explanation of why the MLD is shoaling comes from the Pacific Decadal Oscillation (PDO), which is a mode of interdecadal climate variability that affects the sea surface temperature (SST), sea level pressure and wind strength and direction (Mantua and Hare, 2002). Changes to the wind stress affect Ekman pumping which impacts the pycnocline (Lagerloef, 1995). Recent studies have correlated PDO-induced climate changes with the depth of the pycnocline and have found that the PDO can explain 70-90% of the pycnocline variability over the past 50 years (Cummins and Lagerloef, 2002; Capotondi, et al., 2005) but from 2001-04, changes to the Ekman pumping can only explain 64% of the MLD variability (Li, et al., 2005b).

The second explanation for MLD variability comes from the occurrence of El Nino – Southern Oscillation (ENSO) events because they are often synonymous with shallow winter MLDs at OSP (Whitney and Welch, 2002; Freeland and Cummins, 2005). The effect of ENSO on the Gulf of Alaska can be broken into two phases, the earlier meteorological phase and the later oceanographic phase (Freeland, 2002). The meteorological phase begins at roughly the same time as the ENSO (Freeland, 2002) and is associated with decreased cloud cover (Overland, et al., 2001; Brown and Fu, 2000), latent heat fluxes (Brown and Fu, 2000) and wind speeds (Schwing, et al., 2002; Brown

37

and Fu, 2000). The oceanographic phase results from the northward propagation of Kelvin waves from the equatorial Pacific to latitudes of 40°N (Strub and James, 2002) to 50°N (Whitney and Freeland, 1999; Miller and Schneider, 2002) that are reflected into the NEP as Rossby waves and travel westward at depths of about 200-250m (White and Tabata, 1987) and speeds of 1.8 - 3.5 km/day (Miller and Schneider, 2002). Thus, Rossby waves would be expected to reach OSP roughly 1-3 years after leaving the west coast of North America, which occurs about 6 months after the Kelvin wave leaves the equator (Strub and James, 2002). Since a moderately strong ENSO occurred during the winter of 2002-03 (McPhaden, 2004), it is possible that it can explain the shallow MLD during this year, however no ENSO occurred during the winter of 2003-04.

A third hypothesis to explain the shoaling MLD at OSP comes from the observed temperature and salinity trends above the pycnocline, which are warming and freshening at a rate of 2 ± 1°C and 0.4 ± 0.3 psu per century (Freeland, et al., 1997), resulting in a density that is becoming 0.5 ± 0.2 kgm^{-3} lighter per century. Since there is no similar trend in the waters below the pycnocline (Freeland, et al., 1997), the density gradient between the surface and lower waters is strengthening, thereby making it more difficult for the MLD to deepen through the pycnocline. This explains the trend of MLD shoaling at OSP but does not specifically account for the anomalies seen during the winters of 2002-03 and 2003-04.

In addition to the long-term atmospheric and oceanographic processes, several events occurred over the past few years that have had the potential to affect the MLD. The first event was the appearance of a water mass at 100-150m along Line P, which was up to 2°C colder and 0.5 psu fresher than normal (Freeland, et al., 2003; Crawford, et al.,

38

2005). This water mass was first observed in the summer of 2002 and was still present, although weakened, in the summer of 2003 (Crawford, et al., 2005). It is believed to have been formed in the center of the Alaska gyre during the winter of 2001-02 from enhanced winter mixing (Freeland, et al., 2003; Churchister, et al., 2005) and was propagated southeastward through the following year (Crawford, et al., 2005; Churchister, et al., 2005). This cold anomaly would be expected to strengthen the vertical density gradient in the Gulf of Alaska. The second event (that was observed through Argo data) was the northward migration of the North Pacific Current (NPC) to 52°N along 145°W (which is about 7° - 12°N north of its normal position (Thomson, 1981)), from March – May 2002 (Freeland and Cummins, 2005). A better understanding of how these events affected the MLD in the northeast Pacific is necessary to explain the shallow MLD observed in the winters of 2002-03 and 2003-04.

3.1.2 General Circulation of the Northeast Pacific Ocean

The NPC transports up to 30 Sv relative to 2000 m (Roemmich and McCallister, 1989) and dominates the circulation of the NEP (figure 1). It bifurcates near 45°-50°N and 130°-150°W to form the northward flowing Alaska Current and the southward flowing California Current (Thomson, 1981). The Alaska (California) Current forms into the divergent (convergent) Alaska (subtropical) gyre that undergoes upwelling (downwelling) when strong winds increase the current transport. Strong wind stress in the NEP affects Ekman pumping 8-15 months later (Lagerloef, 1995; Li, et al., 2005b; Capotondi, et al., 2005) and since downwelling pushes down the pycnocline while upwelling pushes up the pycnocline, periods of strong wind stress should cause a deeper MLD in the subtropical gyre and a shallower MLD in the Alaska gyre 8-15 months later.

39

Within the region of the NPC is the subarctic frontal zone, which separates cold, fresh water to the north from warm, salty water to the south. The temperature and salinity difference in the upper 100m between these two regions can be as high as 6°C and 0.8 psu (Yuan and Talley, 1996). The region north of the subarctic front has a permanent halocline and a thermocline in summer when the surface waters warm (Tabata, 1961). The change in density over the change in temperature ($\delta\rho/\delta T$) is much greater in warm waters while the change in density over the change in salinity ($\delta\rho/\delta S$) is consistent throughout the world's oceans so the density calculation north (south) of the subarctic front is dominated by salinity (temperature) (Freeland, et al., 1997; Carmack, 2000).

In this study, the observed MLD based on Argo data was examined at 4 stations (3 in the Alaska gyre and 1 in the subtropical gyre). The atmospheric forcing for the same period from the NCEP/NCAR Reanalysis was analyzed and potential links between the forcing and the observed MLD are discussed. The 1-D General Ocean Turbulence Model (GOTM; Burchard, et al., 2005), was run at each station and issues of reproducing the observed ML variability was examined. Using GOTM, several experiments were then run to determine the sensitivity of the MLD to idealized changes in atmospheric forcing. Finally, the results from these sensitivity experiments were assessed to help understand the observed variability over 2001-05 and to try to relate it to the recent oceanographic events occurring in this region.

3.2. Data and Methods

3.2.1. Oceanographic data

Temperature and salinity data were taken from the Argo dataset (Gould, et al., 2004). Three stations in the Gulf of Alaska and one station in the subtropical gyre were

40

selected (figure 3-1). They were i) OSP on the southern edge of the Alaska gyre (50°N, 145°W) ii) station 16 along oceanographic Line P on the southeastern edge of the Alaska gyre (S16; 49°17N, 134°40W) iii) the center of the Alaska Gyre (CAG, 55°N, 145°W) and iv) the northern edge of the subtropical gyre (NSG, 40°N, 145°W). The study period in the Gulf of Alaska is from July 10, 2001 – July 20, 2005. In the subtropical gyre, floats releases were delayed so the data covers from March 10, 2002 – July 10, 2005. The coverage of Argo floats increased through the study period, from a density (density = number of floats/targeted number of floats where targeted number of floats is 1 per 300km) of 0.8 at OSP, 1.2 at S16, 1.0 at CAG and 0.2 at NSG in March 2002 (Freeland and Cummins, 2005) to 2.0 at OSP, S16 and CAG and 0.6 at NSG on November 16, 2005 (Freeland, 2005). An initial assessment of Argo data found a few extreme temperature readings in March 2004 (for example a temperature of 25°C at 480m) so the temperature and salinity profiles from those days were removed from our dataset. Data from within a 1000km radius of each station were interpolated to that station as outlined in Freeland and Cummins (2005).

3.2.2. Atmospheric Data and Conversions

Atmospheric input in the form of the daily mean of LH, SW, LW, SW, air temperature (T_a), and zonal (u) and meridional (v) wind speeds was taken from the NCEP/NCAR Reanalysis Project (Kalnay, et al., 1996). Values were linearly interpolated from the NCEP to our four stations of interest. Wind stress (τ_{ox}, τ_{oy}) was calculated using the formula (Stewart, 2005)

$$(\tau_{ox}, \tau_{oy}) = \rho_a C_D U_{10}(u, v) \qquad (3.2.2.1)$$

41

where ρ_a, the density of air, is 1.2 kgm^{-3}, U_{10}, the net wind speed at 10 meters above the sea surface was calculated from the NCEP derived wind speeds as,

$$U_{10} = \text{sqrt} (u^2 + v^2) \tag{3.2.2.2}$$

C_D, the drag coefficient, was calculated by

$$C_D = 0.934 \times 10^{-3} + 0.788 \times 10^{-4} U_{10} + 0.868 \times 10^{-4} \delta + -0.616 \times 10^{-5} U_{10}^2 +$$

$$-0.120 \times 10^{-5} \delta^2 + -0.214 \times 10^{-5} U_{10} \delta \tag{3.2.2.3}$$

and δ, the difference between the sea surface temperature (SST) and T_a, is

$$\delta = SST - T_a \tag{3.2.2.4}$$

To compare the atmospheric NCEP values between stations and seasons, the total heat flux (Q_{SF}) and wind speed (U_{10}) was averaged as Q_{AVG} and $\bar{U}$ and were examined during two seasons, winter, which was defined as September 16th to March 15th, and summer, from March 16th to September 15th. To give a relative comparison of seasons when the heat fluxes and wind speeds were especially strong, Q_{SF} was arbitrarily considered significant when it was stronger than −300 Wm^{-2} (200 Wm^{-2}) in with winter (summer) and U_{10} was considered significant when speeds greater than 18.0 m/s were reached

3.2.3. The General Ocean Turbulence Model

GOTM (Burchard, et al., 2005) is a 1-D ML model that calculates the vertical transport of heat, salt and momentum. The upper 250 m of the ocean was simulated using a vertical grid spacing of 1 m. Turbulence closure was based on the generic model (Umlauf and Burchard, 2003) because it has recently been adapted for oceanographic applications and has produced realistic results at OSP (Umlauf, et al., 2003). Initial experiments were run at OSP to determine the best parameters for calculating the MLD.

42

The MLD was calculated according to the turbulent kinetic energy (TKE) criteria

(Umlauf, et al., 2004):

$$k = q^2/2 \qquad (3.2.3.1)$$

where k is TKE and q is the velocity scale of turbulence that was used to calculate the

diffusivities of momentum (v_t) and heat (v'_t) (Umlauf, et al., 2004):

$$v_t = c_u k^{1/2} l, \quad v'_t = c_u' k^{1/2} l \qquad (3.2.3.2)$$

where c_u and c_u' are parameterized stability functions and l is a typical length scale whose

calculation is outlined in Umlauf and Burchard (2003). Using v_t and v'_t, the fluxes of

momentum and heat were calculated as (Umlauf, et al., 2004):

$$(u',w') = -v_t \, \delta u/\delta z, \quad (v',w') = -v_t \, \delta v/\delta z, \quad (w',\theta') = -v_t' \, \delta\theta/\delta z \qquad (3.2.3.3)$$

where u and v are the horizontal velocity in the directions x and y, w is the vertical

velocity in the direction z and θ is the potential temperature. The MLD was defined as the

depth when the k was less than the critical value of 1.0×10^{-5} m^{2}s^{-2}. Note that the

turbulent transport of salt was assumed to be identical to heat so that in the salinity

equation, the sum of the turbulent transport terms (D_S) (Umlauf, et al., 2004):

$$D_S = \delta/\delta z \, ((v'_t + v^S) \, \delta S/\delta z) \qquad (3.2.3.4)$$

is based on the turbulent diffusivity of heat and the molecular diffusivity of salt (v^S).

In addition, the results were more realistic when the internal wave model (Large, et al.,

1994) was implemented and when the background diffusivity was set at 10^{-5} m^{2}s^{-1} (as

suggested by Denman and Pena, 1999).

3.2.4. Sensitivity Experiments

Several experiments were run with GOTM to determine whether some form of

restoring was necessary to maintain the base model state and to prevent model drift.

43

When restoring was not used in the Gulf of Alaska, the upper 100 m became unrealistically warm after 1 year (up to 12°C warmer in the summer and up to 2°C warmer in the winter) and salty (up to 0.2 psu saltier year round). At NSG with 1 year restoring, the upper 100m became up to 5°C colder and 1.0 psu fresher in winter and up to 0.2 psu fresher in summer. The sensitivity experiments were run initially with 30 day restoring that proved too strong, thereby asserting too much control on the MLD and disallowing the true impact of the altered atmospheric forcing to be seen. Thus, 3 month restoring was used at the risk of the surface waters becoming too warm (cold) and salty (fresh) in the Gulf of Alaska (subtropical gyre). Since density variation north (south) of the subarctic front is controlled by salinity (temperature) (Freeland, et al., 1997) and the salinity (temperature) changes were minimal compared to temperature (salinity), the changes to temperature and salinity in the water column would not detrimentally affect our MLD calculation.

The experiments that were run at each station were doubling and zeroing the wind speed to represent the winds associated with strong storms and no storms, doubling and zeroing the outgoing heat fluxes to mimic a significant heat loss and no heat loss from the ocean to the atmosphere and doubling and zeroing the incoming heat fluxes to understand how cloud cover affects the MLD. Initial trials found that the ML cycle can be broken into four different seasons – summer-winter transition when the MLD is deepening, winter when the MLD is deepest, winter-summer transition when the MLD is shoaling and summer when the MLD is shallowest. An objective criterion was developed to determine the start and end of each season.

3.2.5. Criterion to determine the seasonality of the MLD

44

First, the two-week running mean of the MLD was calculated to smooth out daily variability. Second, the daily derivative of MLD was calculated from the two-week running mean. Third, the two-week running mean of the daily derivative of the MLD was calculated because it was found that additional smoothing was needed to discern between normal daily and weekly MLD variability and transition periods.

To confirm the exact start date of the transition, one must examine the two-week running mean of the daily derivative and define the beginning of the summer-winter (winter-summer) transition as the period when the derivative is negative (positive) for a period of time in the fall (spring). If this value is negative (positive) for at least 14 (10) days at the end of summer (winter), then this is the start of the summer-winter (winter-summer) transition. The summer-winter (winter-summer) transition ends when there have been at least 14 (10) days in a row that are either positive (negative), have a value that is less than -0.1 (greater than 0.1), or both. When the summer-winter (winter-summer) transition ends, winter (summer) begins. Generally, the summer-winter transition lasts longer because it deepens at a slower rate than the winter-summer transition shoals, so more time is needed when the daily derivative is minimal before the end of transition is determined.

Once the dates of the transitions were determined, the average MLD during each winter and summer season was calculated and compared to the average MLD from a control experiment (where the MLD that was calculated from the observed atmospheric forcing and 3 months restoring). It was found that the observed length of summer and winter sometimes varied from the modeled and we feel that this is because a smooth transition tends to last longer than a step-like transition and since the modeled MLD was

45

usually smoother than the observed, the modeled MLD tended to have shorter summer and winters than what was observed. However, we felt a criterion that automatically calculated the length of each season was necessary and since the point of this exercise was to compare sensitivity experiments with 3 months restoring to the control MLD with 3 months restoring, we do not feel that this criterion had a significant effect on the results.

3.3. Results

3.3.1. Observed Atmospheric Conditions

Compared to other stations, OSP had the weakest winter Q_{AVG} (defined in section 3.2.2) and the strongest summer Q_{AVG}, which was caused by strong incoming heat fluxes and weak outgoing heat fluxes while CAG had the weakest summer Q_{AVG} and the strongest winter Q_{AVG}, which was caused by strong outgoing heat fluxes and weak incoming heat fluxes (figure 3-2, table 3-1). All stations had a net heat gain into the ocean over the study period with OSP having the greatest net heat gain at 33.6 Wm^{-2} and CAG having the lowest at 0.15 Wm^{-2}.

When examining the interannual variability at OSP, the winter of 2001-02 had the strongest average Q_{AVG} at –55.9Wm^{-2} while the winter of 2003-04 had the strongest daily Q_{SF} at -525.8Wm^{-2} and the winters of 2001-02, 2003-04 and 2004-05 each had 4 days when Q_{SF} was stronger than –300Wm^{-2}. The summer of 2002 had the highest Q_{AVG} at 120.6Wm^{-2}. At S16, the winter of 2001-02 had the strongest Q_{AVG} at –60.1Wm^{-2} but the winter of 2004-05 had the strongest Q_{SF} at –476.3Wm^{-2} and the most number of days, 6, when Q_{SF} was stronger than –300Wm^{-2}. The summer of 2002 had the highest Q_{AVG} at 112.56Wm^{-2}. At CAG, the winter of 2003-04 had the strongest Q_{AVG} at –102.4Wm^{-2}, the strongest daily Q_{SF} at –649.7Wm^{-2} and the most number of days, 13, when Q_{SF} was

46

stronger than -300Wm^{-2}. The summer Q_{AVG} were quite similar during all years but 2003 had a slightly higher average at 95.5Wm^{-2}. At NSG, the winter of 2002-03 had the strongest Q_{AVG} at -67.1Wm^{-2}, the strongest daily Q_{SF} value at -613.5Wm^{-2} and the most number of days, 12, when Q_{SF} was stronger than -300Wm^{-2}. The Q_{AVG} were similar during all summers but 2003 had the greatest Q_{AVG} at 111.0Wm^{-2}.

Overall, OSP had the strongest $\bar{U}$ (defined in section 2.2) except in the summer of 2002 and the winter of 2002-03 (table 3-2). S16 and CAG had the strongest $\bar{U}$ and during the summer of 2002 while NSG had the strongest $\bar{U}$ during the winter of 2002-03. The weakest average wind throughout the study was seen at NSG, with a value of 7.39 m/s.

At OSP, the winter of 2004-05 had the strongest $\bar{U}$ at 9.6m/s while the winter of 2001-02 had the highest U_{10} with a measurement of 18.8m/s. The summer of 2004 had the highest $\bar{U}$ with a value of 7.03m/s. At S16, the winter of 2003-04 had the strongest $\bar{U}$ with a value of 8.8m/s while the winter of 2001-02 had the highest daily value of U_{10} at 20.0m/s. The summer of 2003 had the strongest $\bar{U}$ with a value of 6.8m/s. At CAG, the winter of 2004-05 had the highest $\bar{U}$ at 9.0m/s and the highest U_{10} at 19.8m/s. The summer of 2002 had the weakest $\bar{U}$ with a value of 6.21m/s. At NSG, the winter of 2002-03 had the highest $\bar{U}$ at a value of 9.2m/s and the highest U_{10} at 19.9m/s. The summer of 2004 had the highest $\bar{U}$ with a value of 6.5m/s.

3.3.2. The Observed MLD

The observed MLD was determined by running GOTM with 1 second restoring (figure 3-3). We use this approach so we may consistently report the MLD from both the observations and the model sensitivity studies using the same TKE criterion. Winter and summer were defined using the criterion outlined in section 2.5.

47

At OSP, the winter of 2001-02 had the deepest MLD, with a maximum MLD of -108m, an average of -50.7m and 6 days when the MLD was greater than 100m. In addition, there was an abrupt shoaling of the MLD at the end of January 2002, so although the MLD was deepest, the winter was also shortest. The winter of 2002-03 had the shallowest MLD at OSP, with a maximum of -66m (which is similar to the value of -70m observed by Freeland and Cummins, 2005) and an average of -32.9m. At S16, the winter of 2003-04 had the deepest MLD, with a maximum of -103m, an average of -54.6 m and 3 days when the MLD was greater than -100m. The winter of 2002-03 had the shallowest MLD, with a maximum of -60m and an average of -37.6m. At CAG, the winter of 2001-02 had the deepest average MLD at -43.5m but the winter of 2003-04 had the maximum winter MLD at -105m and 9 days when the MLD was greater than -100m. The winter of 2004-05 had the shallowest maximum MLD at -64m and the shallowest average MLD at -31.2m. At NSG, the winter of 2004-05 had the deepest winter MLD with a maximum MLD of -133m, an average MLD of -58.7m and 11 days when the MLD was greater than -100m. The winter of 2003-04 had the shallowest MLD with a maximum of -79m, an average of -38.8m and no days when the MLD was greater than -100m.

3.3.3. Modeled MLD compared to observed MLD

A comparison between the average modelled MLD (MLDmod) with 3 months restoring and the average observed MLD (MLDobs) with 1 second restoring (table 3-3, figure 3-3) found that the MLDmod was always deeper than the MLDobs in the winter by up to 51.5m. In summer, the MLDmod was usually shallower than the MLDobs by up to 3m. In addition, the number of days in winter was always less for MLDmod than

MLDobs while the number of days in summer was closer (table 3-4). We explain this discrepancy by the fact that the model smoothes out a lot of the step-like behaviour of the observed MLD and since the criterion to determine the seasonality of the MLD bases the start and end of the seasons on sudden changes to the MLD, the smoothness of the modeled MLD results in a longer summer-winter transition and a shorter winter. The difference between MLDmod and MLDobs (MLDdif = MLDmod - MLDobs) was calculated.

Overall, the greatest MLDdif throughout the study period was seen at CAG with an average of -12.6m and the smallest MLDdif was seen at NSG with an average of -2.1 m. At OSP, the greatest difference between MLDdif was seen in 2001-02, where the MLDmod was 42.6m deeper than the MLDobs. This can be explained be the shortness of the MLDmod winter calculated from the criterion, which was only 9 days long, while the MLDobs winter was 104 days long. Besides the winter of 2001-02, the winter of 2004-05 had the greatest value of MLDdif at -24.3m. At S16, the greatest MLDdif was seen during the winter of 2001-02, where the MLDmod was 32.0m deeper than the MLDobs. At CAG, the winter of 2001-02 had the greatest MLDdif, where the MLDmod was 51.5m deeper than MLDobs. Again, this can be explained by the shortness of the MLDmod winter, which was only 1 day whereas the MLDobs winter was 114 days. At NSG, the winter of 2002-03 had the highest value of MLDdif where the MLDmod was 16.0m deeper than MLDobs.

Some of the variability in MLDdif can be explained by horizontal advection that would be expected to affect how well the model calculates the MLD. A recent paper (Chapter 2) that estimated advection by the monthly change of heat content at the same

49

stations showed that the greatest advection at OSP and S16 was in the winter of 2004-05, at CAG was in the winters of 2004-05 and at NSG there were periods of strong advection throughout the study period. Since the MLDdif was greatest at OSP during the winter of 2004-05, we suggest part of the reason that the 1-D model performed poorly was because it did not compensate for the horizontal transport during this period. However, the greatest MLDdif at S16 was in the winter of 2001-02, when there was little advection, while the smallest MLDdif was during the winter of 2004-05 despite strong advection. The MLDdif at CAG was high throughout the winters of the study period even though this station that experienced the least amount of advection. Finally, the MLDdif was the smallest at NSG despite strong advection. Thus, another mechanism must caused the MLDdif to be so big at CAG and small at NSG.

We suggest that beyond advection, the discrepancies between the observed and modeled MLD can be explained by the fact that this version of GOTM calculates the turbulent diffusivity so that it is based on heat, not buoyancy, fluxes and there is no direct forcing of evaporation minus precipitation (Burchard, et al., 2005). Although the turbulent diffusivity for the temperature and salinity flux should be similar (Mellor, 1996), if there was a difference and the salinity flux was not calculated separately then it would likely affect the density calculation in beta oceans. A comparison of the difference between modeled and observed salinity (figure 3-5) and temperature (figure 3-6) at CAG and NSG, the stations with the greatest and smallest MLDdif is displayed. At CAG, with the exception of the winter of 2001-02, the model calculated salinity so that the upper 100m was up to 0.2 psu saltier than the observed salinity with the greatest difference in the fall while temperature in the summer was up to 5°C warmer above the MLD and 4°C

50

colder below the MLD. At NSG, with the exception of the summer of 2004, the modeled salinity in the upper 100m was up to 0.4 psu fresher than the observed salinity, with the greatest difference in the fall while the temperature in summer was up to 5°C warmer above the MLD and 4°C below the MLD. Thus at CAG, a small difference in the modeled salinity had a great affect on the modeled density and MLD whereas at NSG a large difference in both the modeled salinity and temperature did not have a large affect on the density and MLD because GOTM algorithms are more suited to this location. This suggests that since NSG underwent significant advection much more frequently than CAG (Chapter 2), the inaccurate calculation of turbulent diffusivity had a greater impact on the MLD than using a 1-D model in region that undergoes advection.

Despite the inconsistencies between stations when calculating the MLDmod, we do not feel that the results of this study are compromised. Since both the control MLD and the sensitivity experiments were run with 3 months restoring, the comparison between these should reflect how changing the atmospheric forcing affects the MLDmod, not how the MLDmod performs compared to the MLDobs.

3.3.4. GOTM Sensitivity Experiments

The results from the sensitivity experiments are displayed as the average summer and winter MLD at each station in table 5 and as the difference between the controlled MLD and the MLD with manipulated atmospheric forcing in figures 3-7 (winter) and 3-8 (summer).

Throughout the study period, the MLD at OSP increased the most (to an average MLD of -67.6m) when SW was zeroed and decreased the most (to an average MLD of -12.4m) when the wind speed was zeroed. During the winter the MLD was the most

51

sensitive to doubling the wind speed, causing an average deepening of 39.7m whereas during the summer the MLD was the most sensitive to zeroing the SW causing an average deepening of 33.5m At S16, the MLD increased the most (to an average MLD of -72.0m) when SW was zeroed and decreased the most (to an average MLD of -15.1m) when the outgoing heat fluxes were zeroed. During the winter, the MLD was the most sensitive to zeroing the outgoing heat fluxes, with average shoaling of 39.2m while during the summer, the MLD was the most sensitive to zeroing the SW, with an average deepening of 34.2m. At CAG, the MLD increased the most (to an average MLD of -72.1 m) when the winds were doubled and decreased the most (to an average MLD of -17.0 m) when the outgoing heat fluxes were zeroed. During the winter, the MLD was the most sensitive to zeroing the outgoing heat fluxes, with average shoaling of 49.4m while during the summer, the MLD was the most sensitive to doubling the wind speed, with an average deepening of 33.2m. At NSG, the MLD increased the most (to an average MLD of -88.0m) when SW was zeroed and decreased the most (to an average MLD of -13.9m) when the outgoing heat fluxes were zeroed. The MLD was the most sensitive to zeroing the SW in the winter and summer, with an average deepening of 57.5m and 40.2m respectively.

To examine which stations had the greatest reaction to each experiment, we again compared the average MLD change at each station in winter and summer. Overall, the MLD at NSG was the most sensitive to doubling the wind speed in the winter with an average deepening of 47.7m while CAG was the most sensitive in the summer with an average deepening of 33.2m. The MLD at OSP was the most sensitive to zeroing the wind speed in winter with an average shoaling of 32.8m while NSG was the most

52

sensitive in summer with an average MLD shoaling of 12.4m. The result from OSP makes sense since it had the strongest winter winds, however NSG had the weakest summer winds but strong winter winds, suggesting that when the winds were zeroed, other processes such as Ekman pumping were also reduced. The MLD at NSG was the most sensitive to doubling the outgoing heat fluxes in the winter with an average deepening of 36.8m per year while S16 was the most sensitive in the summer with an average deepening of 8.2m per summer. It would be thought that CAG would be the most sensitive to increasing the outgoing heat fluxes year round since they dominated most in the winter and summer so another mechanism must have prevented the MLD at CAG from deepening when the outgoing heat fluxes were doubled. The MLD at CAG shoaled the most when the outgoing heat fluxes were zeroed, with an average shoaling of 49.4m while in the summer, the MLD at NSG was the most sensitive, with an average decrease of 5.2m per summer. The MLD at NSG was the most sensitive to doubling the SW during winter and summer with the average MLD shoaling by 35.4m and 8.0m respectively. Similarly, the MLD at NSG was the most sensitive to zeroing the SW during winter and summer with the average deepening by 57.5m and 40.2m respectively. We would expect NSG to be the most sensitive to SW because although the summer Q_{AVG} are greater at OSP than NSG, the general period when Q_{AVG} was positive at NSG, from February to October, is 1 month longer than the period at OSP that is from March to October.

3.4. Discussion

3.4.1. How the 2002-03 ENSO Affected the MLD

The 2002-03 ENSO was a mid-strength event (it had a value of 1.1 on NOAA-CIRES's multivariate ENSO index from the Climate Diagnostic Center at the University

of Colorado at Boulder) that peaked in January 2003 (McPhaden, 2004) and followed 3-4 years of La Nina conditions. The response of ENSO at the different stations depends on several factors. Flatau, et al. (2000) suggested that the NPC is the division between positive (negative) SST anomalies in the Alaska Gyre (subtropical gyre). During 2002-03, the most positive SST anomaly of 3°C was observed near OSP while S16, CAG and NSG had anomalies of 2°C, 2°C and 1°C respectively (Murphee, et al., 2003). Thus, although NSG was south of the NPC, the SST still responded as a weak subarctic station to the SST anomaly induced by the 2002-03 ENSO. However, differences in the outgoing heat fluxes and wind speeds between the subarctic and subtropical stations (tables 3-1 and 3-2) show that OSP, S16 and CAG had the weakest atmospheric forcing while NSG the strongest during the ENSO. Thus, although the SST at NSG responded as a subarctic station, the atmospheric forcing did not.

At the end of January of 2002, the wind speeds at OSP abruptly decreased, which could have been an early response to the initial meteorological phase of the ENSO, and could have caused the subsequent shoaling of the MLD that was observed at OSP (figure 3-3a). If true, it is odd that the MLD at OSP responded so dramatically to the average wind speeds of 10.8m/s, 9.3m/s and 8.2m/s in January, February and March of 2002 because during the strong ENSO of 1997-98 (a value of 2 on the NOAA-CIRES multivariate ENSO index) the average wind speeds were 6.0m/s, 5.0m/s and 6.3m/s in January, February and March of 1997 (Brown and Fu, 2000) but the MLD did not shoal early (Whitney and Welch, 2002). Also, since this early shoaling was not observed at other stations and the meteorological phase of ENSO was region-wide, it is unlikely that ENSO caused the early transition at OSP.

54

As the ENSO progressed into the winter of 2002-03, there was an observed decrease in the outgoing heat fluxes and wind speeds (tables 3-1 and 3-2) at all stations in the Gulf of Alaska. These resulted in a decreased MLD, with the shallowest seen at OSP (figure 3-3, table 3-3). The MLD in the Gulf of Alaska responded differently to the reduced forces, with OSP being more sensitive to changes to the wind speed and S16 and CAG being more sensitive to changes to the outgoing heat fluxes (figure 3-7). In addition, the MLD was not able to deepen more than 38.8m at OSP, 30.4m at SEAG and 22.7m at CAG when the weak atmospheric forcing was corrected, suggesting that some process beyond the ENSO was preventing the MLD from deepening past 100m. At NSG (figure 3-7d) the MLD at this station was deepest during the winter of 2002-03 of the years observed, which can be explained by the strong outgoing heat fluxes (figure 3-2d) and wind speeds (table 3-2). Interestingly, results show that the MLD at NSG was very sensitive to zeroing the SW, suggesting that the decreased cloud cover associated with El Nino also affected that southern station.

3.4.2. How the 2002 subsurface cold water anomaly affected the MLD

The abnormally cold, fresh water, which was found at depths of about 50 – 150 m along Line P in the summer of 2002 (Freeland, et al., 2003; Crawford, et al., 2005) furthered stratification by increasing the density gradient between surface and subsurface waters. It was still present, albeit weakened, under OSP and S16 in the summer of 2003 (Crawford, et al., 2005). The cold anomaly explains why the MLD during the winter of 2002-03 was so shallow and was prevented from deepening past 100m even when strong wind speeds and outgoing heat fluxes and weak SW was applied. This cold water anomaly was not present during the ENSO of 1982-83 and 1997-98 (Robert, 2005),

55

explaining why the MLD during those winters did not shoal to the same extent that the MLD of 2002-03 did. Thus the second mechanism that caused the MLD shoaling during the winter of 2002-03 at OSP and S16 was the subsurface cold water mass.

3.4.3. How the migration of the NPC affected the MLD

The NPC migrated to 52°N at 145°W where it resided from March – May 2002, up to 12° further north than what was previously thought to be its most northerly range (Freeland and Cummins, 2005), thereby changing the environment of OSP from one that was inside the Alaska Gyre to one that was within the NPC. By mid-2003, the current had migrated back to the latitude of 40°- 42°N at 145°W. Despite this flow through OSP, a recent study (Chapter 2) found that there was no significant change in the heat content from advection during this period, suggesting that the NPC did not have as great an affect on OSP as would be expected. However, the advection that did occur resulted in a net loss of heat from OSP, suggesting that either the NPC transported cold water to OSP or pushed heat away from OSP. Either way, we would expect that the heat loss would make the water denser, thereby increasing the MLD, yet the MLD shoaled abruptly at the end of January 2002, when the outer edges of the NPC would be expected to reach OSP. Thus, it is possible that change in water properties from the passage of the NPC at OSP caused the early winter shoaling of 2001-02.

3.4.4. An explanation for the variable MLD seen during the winters of 2003-04 and 2004-05

Results from this study indicate that the MLD during the winters of 2003-04 and 2004-05 was unusual in the Gulf of Alaska because although the atmospheric forcing was high (figures 3-2), the MLD was still shallow (figure 3-3), with the maximum winter

56

MLD well below normal (Whitney and Freeland, 1999; Li, et al., 2005a). In addition, the winter of 2004-05 was unusually long with both a longer period when the outgoing heat fluxes were dominant (figure 3-2) and a longer time when the MLD was in winter-mode.

Observations from the February 2004 Line P cruise (Robert, 2005) show that there was an anomalously cold, salty water mass at about 100 – 150m along Line P above which the water was anomalously warm and fresh. Thus, another strong density gradient was present that prevented the MLD from deepening in the winter of 2003-04. Had the winds from the winter of 2002-03 been strong then upwelling from Ekman pumping could explain the gradient, however the winds were abnormally weak. As with the previous cold-water anomaly seen during the winter of 2002-03, the MLD at CAG was the least affected, indicating that this anomaly was not basin-wide.

The water along Line P during February 2005 was anomalously warm and fresh through the entire water column (Robert, 2005), explaining the strong outgoing heat fluxes that lasted throughout the winter. However, the water properties do not account for why the MLD during the winter of 2005 was so shallow because if anything, it would be expected that the smaller density gradient would allow the MLD to deepen further. In addition, an examination of the same four stations showed that OSP and NSG experienced a large advection of heat during this winter, which brought large changes in the heat content (Chapter 2).

3.5. Conclusions

The observed winter MLD was deepest at stations in the Gulf of Alaska during the winter of 2001-02 and the shallowest in the winter of 2002-03. At NSG, the winter MLD was deepest during 2004-05 and shallowest during 2003-04. Our analyses show

that the strength of atmospheric forcing in the form of wind speed and surface heat fluxes can explain some of the MLD variability in the NEP. Of the four stations studied, the incoming heat fluxes and wind speeds were strongest at OSP whereas the outgoing heat fluxes were strongest at CAG. Overall, the MLD at OSP was the most sensitive to changing the wind speeds in the winter and SW in the summer, the MLD at S16 was the most sensitive to changing the outgoing heat fluxes in the winter and SW in the summer, the MLD at CAG was the most sensitive to changing the outgoing heat fluxes in the winter and the wind speed in the summer and the MLD at NSG was the most sensitive to changing the SW in both the winter and the summer. However, the MLD did not respond the same way to these experiments each year and anomalous atmospheric and oceanographic events can explain some of the MLD variability. The decreased (increased) outgoing heat fluxes and winds in the Gulf of Alaska (subtropical gyre) during the 2002-03 ENSO can partially explain why the MLD at OSP, S16 and CAG (NSG) was so shallow (deep). In addition to ENSO, the subsurface cold water mass observed along Line P from the summer of 2002 to the summer of 2003 created a large density gradient that prevented the MLD from deepening further. The northward migration of the NPC observed in early 2002 could have caused the MLD to shoal in late January 2002. An anomalous cold, salty water mass that resided around 100–150m along Line P in the winter of 2003-04 separated the warm, fresh surface waters from the bottom water. Again, we believe that the strong density gradient created by this water mass prevented the MLD from deepening to a level that the relatively strong atmospheric forcing would suggest, resulting in a shallow MLD. The water column along Line P in the winter of 2004-05 was anomalously warm and fresh, however despite strong

58

atmospheric forcing and a weak density gradient, the MLD was very shallow throughout the Gulf of Alaska.

We feel that one of the most important results from our study is that 1-D mixed layer models, where the turbulence diffusivities are calculated only by temperature and not salinity fluxes, are better at estimating the MLD in alpha oceans, where temperature dominates the density equation than in beta oceans, where salinity dominates the density equation.

The average winter MLD in the Gulf of Alaska continues to be shallower than the historical average and this study clearly shows that although atmospheric forcing has a lot of control on the MLD, oceanographic events also influence it. Further study of the MLD in the Gulf of Alaska, both in time and space, is necessary to gain a better understanding of the underlying causes behind the continued shoaling.
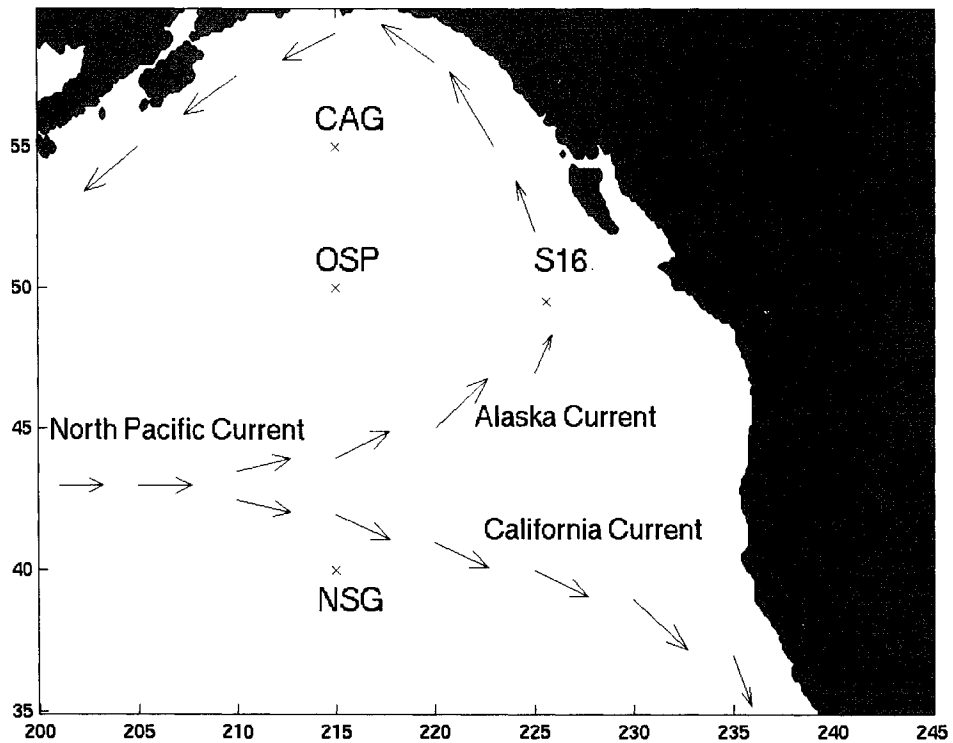
Figure 3-1: A map of the North Pacific Ocean with surface currents and labeled stations.

Table 3-1: A comparison of the winter and summer Q_{AVG} (Wm^{-2}) with standard deviation (n=183) and average Q over study period with standard deviation (n=1471) at the four stations. Negative values indicate that there is a heat loss from the ocean.

	OSP	S16	CAG	NSG
Winter 2001-02	-55.9 ± 97.9	-60.1 ± 81.8	-100.7 ± 109.1	-47.2 ± 113.1
Summer 2002	120.6 ± 62.5	112.6 ± 64.6	93.5 ± 61.9	109.6 ± 69.7
Winter 2002-03	-24.3 ± 85.9	-39.2 ± 87.4	-60.3 ± 87.9	-67.1 ± 142.4
Summer 2003	109.7 ± 65.8	96.5 ± 74.6	95.5 ± 71.3	111.0 ± 74.3
Winter 2003-04	-49.6 ± 101.0	-55.8 ± 99.4	-102.4 ± 127.8	-59.3 ± 139.5
Summer 2004	117.2 ± 64.7	101.5 ± 64.4	94.0 ± 79.7	108.4 ± 81.1
Winter 2004-05	-47.4 ± 101.0	-57.0 ± 112.9	-83.9 ± 113.1	-63.9 ± 112.6
Average 2001-05	33.6 ± 115.0	24.8 ± 114.1	0.15 ± 129.2	23.1 ± 134.4

60
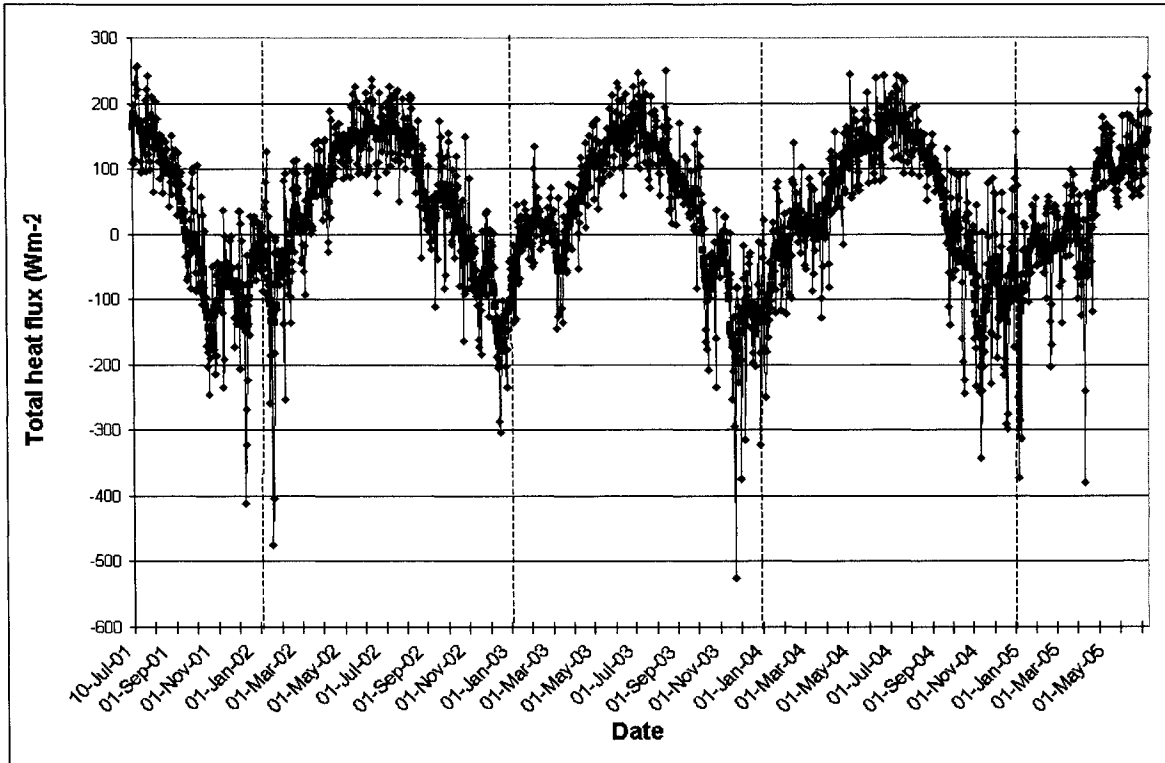
Figure 3-2a: The total heat flux at OSP for July 10, 2001–June 30, 2005 from NCEP. Blue lines represent daily-calculated total heat flux and pink lines represent 2-week running mean of total heat flux. Vertical dashed lines intersect on January 1st of every year.

Figure 3-2b: As in figure 3-2a except at S16

61

Figure 3-2c: As in figure 3-2a except at CAG
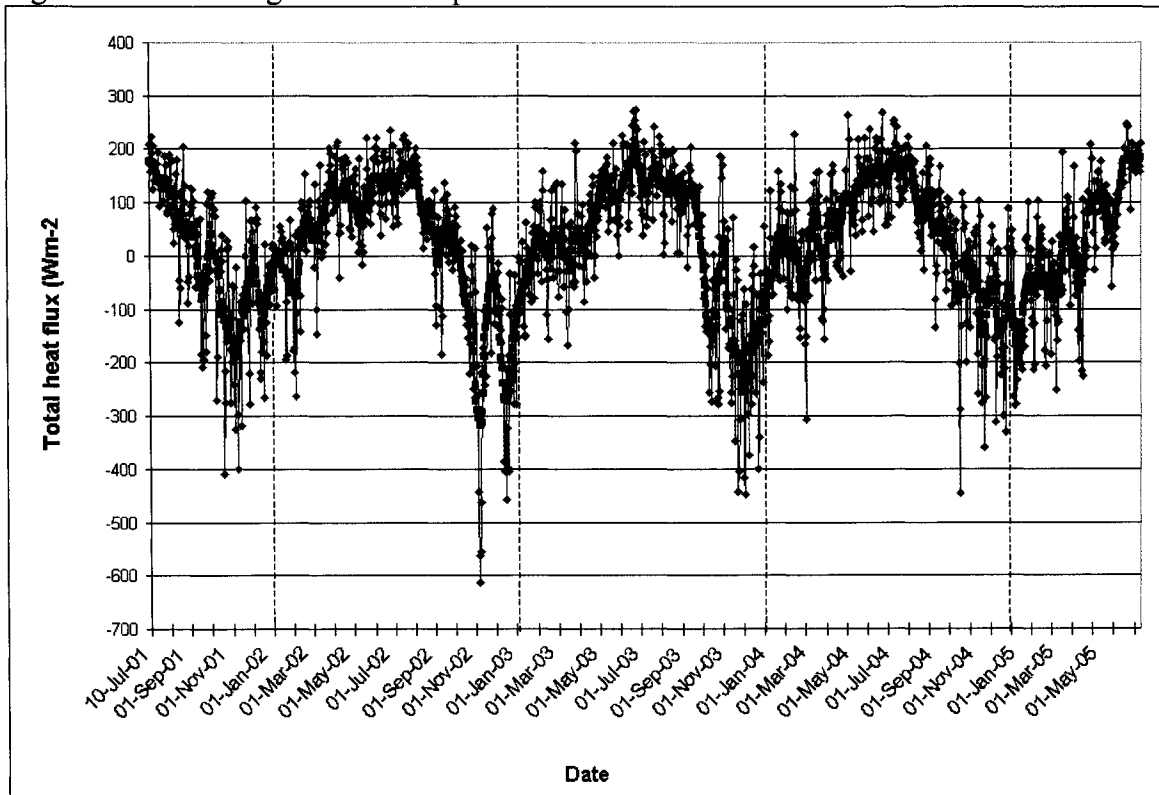
Figure 3-2d: As in figure 3-2a except at NSG

62

Table 3-2: A comparison of the winter and summer Ū (m/s) at the four stations with standard deviation (n=183).

	OSP	S16	CAG	NSG
Winter 2001-02	9.09 ± 3.8	8.54 ± 3.7	8.71 ± 3.9	8.05 ± 3.5
Summer 2002	5.99 ± 3.0	6.21 ± 2.9	6.21 ± 2.9	5.92 ± 2.6
Winter 2002-03	8.26 ± 3.4	7.85 ± 3.3	8.27 ± 3.4	9.23 ± 3.6
Summer 2003	6.98 ± 3.3	6.80 ± 2.9	6.42 ± 2.9	6.48 ± 3.0
Winter 2003-04	9.14 ± 3.8	8.76 ± 3.5	8.55 ± 3.7	8.62 ± 3.5
Summer 2004	7.03 ± 3.3	6.46 ± 2.8	6.52 ± 3.1	6.52 ± 3.3
Winter 2004-05	9.58 ± 3.8	8.68 ± 3.6	9.01 ± 3.8	7.92 ± 3.4
Average 2001-05	7.96 ± 3.7	7.47 ± 3.4	7.42 ± 3.6	7.39 ± 3.5

Table 3-3: A comparison of the average observed winter and summer MLD (m) at the four stations with standard deviation (n= length of season as in table 3-5) and the average MLD over the study period with the standard deviation (n=1471 for OSP, SEAG and CAG, n=1228 for NSG). Negative values represent measurement from sea surface, where MLD = 0m

	OSP	S16	CAG	NSG
Winter 2001-02	-50.7 ± 18.7	-46.5 ± 18.7	-43.5 ± 16.2	-
Summer 2002	-11.8 ± 6.15	-14.9 ± 9.7	-10.2 ± 6.2	-15.5 ± 7.4
Winter 2002-03	-33.1 ± 14.4	-37.6 ± 12.3	-34.2 ± 17.4	-52.1 ± 20.5
Summer 2003	-13.9 ± 7.0	-14.5 ± 7.6	-12.9 ± 6.4	-12.1 ± 7.2
Winter 2003-04	-37.4 ± 16.8	-56.6 ± 19.8	-42.5 ± 23.5	-38.8 ± 18.0
Summer 2004	-11.1 ± 8.0	-11.1 ± 7.0	-9.6 ± 5.4	-15.6 ± 9.5
Winter 2004-05	-31.3 ± 15.9	-43.0 ± 21.3	-31.2 ± 12.2	-58.7 ± 33.6
Average 2001-05	-27.2 ± 18.4	-28.9 ± 19.8	-26.1 ± 19.7	-32.3 ± 24.6
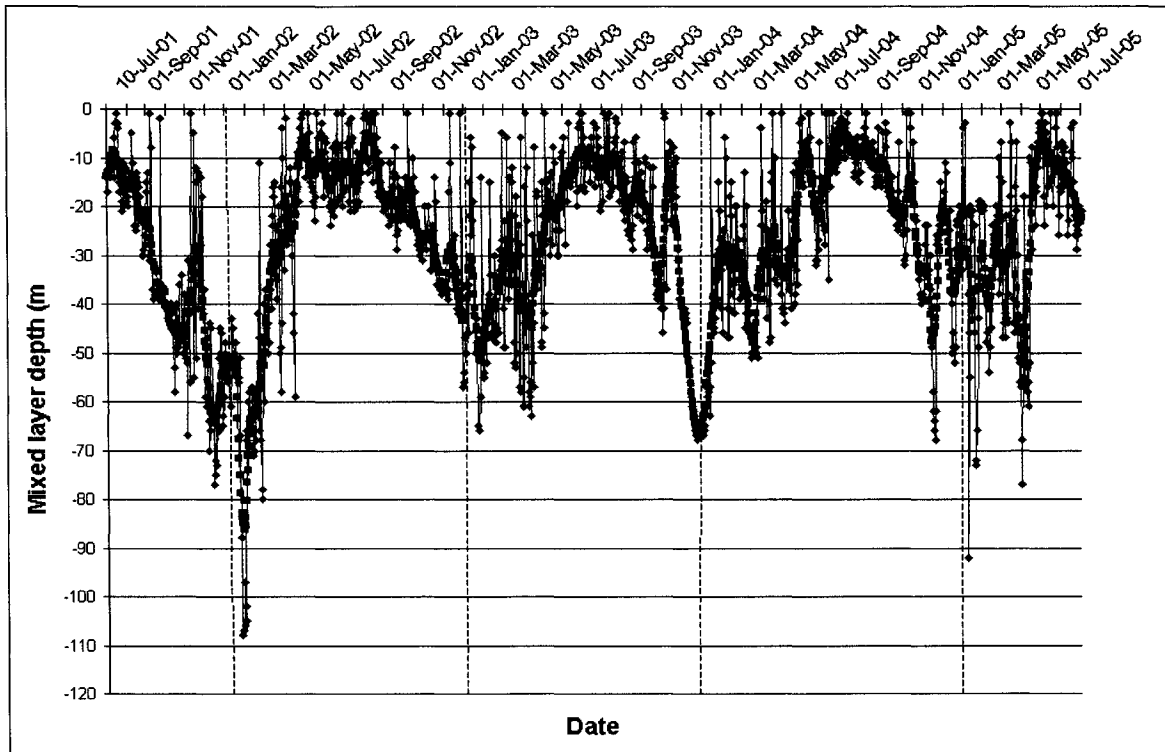
Figure 3-3a: Observed MLD at OSP using the GOTM TKE criterion (with 1 second restoring). Blue line represents the MLD and pink line represents 2-week running mean of MLD. Vertical dashed lines intersect on January 1st of every year.
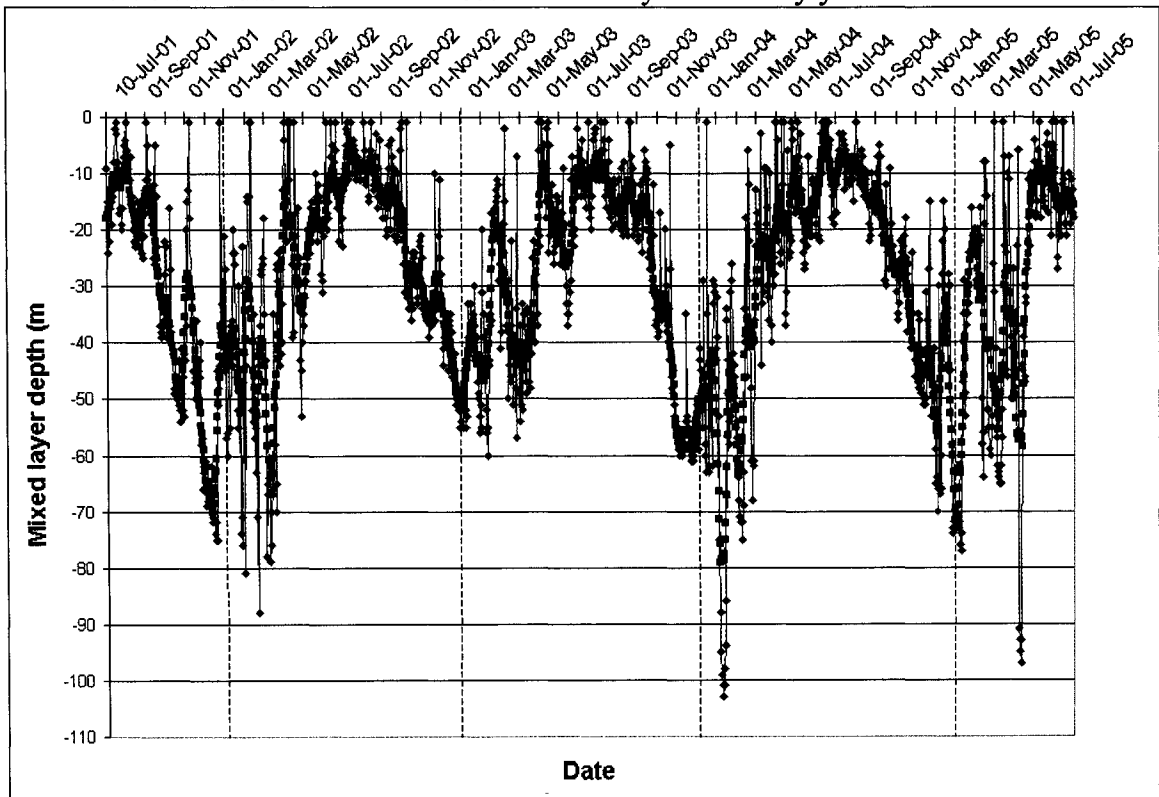
Figure 3-3b: As in figure 3-3a except at S16.

64
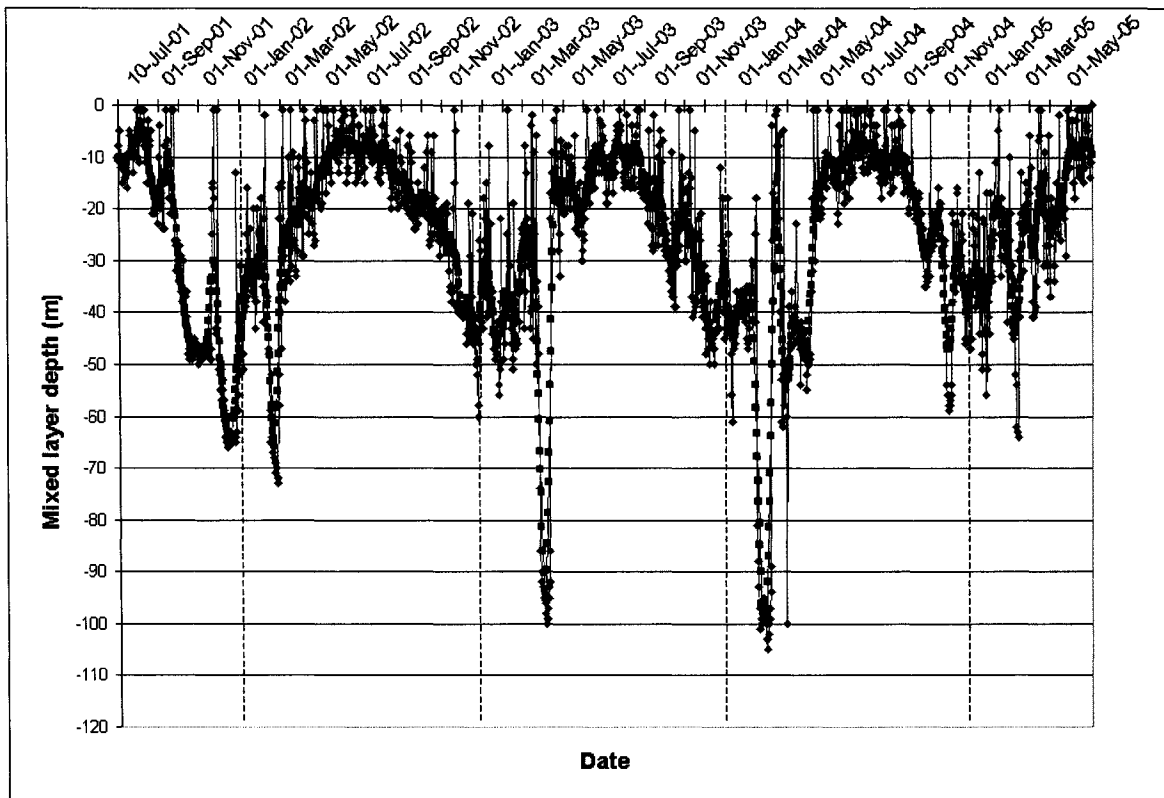
Figure 3-3c: As in figure 3-3a except at CAG
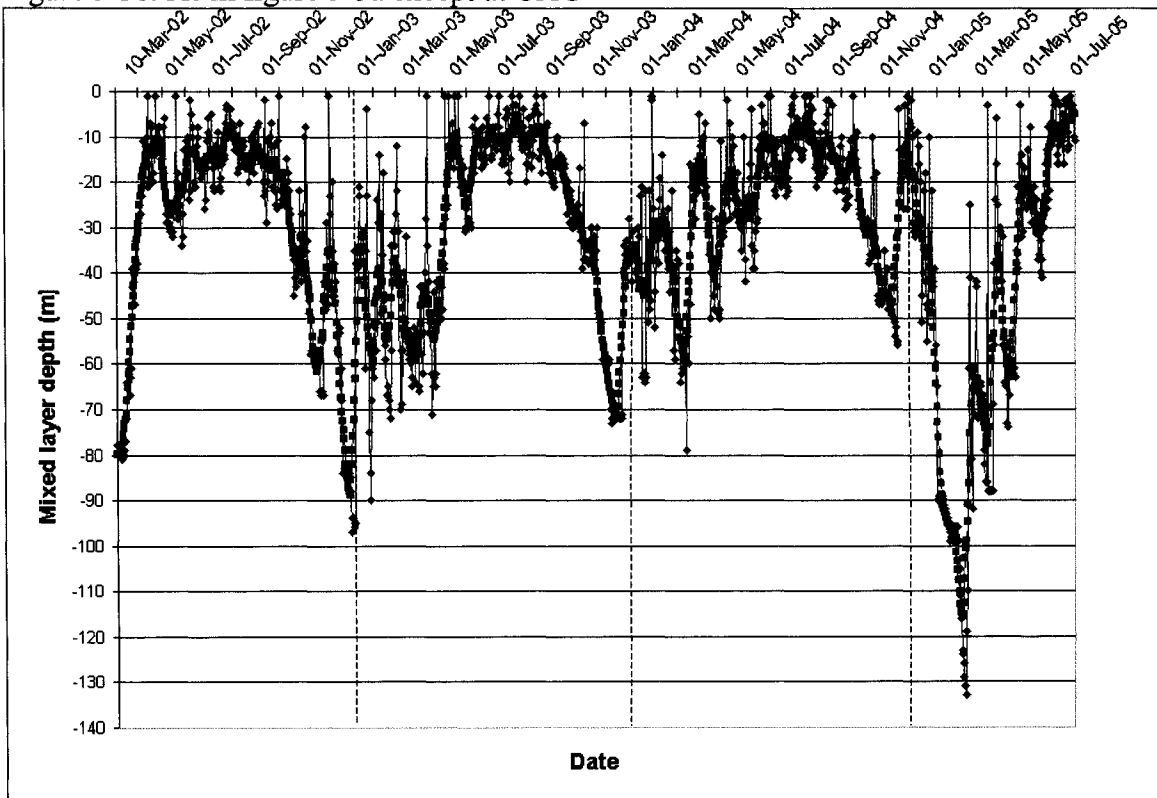
Figure 3-3d: As in figure 3-3a except at NSG

65

Table 3-4: A comparison of the average MLDmod (m) with standard deviation (n= length of season as in table 3-5), the MLDdif during each season and the average MLDmod and MLDdif with standard deviation (n=1471 for OSP, S16 and CAG, n=1228 for NSG) throughout the study period. Positive values of MLDdif indicate that the MLDobs is deeper than the MLDmod

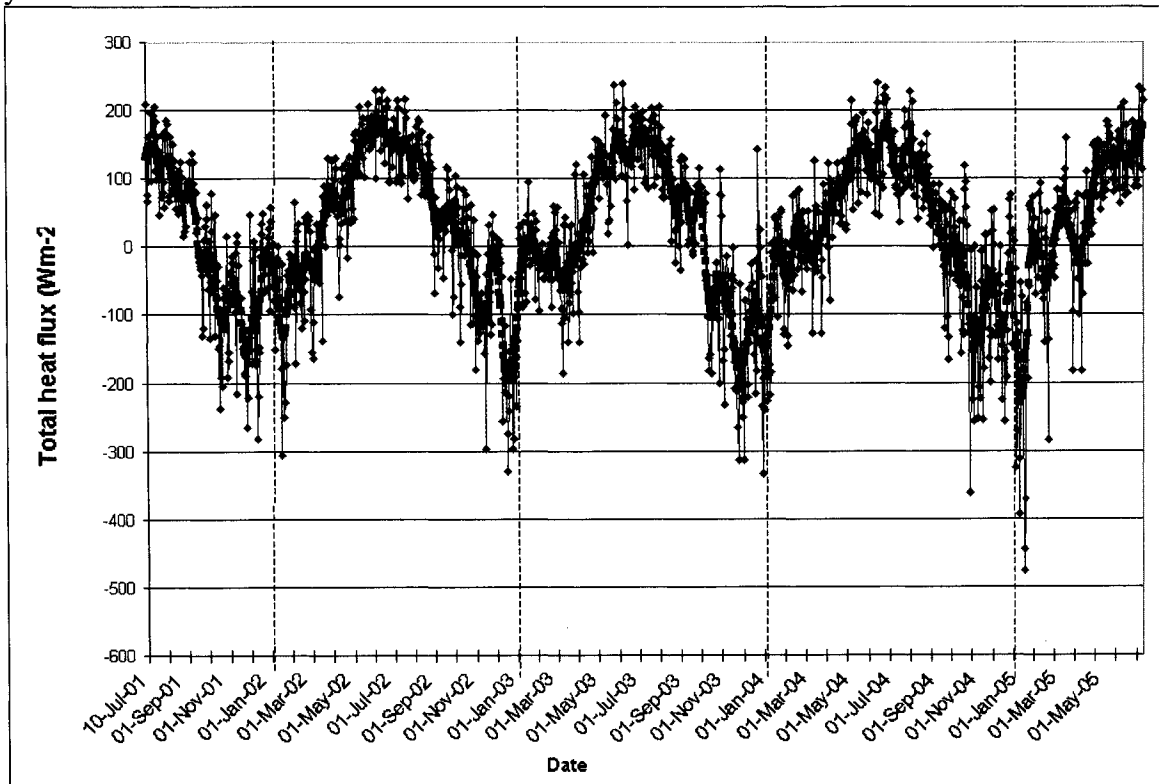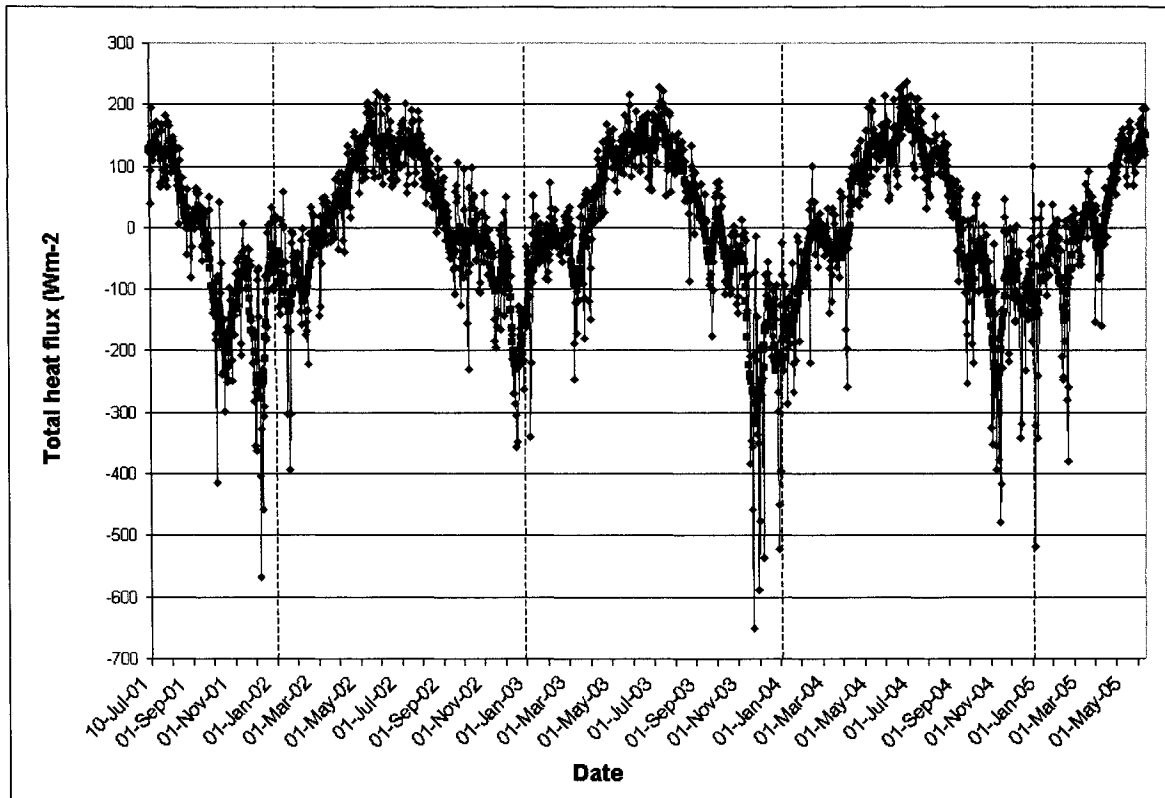|	OSP		S16		CAG		NSG	
	MLD mod	MLD dif	MLD mod	MLD dif	MLD mod	MLD dif	MLD mod	MOD dif
Winter 2001-02	-93.3 ± 1.9	-42.6	-78.5 ± 24.2	-32.0	-95.0 ± 0	-51.5	-	-
Summer 2002	-9.2 ± 7.5	2.6	-12.0 ± 9.5	2.9	-12.6 ± 13.1	-2.4	-13.9 ± 8.4	1.6
Winter 2002-03	-49.9 ± 13.6	-16.8	-55.9 ± 15.7	-18.3	-65.7 ± 13.1	-31.5	-68.1 ± 23.2	-16.0
Summer 2003	-10.7 ± 6.4	3.2	-12.1 ± 6.3	2.4	-11.2 ± 6.9	1.7	-12.0 ± 7.9	0.1
Winter 2003-04	-56.7 ± 19.5	-19.3	-65.8 ± 17.0	-9.2	-78.5 ± 17.9	-36.0	-48.9 ± 24.7	-10.1
Summer 2004	-9.8 ± 7.2	1.3	-10.0 ± 6.3	1.1	-8.2 ± 5.1	1.4	-16.1 ± 11.2	-0.5
Winter 2004-05	-55.6 ± 18.2	-24.3	-50.6 ± 24.5	-7.6	-62.8 ± 24.5	-31.6	-67.3 ± 23.6	-8.6
Average 2001-05	-32.9 ± 24.8	-5.6 ± 11.8	-33.4 ± 26.4	-4.5 ± 13.3	-38.7 ± 29.6	-12.6 ± 17.9	-34.3 ± 26.1	-2.1 ± 13.3

Table 3-5: A comparison between the observed and modeled number of days in each season at each station.

	OSP		S16		CAG		NSAG	
	MLD mod	MLD obs	MLD mod	MLD obs	MLD mod	MLD obs	MLD mod	MOD obs
Winter 2001-02	9	104	85	139	1	116	-	-
Summer 2002	130	101	171	162	117	118	116	148
Winter 2002-03	99	198	91	147	72	189	78	151
Summer 2003	98	135	152	153	101	103	105	106
Winter 2003-04	71	189	33	74	52	197	100	131
Summer 2004	89	88	98	91	100	104	126	125
Winter 2004-05	89	184	84	128	84	133	69	155

66
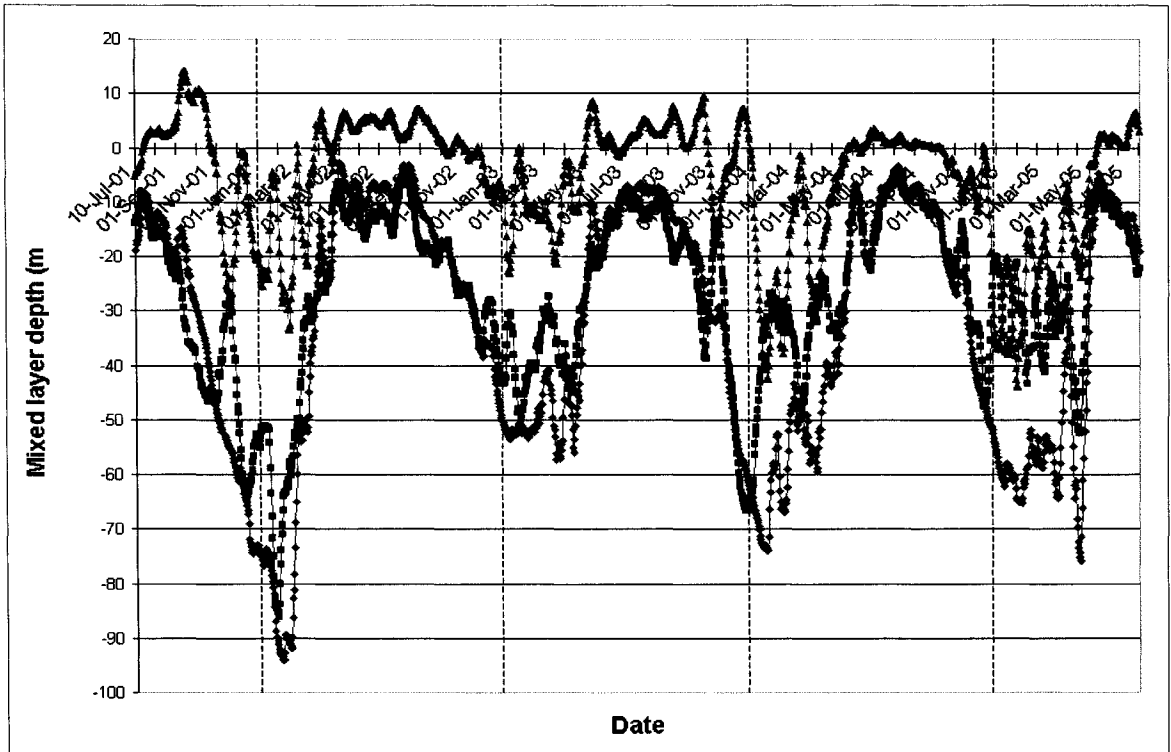
Figure 3-4a: A comparison of the observed and modelled MLD at OSP. Pink line is observed MLD, blue line is modelled MLD and green line is difference between modelled and observed where positive values indicate the observed MLD is deeper than modelled. Vertical dashed lines intersect on January 1st of every year.
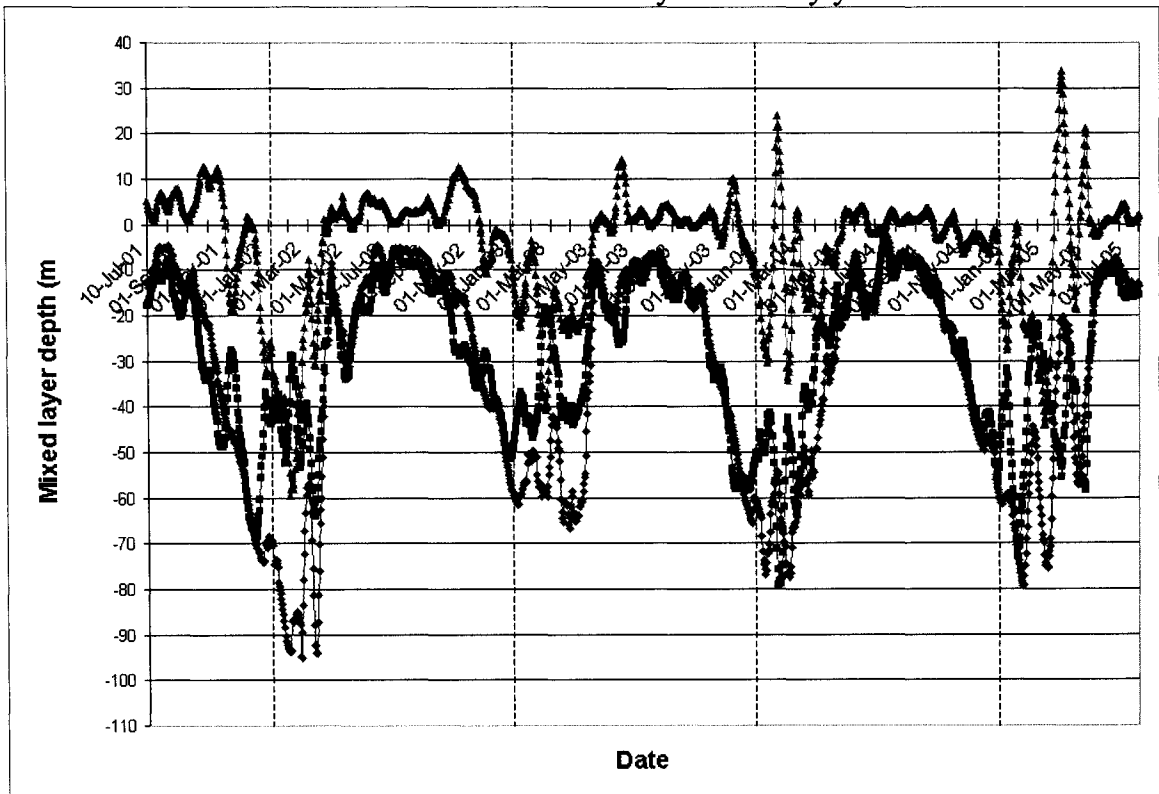
Figure 3-4b: As in figure 3-4a except at S16.

67
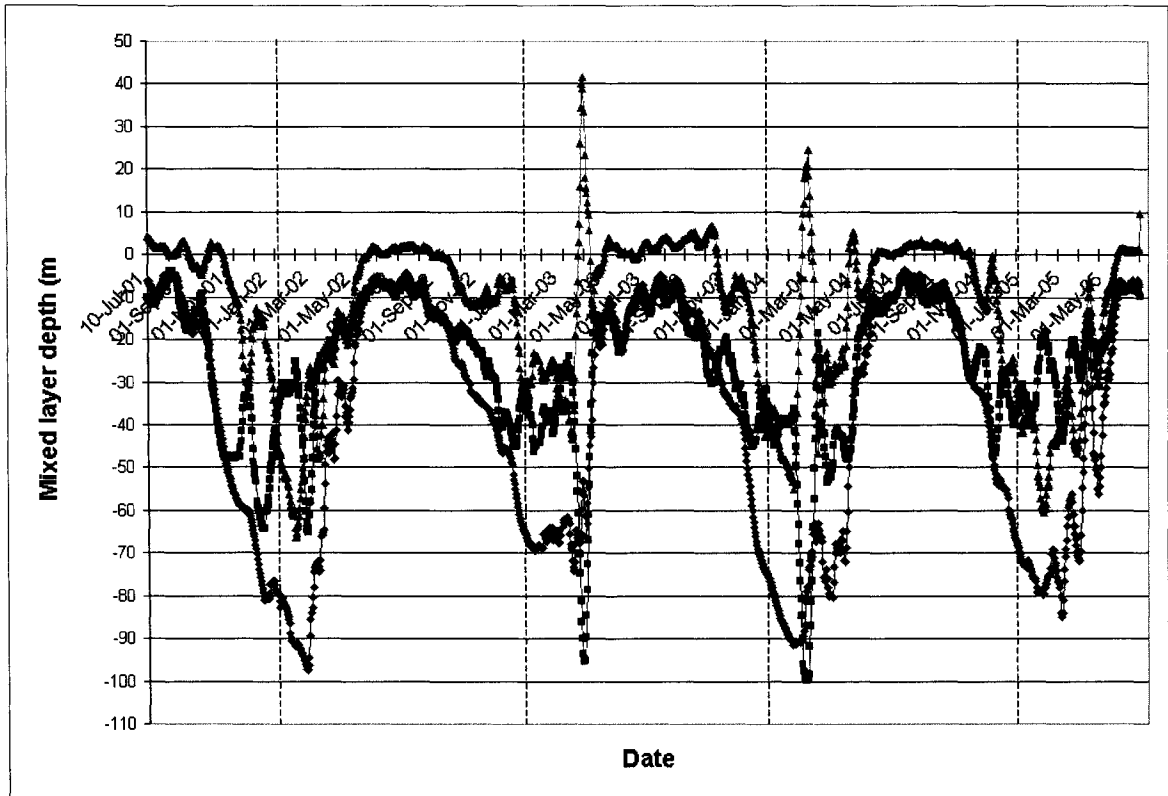
Figure 3-4c: As in figure 3-4a except at CAG.
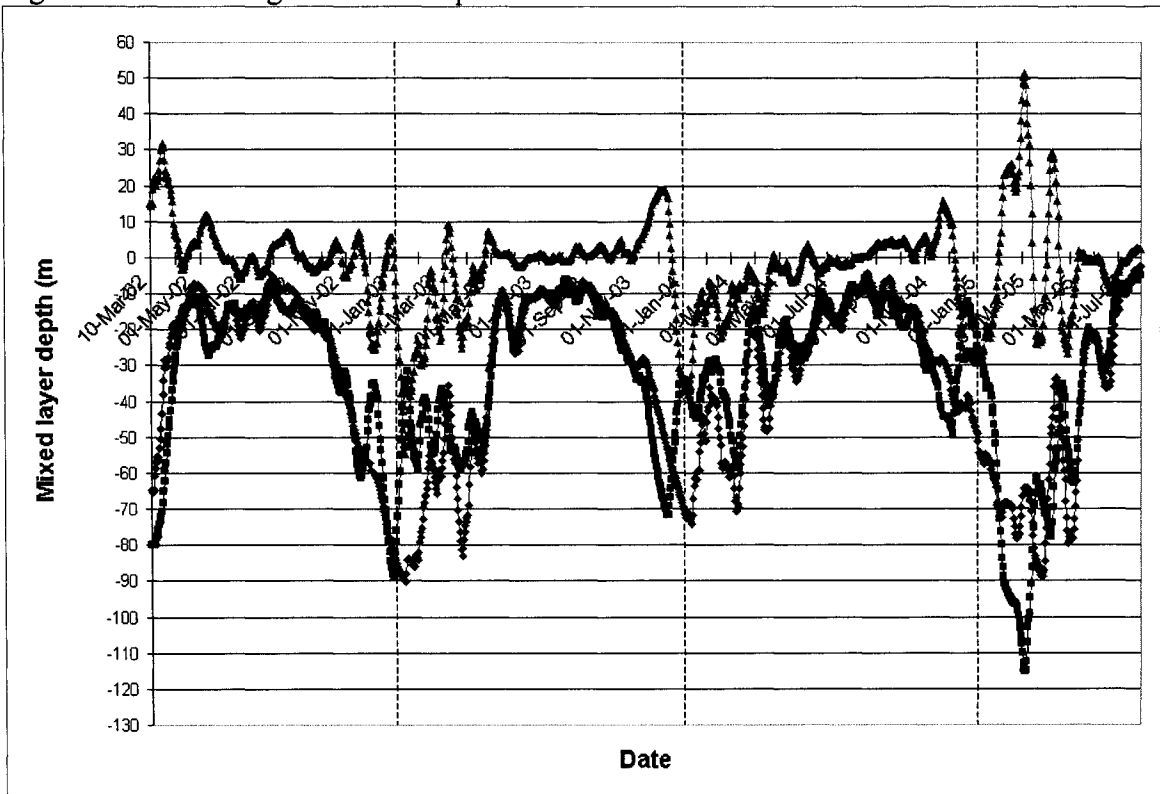
Figure 3-4d: As in figure 3-4a except at NSG

68
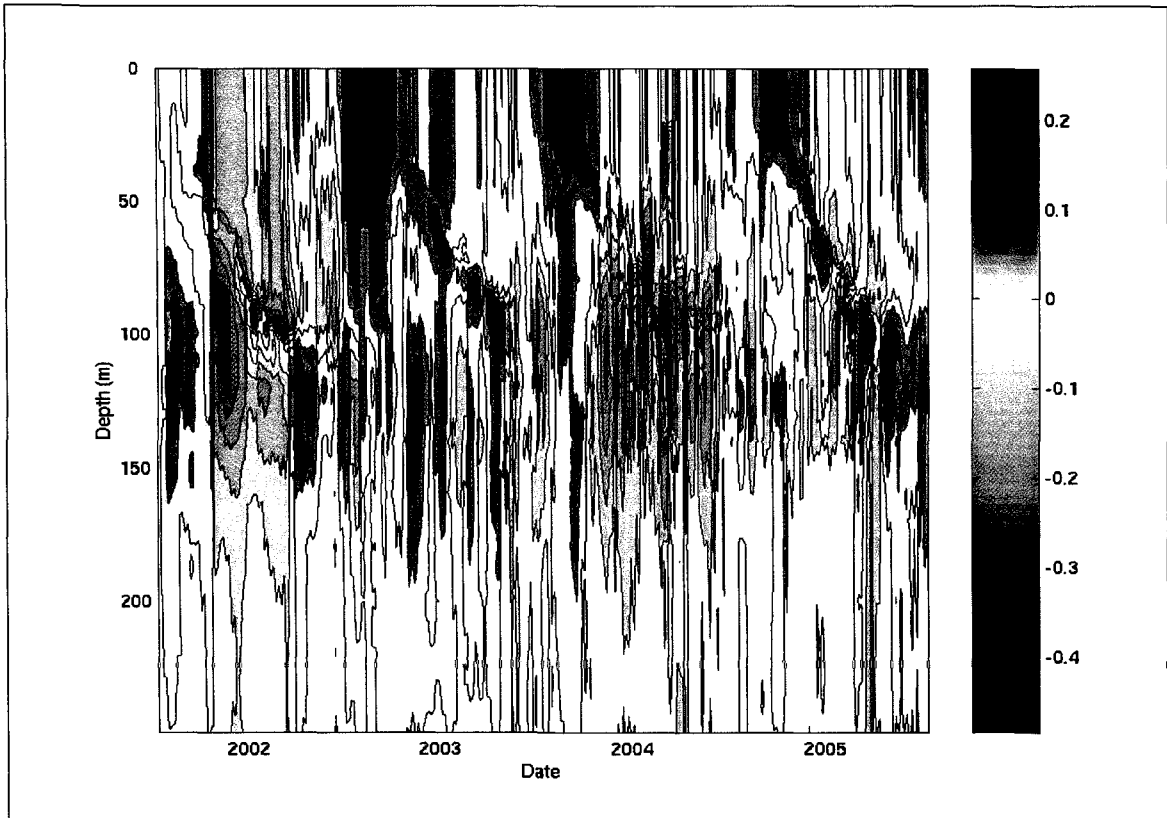
Figure 3-5a: Difference between observed salinity and modeled salinity at CAG. Positive values indicate that model results are saltier than observed.
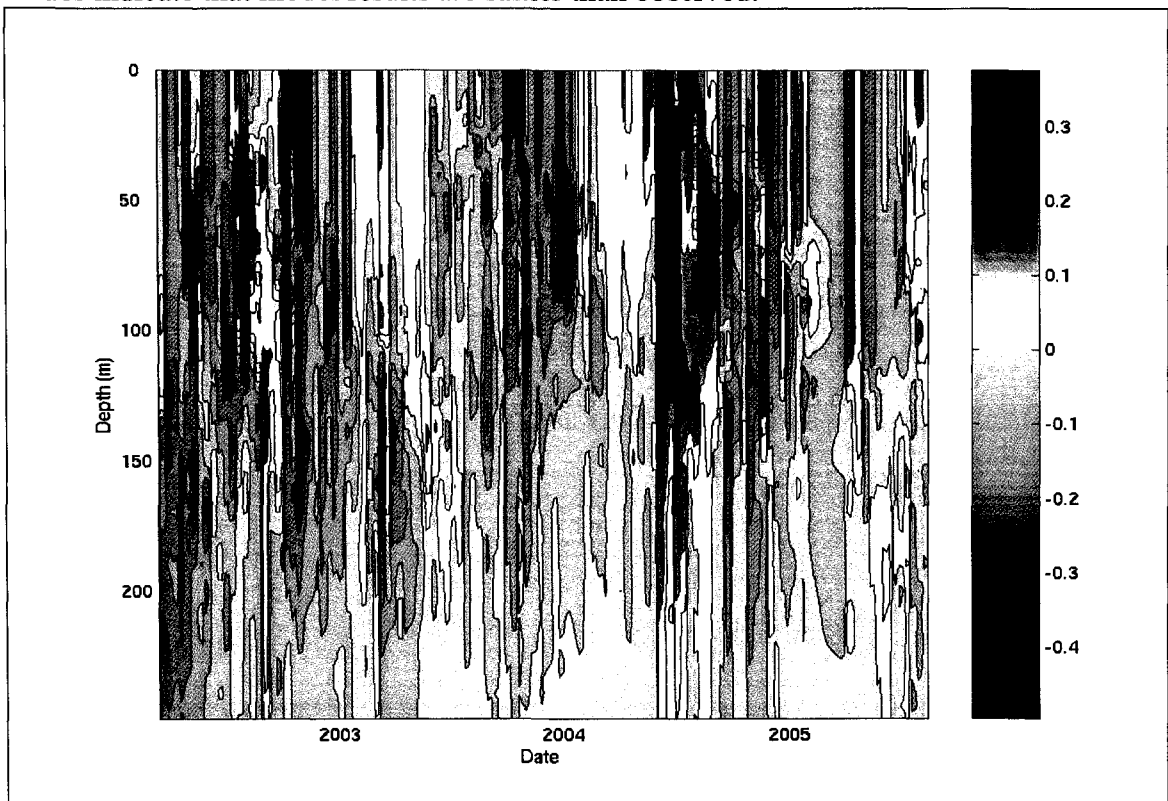
Figure 3-5b: As in figure 3-5a except at NSG

69
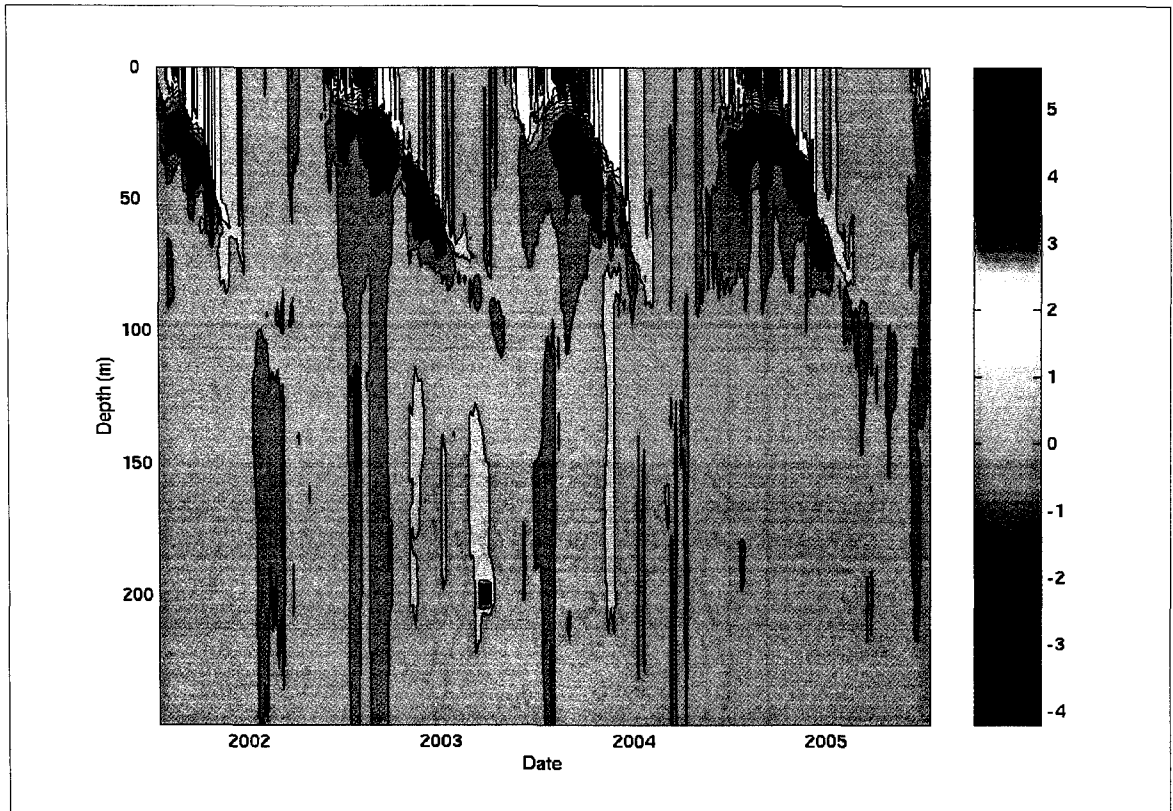
Figure 3-6a: Difference between observed temperature and modeled temperature at CAG. Positive values indicate that model results are warmer than observed.
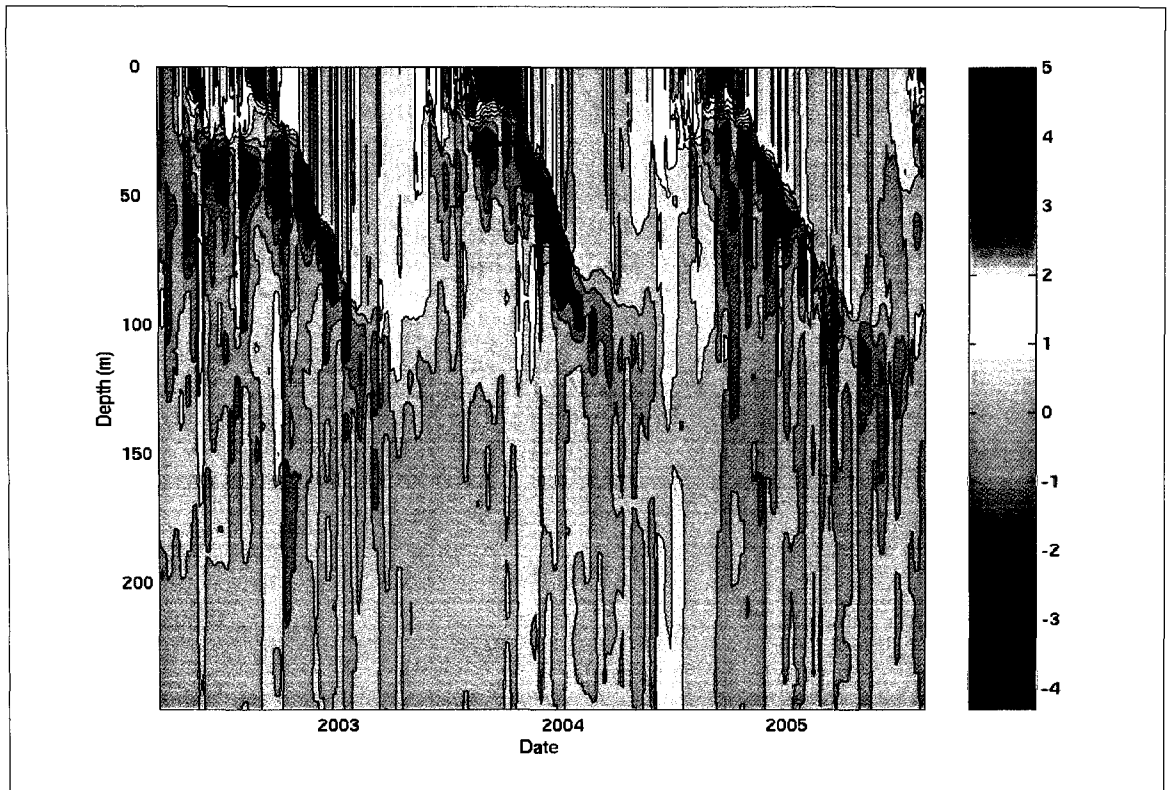
Figure 3-6b: As in figure 3-6a except at NSG.

70

Table 3-6a: A comparison of the how changing the atmospheric forcing affected the average winter and summer MLD with standard deviation (n=variable, depends on length of season) and MLD over study period (n=1471) at OSP

	MLD control	Double wind speed	Zero wind speed	Double SH, LH and LW	Zero SH, LH and LW	Double SW	Zero SW
Winter 2001-02	-92.2 ± 1.9	-127.0 ± 37.1	-47.1 ± 34.1	-103.3 ± 18.4	-30.3 ± 11.3	-63.9 ± 7.8	-93.4 ± 24.4
Summer 2002	-9.1 ± 7.5	-25.2 ± 17.7	-1.3 ± 0.8	-15.0 ± 11.9	-6.5 ± 5.07	-3.4 ± 1.9	-40.2 ± 8.8
Winter 2002-03	-50.0 ± 13.6	-88.8 ± 29.5	-15.2 ± 19.0	-76.2 ± 15.3	-22.0 ± 9.3	-28.2 ± 10.8	-80.6 ± 9.6
Summer 2003	-10.7 ± 6.4	-32.5 ± 15.5	-1.2 ± 0.5	-14.5 ± 9.6	-7.8 ± 4.1	-5.1 ± 2.7	-47.0 ± 11.3
Winter 2003-04	-57.0 ± 19.5	-94.3 ± 38.1	-38.9 ± 30.4	-79.8 ± 21.5	-25.7 ± 11.2	-30.7 ± 14.9	-85.3 ± 14.1
Summer 2004	-9.7 ± 7.2	-31.1 ± 21.3	-1.8 ± 2.9	14.5 ± 11.1	-7.4 ± 4.7	-4.7 ± 2.9	-42.8 ± 10.1
Winter 2004-05	-55.6 ± 18.2	-103.5 ± 45.6	-22.5 ± 21.8	-82.3 ± 24.2	-25.2 ± 9.9	-31.3 ± 12.2	-89.0 ± 14.4
Average 2001-05	-32.9 ± 24.8	-64.8 ± 46.6	-12.4 ± 20.8	-47.4 ± 34.8	-17.7 ± 12.3	-18.2 ± 15.9	-67.6 ± 24.2

Table 3-6b: As in table 3-6a except at S16.

	MLD control	Double wind speed	Zero wind speed	Double SH, LH and LW	Zero SH, LH and LW	Double SW	Zero SW
Winter 2001-02	-78.5 ± 24.2	-117.3 ± 29.6	-55.9 ± 35.7	-110.6 ± 25.9	-26.0 ± 10.4	-42.7 ± 16.5	-104.7 ± 20.9
Summer 2002	-11.9 ± 9.5	-33.0 ± 20.4	-1.5 ± 1.1	-20.9 ± 20.0	-7.8 ± 5.9	-5.8 ± 4.5	-43.8 ± 7.73
Winter 2002-03	-56.4 ± 15.7	-78.8 ± 27.2	-27.7 ± 22.4	-84.6 ± 19.6	-22.0 ± 8.9	-27.8 ± 12.3	-86.8 ± 11.4
Summer 2003	-12.1 ± 6.3	-30.3 ± 11.3	-1.4 ± 0.9	-20.7 ± 11.8	-7.3 ± 3.6	-5.2 ± 2.6	-50.1 ± 9.2
Winter 2003-04	-65.4 ± 17.0	-98.6 ± 36.0	-43.0 ± 29.9	-86.7 ± 21.2	-25.5 ± 11.0	-37.7 ± 13.2	-88.8 ± 11.7
Summer 2004	-9.9 ± 6.3	-22.7 ± 10.8	-2.9 ± 7.2	-16.9 ± 11.2	-8.6 ± 6.0	-4.4 ± 2.3	-42.6 ± 5.5
Winter 2004-05	-50.5 ± 24.5	-85.1 ± 29.8	-35.0 ± 27.8	-75.9 ± 27.6	-20.7 ± 11.5	-25.4 ± 16.4	-81.2 ± 14.8
Average 2001-05	-33.4 ± 26.4	-60.1 ± 39.1	-15.6 ± 24.4	-51.6 ± 36.4	-15.1 ± 10.6	-17.0 ± 15.2	-72.0 ± 23.8

71

Table 3-6c: As in table 3-6a except at CAG

	MLD control	Double wind speed	Zero wind speed	Double SH, LH and LW	Zero SH, LH and LW	Double SW	Zero SW
Winter 2001-02	-95.0 ± 0	-99.2 ± 36.2	-65.3 ± 31.7	-102.7 ± 17.6	-31.4 ± 13.2	-80.5 ± 0	-94.0 ± 11.9
Summer 2002	-12.6 ± 13.1	-50.5 ± 27.0	-2.4 ± 3.1	-10.8 ± 5.9	-7.3 ± 5.8	-5.8 ± 5.5	-29.5 ± 0
Winter 2002-03	-66.4 ± 13.1	-80.2 ± 29.1	-39.0 ± 26.4	-89.1 ± 9.5	-24.9 ± 11.0	-40.6 ± 16.2	-77.4 ± 16.0
Summer 2003	-11.1 ± 6.9	-36.6 ± 18.1	-1.3 ± 0.6	-18.7 ± 12.1	-6.6 ± 3.6	-4.8 ± 2.6	-46.5 ± 7.7
Winter 2003-04	-77.9 ± 17.9	-98.8 ± 29.8	-49.3 ± 38.4	-99.7 ± 15.3	-25.4 ± 12.3	-44.1 ± 23.0	-90.6 ± 12.8
Summer 2004	-8.1 ± 5.2	-44.4 ± 32.0	-1.0 ± 0.2	-12.7 ± 7.9	-5.4 ± 3.3	-3.8 ± 2.1	-41.0 ± 6.1
Winter 2004-05	-65.5 ± 24.5	-87.5 ± 37.9	-39.6 ± 32.6	-94.2 ± 18.8	-23.4 ± 11.6	-53.5 ± 11.3	-94.4 ± 7.9
Average 2001-05	-38.7 ± 29.6	-72.4 ± 38.4	-22.6 ± 29.5	-57.8 ± 37.6	-17.0 ± 13.2	-23.2 ± 22.7	-71.8 ± 23.4

Table 3-6d: As in table 3-6a except at NSG

	MLD control	Double wind speed	Zero wind speed	Double SH, LH and LW	Zero SH, LH and LW	Double SW	Zero SW
Summer 2002	-13.9 ± 8.4	-40.2 ± 16.1	-1.7 ± 1.4	-21.7 ± 12.1	-9.3 ± 5.4	-6.6 ± 3.4	-68.1 ± 20.9
Winter 2002-03	-68.1 ± 23.2	-120.0 ± 54.2	-25.8 ± 35.9	-109.2 ± 40.5	-21.9 ± 8.1	-32.9 ± 12.5	-125.9 ± 18.2
Summer 2003	-12.1 ± 7.9	-34.3 ± 14.5	-1.2 ± 0.5	-17.6 ± 11.9	-8.4 ± 5.2	-5.9 ± 3.7	-47.4 ± 9.7
Winter 2003-04	-48.6 ± 24.7	-100.1 ± 49.1	-27.6 ± 27.0	-81.5 ± 48.5	-17.0 ± 7.4	-20.5 ± 11.2	-100.4 ± 28.6
Summer 2004	-16.2 ± 11.2	-40.9 ± 26.0	-2.0 ± 2.1	-23.8 ± 17.7	-8.8 ± 5.0	-5.7 ± 3.2	-47.3 ± 10.2
Winter 2004-05	-67.3 ± 23.6	-107.1 ± 33.6	-37.9 ± 35.4	-103.8 ± 41.7	-19.1 ± 7.5	-24.3 ± 12.1	-130.4 ± 16.4
Average 2001-05	-34.3 ± 26.1	-69.5 ± 46.3	-14.1 ± 24.0	-60.2 ± 47.0	-13.9 ± 8.3	-15.8 ± 12.3	-88.0 ± 33.5

72
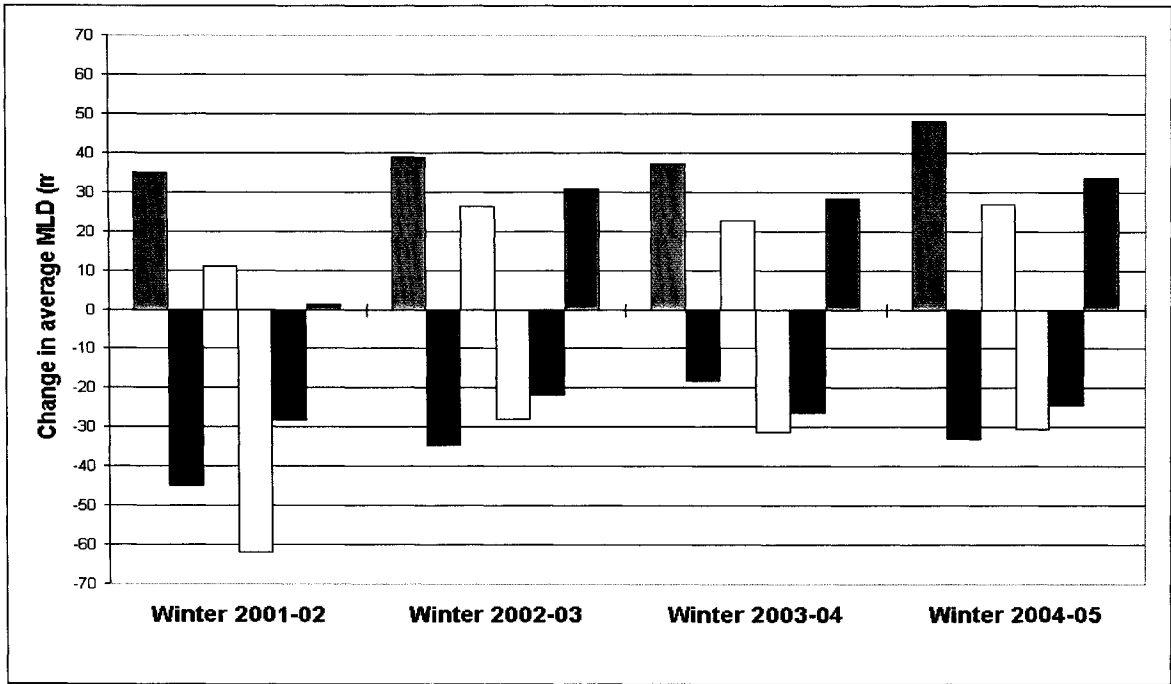
Figure 3-7a: A comparison of the sensitivity of the average winter MLD at OSP to various experiments that changed the atmospheric forcing. Dark blue bars represent doubling the wind speed, light burgundy bars are zeroing the wind speed, yellow bars are doubling the outgoing heat fluxes, light blue bars are zeroing the outgoing heat fluxes, dark burgundy bars are doubling the SW and pink bars are zeroing the SW. Positive values indicate that the MLD increased.
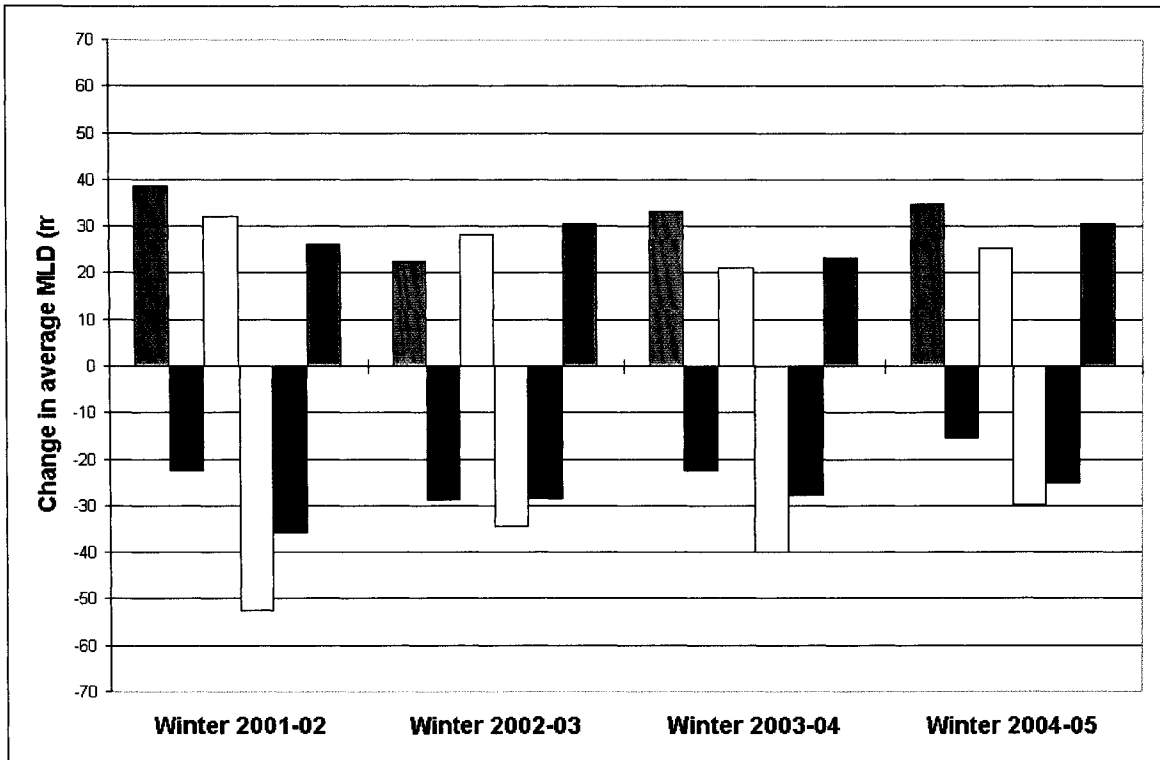
Figure 3-7b: As in figure 3-7a except at S16.

73
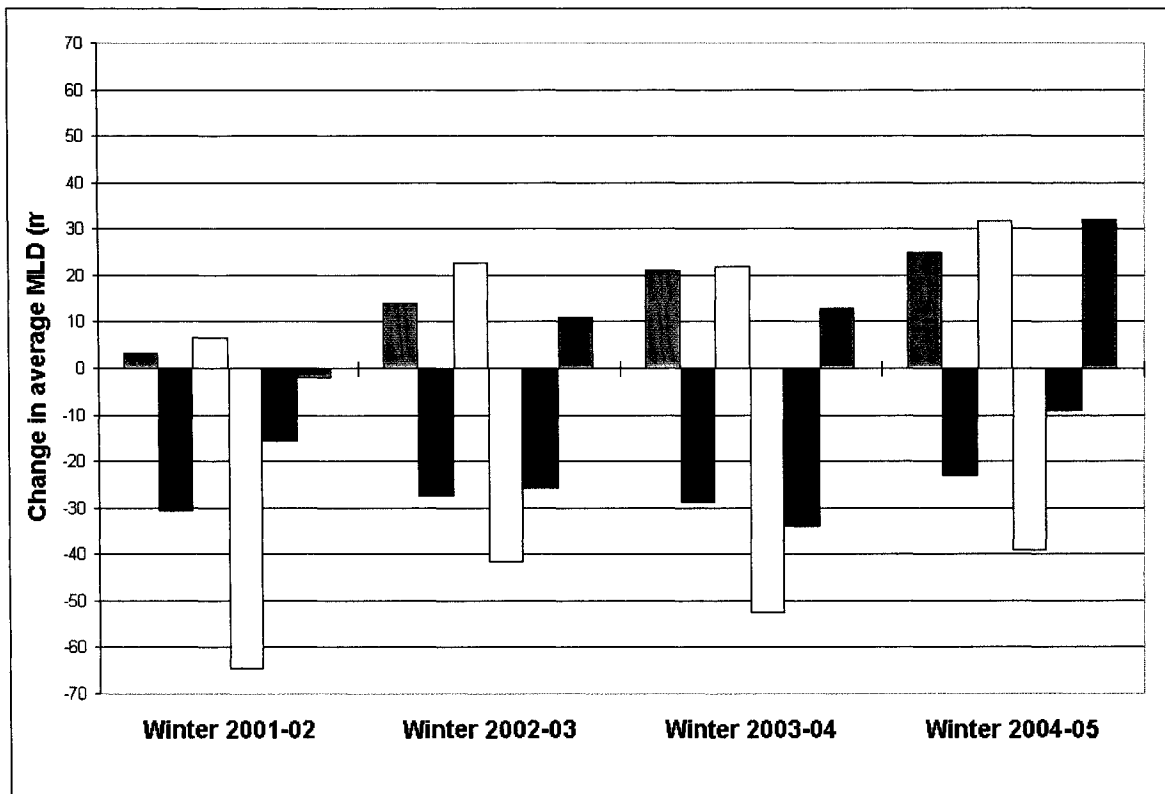
Figure 3-7c: As in figure 3-7a except at CAG.
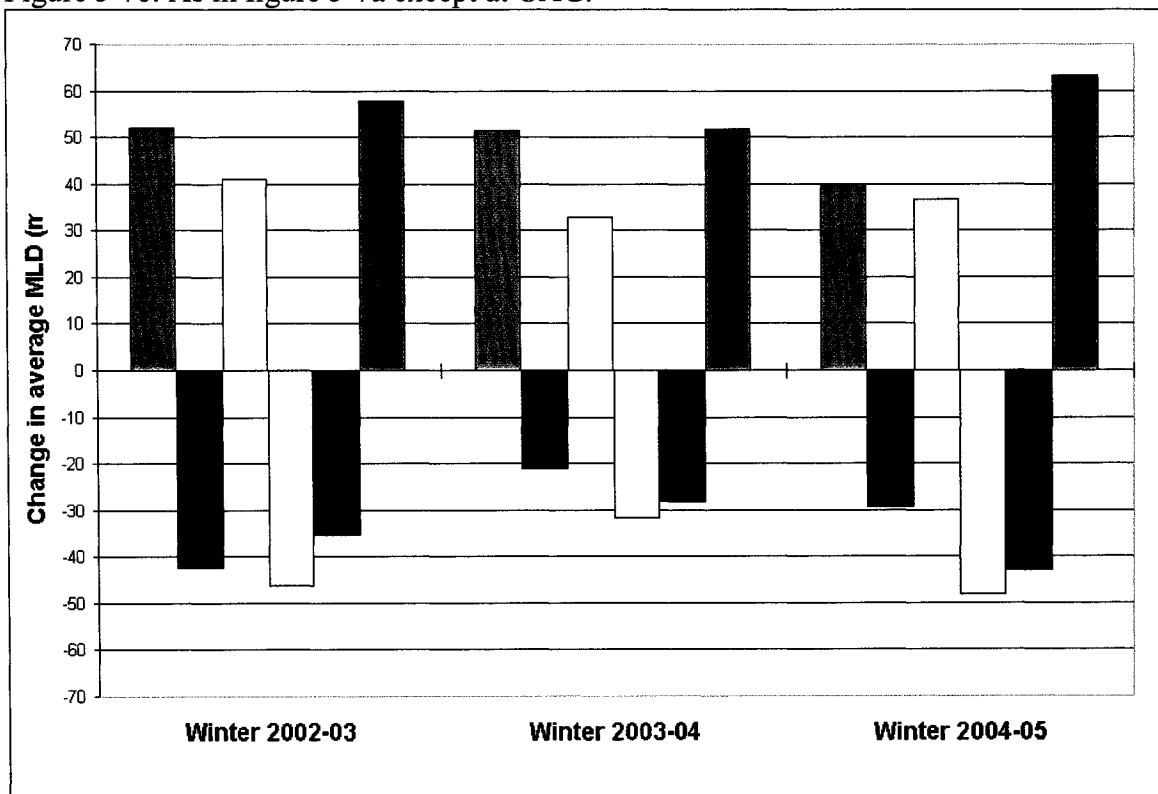
Figure 3-7d: As in figure 3-7a except at NSG.

74
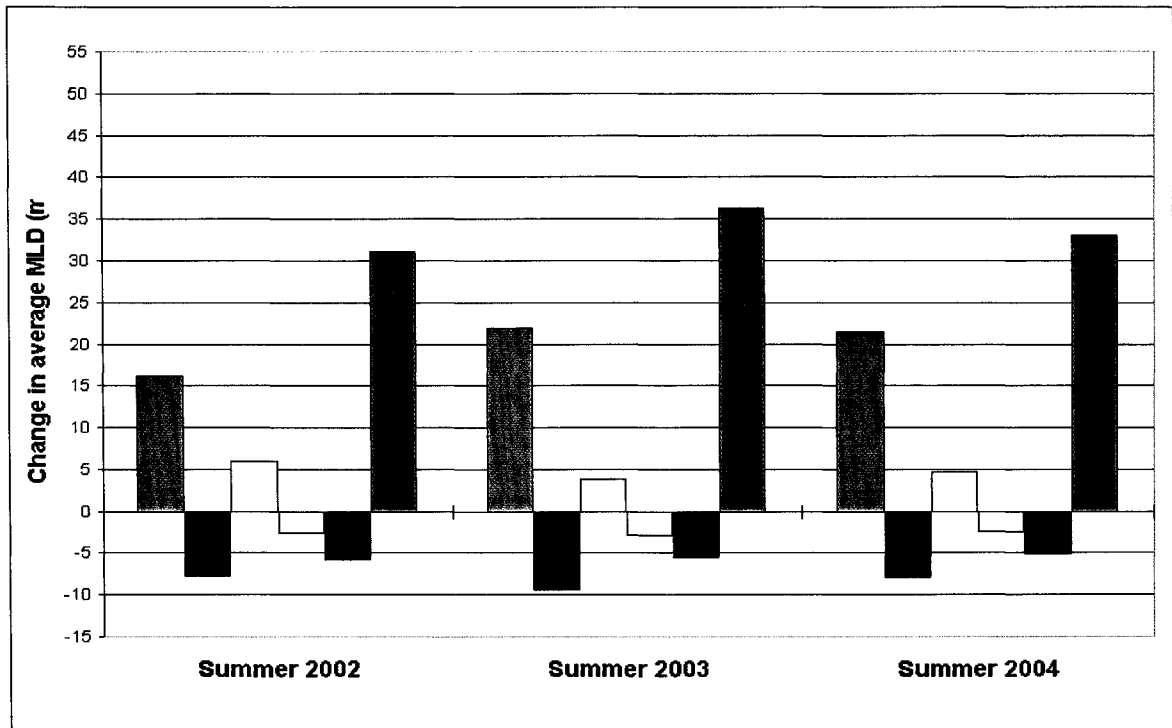
Figure 3-8a: A comparison of the sensitivity of the average summer MLD at OSP to various experiments that changed the atmospheric forcing. Dark blue bars represent doubling the wind speed, light burgundy bars are zeroing the wind speed, yellow bars are doubling the outgoing heat fluxes, light blue bars are zeroing the outgoing heat fluxes, dark burgundy bars are doubling the SW and pink bars are zeroing the SW. Positive values indicate that the MLD increased.
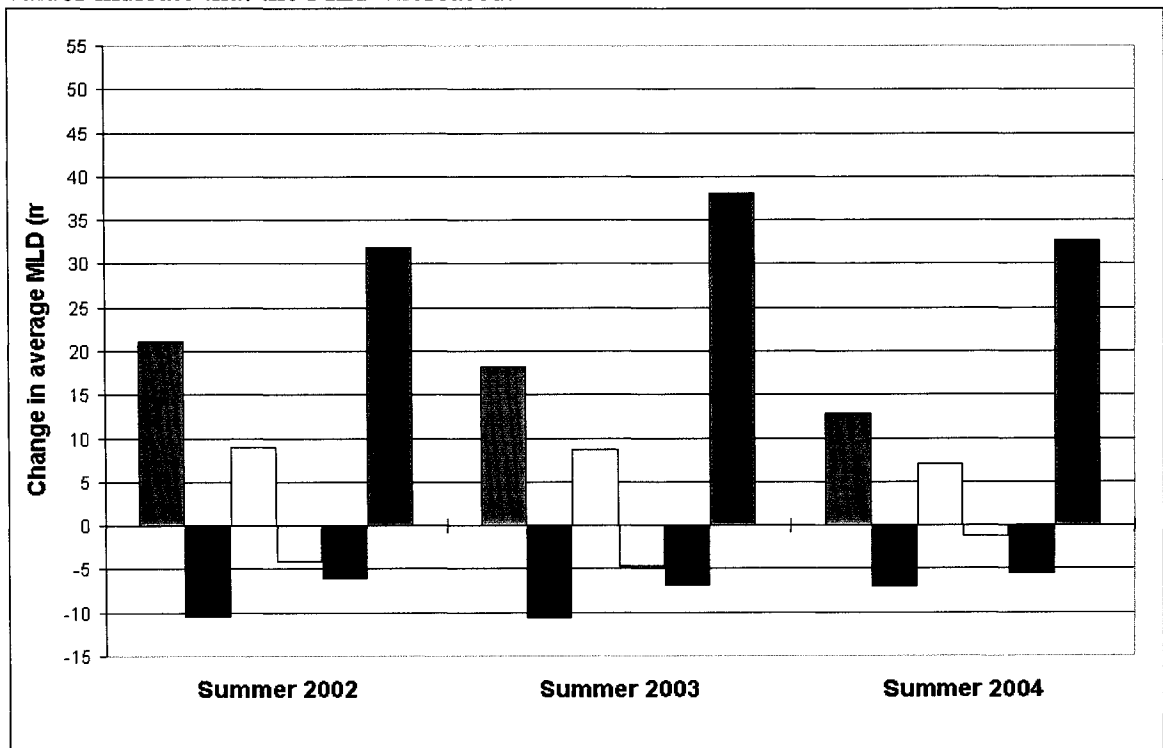
Figure 3-8b: As in figure 3-8a except at S16.

75
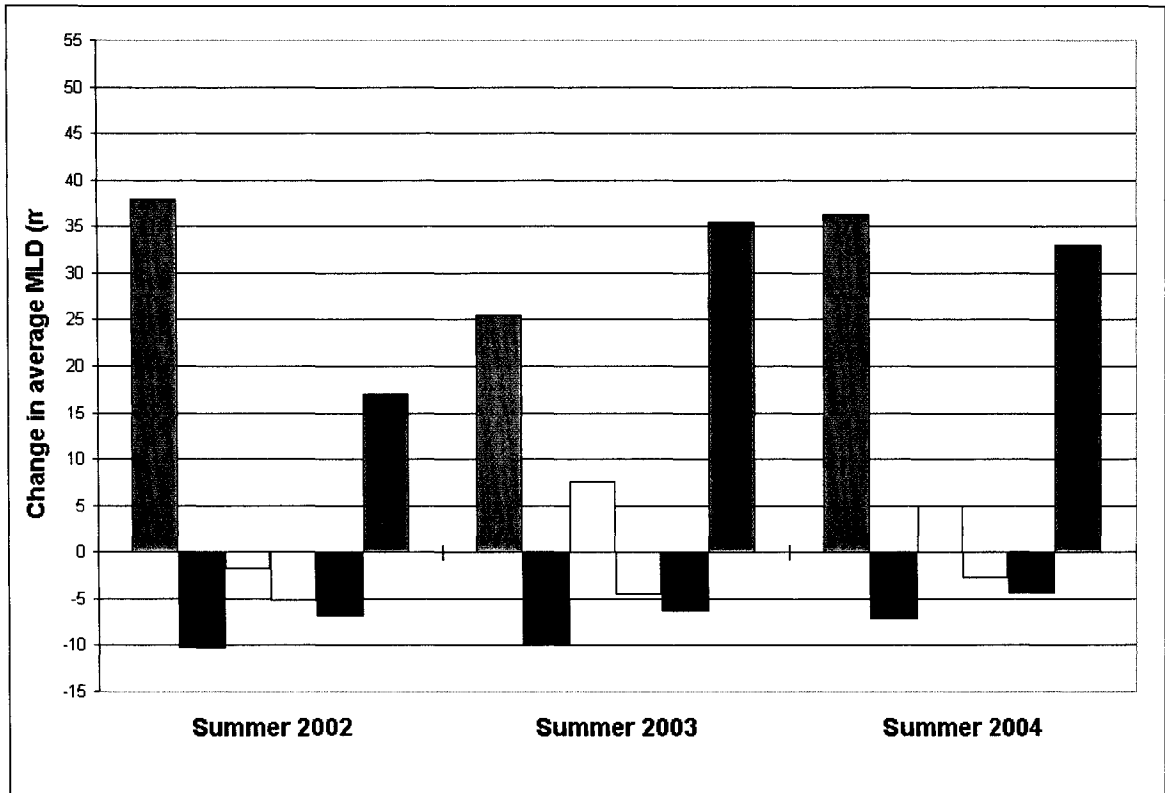
Figure 3-8c: As in figure 3-8a except at CAG.
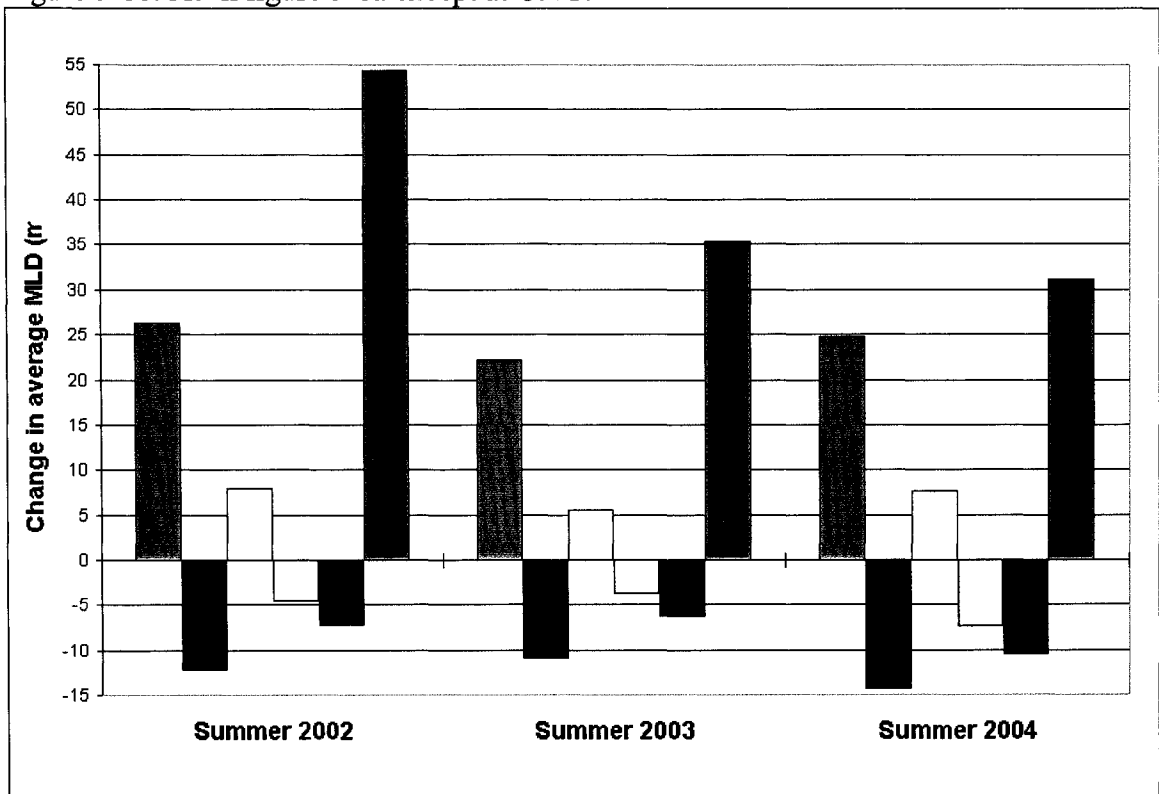
Figure 3-8d: As in figure 3-8a except at NSG.

76

3.6 Bibliography

Adamec, D. and R.L. Elsberry. 1984 Sensitivity of Mixed Layer Predictions at Ocean

Station Papa to Atmospheric Forcing Parameters. *Journal of Physical Oceanography*,

14(4), 769-780.

Alexander, M.A. and C. Penland. 1996. Variability in a Mixed Layer Ocean Model

Driven by Stochastic Atmospheric Forcing. *Journal of Climate*, 9, 2424 – 2442.

Brown, R.G. and L.L. Fu. 2000. An Examination of the Spring 1997 Mid-Latitude East

Pacific Sea Surface Temperature Anomaly. *Atmosphere-Ocean*, 38(4), 577-599.

Burchard, H., K. Bolding and L. Umlauf. 2005. GOTM – The General Ocean Turbulence

Model. http://www.gotm.net

Carmack, E.C. 2000. The Arctic Ocean's Freshwater Budget: Sources, Storage and

Export. In *The Freshwater Budget of the Arctic Ocean*, Kluwer Academic Publishers,

The Netherlands, 91-126.

Capotondi, A., M.A. Alexander, C. Deser and A.J. Miller. 2005. Low-frequency

Variability in the Northeast Pacific. *Journal of Physical Oceanography*, 35, 1403-1420.

Churchister, E.M., D.B. Haidvogel, A.J. Hermann, E.L. Dobbins, T.M. Powell, and A.

Kaplan. 2005. Multi-scale modeling of the North Pacific Ocean: Assessment and

Analysis of simulated basin-scale variability, *Journal of Geophysical Research*, 110,

C11021, doi:10.1029/2005JC002902.

Crawford, W., P. Sutherland and P. van Hardenberg. 2005. Cold water intrusion in the

Eastern Gulf of Alaska in 2002. *Atmosphere-Ocean*, 43(2), 119-128.

Cummins, P.F. and G.S.E. Lagerloef. 2002. Low-Frequency Pycnocline Depth

Variability at Ocean Weather Station P in the Northeast Pacific. 2002. *Journal of*

Physical Oceanography, 32, 3207-3215.

de Boyer Montegut, C., G. Madec, A.S. Fischer, A. Lazar and D. Iudicone. 2004. Mixed

layer depth over the global ocean: An examination of profile data and a profile-based

climatology. *Journal of Geophysical Research*, 109, C12003,

doi:10.1029/2004JC002378.

Denman, K.L. 1973. A Time-Dependent Model of the Upper Ocean. *Journal of Physical

Oceanography*, 3, 173-184.

Denman, K.L. and M.A. Pena. 1999. A coupled 1-D biological/physical model of the

northeast subarctic Pacific Ocean with iron limitation. *Deep-Sea Research II*, 46, 2877-

2908.

Flatau, M., L. Talley and D. Musgrave. 2000. Interannual Variability in the Gulf of

Alaska during the 1991-94 El Nino. *Journal of Climate*, 13, 1664-1673.

Freeland, H. 2002.The Heat Flux across Line-P 1996-1999. *Atmosphere-Ocean*, 40(1),

81-89.

Freeland, H.J. 2005. *Argo Status Globally and in the Gulf of Alaska*.

http://www-sci.pac.dfo-mpo.gc.ca/osap/projects/argo/status_e.htm

Freeland, H.J. and P.F. Cummins. 2005. Argo: A new tool for environmental monitoring

and assessment of the world's oceans, and example from the N.E. Pacific. *Progress in

Oceanography*, 64, 31-44.

Freeland, H., K. Denman, C.S. Wong, F. Whitney and R. Jacques. 1997. Evidence of

Change in the winter mixed layer in the Northeast Pacific Ocean. *Deep-Sea Research I*,

44(12), 2117-2129.

Freeland, H.J., G. Gatien, A. Huyer and R.L. Smith. 2003. Cold halocline in the northern

California Current: An invasion of subarctic water. *Geophysical Research Letters,* 30(3), 1141, doi:10.1029/2002GL016663.

Gould, J., D. Roemmich, S. Wijffels, H. Freeland, M. Ignaszewsky, X. Jianping, S. Pouliquen, Y. Desaubies, U. Send, K. Radhakrishnan, K. Takeuchi, K. Kim, M. Danchenkov, P. Sutton, B. King, B. Owens and S. Riser. Argo Profiling Floats Bring New Era of In Situ Ocean Observations. *EOS Transactions, AGU,* 85(19), 185-190.

Jackson, J.M., P.G. Myers and D. Ianson. 2005. An Examination of Advection in the Northeast Pacific Ocean, 2001-05. *Geophysical Research Letters,* submitted.

Kalnay, E., M. Kanamitsu, R. Kistler, W. Collins, D. Deaven, L.Gandin, M. Iredell, S. Saha, G. White, J. Woollen, Y. Zhu, A. Leetmaa, B. Reynolds, M. Chelliah, W. Ebisusaki, W. Higgins, J. Janowiak, K.C. Mo, C. Ropelewski, J. Wang, R. Jenne and D. Joseph. 1996. The NCEP/NCAR 40-Year Reanalysis Project. *Bulletin of the American Meteorological Society,* 77(3), 437-471.

Lagerloef, G.S.E. 1995. Interdecadal Variations in the Alaska Gyre. *Journal of Physical Oceanography,* 25, 2242-2258.

Large, W.G. and C.B. Crawford. 1995. Observations and Simulations of Upper-Ocean Response to Wind Events during the Ocean Storms Experiment. *Journal of Physical Oceanography,* 25, 2831-2852.

Large, W.G., J.C. McWilliams and S.C. Doney. 1994. Oceanic vertical mixing: a review and a model with nonlocal boundary layer parameterization. *Reviews of Geophysics,* 32, 363-403.

Li, M., P.G. Myers and H. Freeland. 2005a. An examination of historical mixed layer depths along Line P in the Gulf of Alaska. *Geophysical Research Letters,* 32, L05613,

doi:1029/2004GL021911.

Li, M., H. Freeland and P.G. Myers, 2005b. An Examination of Mixed Layer Depth in the Gulf of Alaska using Argo Data. *Geophysical Research Letters,* submitted.

Mantua, N.J. and S.R. Hare. 2002. The Pacific Decadal Oscillation. *Journal of Ocean Oceanography*, 58, 35-44.

McPhaden, M.J. 2004. Evolution of the 2002/03 El Nino. *Bulletin of the American Meteorological Society*, 85, 677 – 695.

Mellor, G.L. 1996. *Introduction to Physical Oceanography*, Springer-Verlag, New York, 260 pp.

Miller, A.J. and N. Schneider. 2000. Interdecadal climate regime dynamics in the North Pacific Ocean: theories, observations and ecosystem impacts. *Progress in Oceanography,* 47, 355-379.

Murphee, T., S.J. Bograd, F.B. Schwing and B. Ford. 2003. Large scale atmosphere-Ocean anomalies in the northeast Pacific during 2002. *Geophysical Research Letters,* 30(15), 8026, doi:10.1029/2003GL017303.

Overland, J.E., N.A. Bond and J.M. Adams. 2001. North Pacific Atmospheric and SST Anomalies in 1997: Links to ENSO? *Fisheries Oceanography*, 10(1), 69-80.

Polovina, J.J., G.T. Mitchum and G.T. Evans. 1995. Decadal and basin-scale variation in mixed layer depth and the impact on biological production in the Central and North Pacific, 1960-88. *Deep-Sea Research,* 42(10), 1701-1716.

Robert, M. 2005. *Line P Oceanographic Data.* http://www-sci.pac.dfo-mpo.gc.ca/osap/data/linep/linepselectdata_e.htm

Roemmich, D. and T. McCallister. 1989. Large scale circulation of the North Pacific

Ocean. *Progress in Oceanography*, 22, 171-204.

Schwing, F.B., T. Murphee, L. deWitt and P.M. Green. 2002. The evolution of oceanic and atmospheric anomalies in the northeast Pacific during the El Nino and La Nina events of 1995-2001. *Progress in Oceanography,* 54, 459-491.

Stewart, R.H. 2005. *Introduction to Physical Oceanography*. On-line textbook: http://oceanworld.tamu.edu/home/course_book.htm

Strub, P.T. and C. James. 2002. The 1997-98 oceanic El Nino signal along the southeast and northeast Pacific boundaries – an altimetric view. *Progress in Oceanography*, 54, 439-458.

Tabata, S. 1961. Temporal Changes of Salinity, Temperature, and Dissolved Oxygen Content of the Water at Station "P" in the Northwest Pacific Ocean, and Some of Their Determining Factors. *Journal of the Fisheries Research Board of Canada*, 18(6), 1073-1124.

Thomson, R.E. 1981. Oceanography of the British Columbia Coast. *Canadian Special Publication of Fisheries and Aquatic Sciences*, 56, 291 p.

Thomson, R.E. and I.V. Fine. 2003. Estimating Mixed Layer Depth from Oceanic Profile Data. *Journal of Atmospheric and Oceanic Technology,* 20, 319-329.

Umlauf, L. and H. Burchard. 2003. A generic length-scale equation for geophysical turbulence models. *Journal of Marine Research,* 61, 235-265.

Umlauf, L., H. Burchard and K. Hutter. 2003. Extending the k-ω turbulence model towards oceanic applications. *Ocean Modelling,* 5, 195-218.

Umlauf, L., H. Burchard and K. Bolding. 2004. *GOTM: Sourcecode and Test Case Documentation, version 3.0,* http://www.gotm.net

White, W.B. and S. Tabata. 1987. Interannual Westward-Propagating Baroclinic Long-

Wave Activity on Line P in the Eastern Midlatitude North Pacific. *Journal of Physical*

Oceanography, 17, 385-395.

Whitney, F.A. and H.J. Freeland. 1999. Variability in upper-ocean water properties in the

NE Pacific Ocean. *Deep-Sea Research II*, 46, 2351-2370.

Whitney, F.A. and D.W. Welch. 2002. Impact of the 1997-1998 El Nino and 1999 La

Nina on nutrient supply in the Gulf of Alaska. *Progress in Oceanography*, 54, 405-421.

Yuan, X. and L.D. Talley. 1996. The subarctic frontal zone in the North Pacific:

Characteristics if frontal structure from climatological data and synoptic surveys.

Journal of Geophysical Research, 101(C7), 16,491 – 16,508.

Chapter 4

Conclusions

This study has shown that several periods in the years from 2001-05 exhibited an anomalously large change in heat content due to horizontal advection in the northeast Pacific Ocean (Chapter 2) and several winters in the Gulf of Alaska when the observed MLD was anomalously shallow (Chapter 3). I suggest that there are periods during this study when these anomalies may be related.

At OSP, there was minimal horizontal advection during the year 2001-02 (Chapter 2), the MLD was the deepest of the years studied and the wind speeds and outgoing heat fluxes were relatively high (Chapter 3). The sensitivity analyses show that the MLD shoaled the most during the winter when the outgoing heat fluxes and wind speeds were zeroed, suggesting that the MLD had reached a threshold where it could not have deepened much further even with increased wind speeds and outgoing heat fluxes

(Chapter 3). The MLD shoaled in early February, which is earlier than other winters, and this was likely caused by the reduced outgoing heat fluxes and wind speeds observed at the end of January 2002, which may have been triggered by an early onset of the meteorological phase of the 2002-03 ENSO (McPhaden, 2004). During the summer of 2002, as in all summers at OSP during this study period, the MLD was the most sensitive to zeroing the SW and doubling the wind speeds (Chapter 3).

During the winter of 2002-03 there was one period of significant advection in December (Chapter 2), the MLD was the shallowest of all the years observed and the outgoing heat fluxes and wind speeds were weak (Chapter 3). The MLD was the most sensitive to changing the wind speeds, suggesting that the decreased wind speeds, another effect of the 2002-03 ENSO (Brown and Fu, 2000), were the main reason why the MLD was so shallow during this year. In addition, I suggest that an observed cold water anomaly from the summer of 2002 – the summer of 2003 at a depth of 100-150 m (Freeland, et al., 2003; Crawford, et al., 2005) created a large density gradient that also prevented the MLD from deepening. This anomalous water mass was likely a remnant of the North Pacific Current since it appeared at roughly the same time as the when the North Pacific Current migrated south (Freeland and Cummins, 2005) and I found no evidence that it was advected into the region near OSP at that time (Chapter 2).

During the winter of 2003-04, there were no periods with significant advection (Chapter 2), the MLD was shallower than normal and the outgoing heat fluxes and wind speeds were relatively strong (Chapter 3). The MLD was the most sensitive to doubling the wind speeds, suggesting stronger winds could have deepened the MLD further, however it would be expected that given the strength of the atmospheric forcing, the

84

shallow MLD was caused by another process (Chapter 3). It is likely that the strong

density gradient that was caused by a subsurface cold water anomaly prevented the MLD

from deepening.

During the winter of 2004-05, OSP experienced several periods of strong

advection (Chapter 2), a relatively shallow MLD and strong winds speeds and outgoing

heat fluxes (Chapter 3). In addition, the modeled MLD was the least accurate when

compared to the observed MLD during this winter, suggesting that the 1-D assumption of

the model was not realistic during this period of high advection (Chapter 3). Coupled

with the strong advection were rapid changes in the heat content, with the water in the

upper 250m alternating between gaining and losing heat (Chapter 2). The sensitivity

studies show that the MLD was very sensitive to doubling the wind speed, suggesting

that there was no oceanographic process that would have prevented deepening (Chapter

3). I propose that these anomalies may have been caused by the passage of a Rossby

wave from the 2002-03 ENSO although further studies would need to be performed to

confirm this theory.

At S16, the winter of 2001-02 had minimal advection (Chapter 2), a relatively

deep MLD, strong outgoing heat fluxes and moderate wind speeds (Chapter 3). The MLD

was the most sensitive to zeroing the outgoing heat fluxes, indicating that they were the

main mechanism that caused MLD deepening (Chapter 3). The observed MLD did not

shoal in January as was seen at OSP, nor did the wind speeds and heat fluxes decrease,

suggesting that the process that caused these anomalies at OSP was not region-wide

(Chapter 3). In addition, this winter was the period when the modeled MLD was least

similar to the observed MLD (Chapter 3) and since advection was minimal, I propose that

the large difference between the modeled and observed MLD occurred because the density calculation during this year was dominated by salinity (Chapter 3). This change could be caused by the southward migration of the subarctic front because in the spring of 2002, the flow from the North Pacific Current into the California (Alaska) Current was strengthened (weakened) (Freeland, et al., 2003) and there was a displacement of subarctic water as far as 1200 km south (Bograd and Lynn, 2003; Freeland, et al., 2003). During all summers at S16, the MLD was the most sensitive to zeroing the SW signifying that this was the dominant control on the MLD in the summer (Chapter 3).

In the winter of 2002-03, there was a period of strong advection in February 2003 (Chapter 2), the MLD was anomalously shallow and the outgoing heat fluxes and wind speeds were weak (Chapter 3). The MLD was the most sensitive to zeroing the outgoing heat fluxes and did not deepen as much as would be expected when the winds and outgoing heat fluxes increased, indicating that in addition to having weakened atmospheric forcing from the ENSO, a mechanism was in place that prevented the ML from deepening (Chapter 3). Again, I suggest that the subsurface cold water anomaly (Crawford, et al., 2003) created a large vertical density gradient that prevented the MLD from deepening. I attribute the strong advection in February to the passage of the Alaska Current (Chapter 2), signifying that the increased southward flow from the North Pacific Current into the California Current (Freeland, et al., 2003) had abated.

During the winter of 2003-04, there was significant advection in February (Chapter 2), the observed MLD had a period of deepening at the end of January where it reached more than 100m, and the outgoing heat fluxes and wind speeds were moderately strong (Chapter 3). The MLD was the most sensitive to zeroing the outgoing heat fluxes

86

(Chapter 3). I suggest that the MLD deepening at the end of January was caused by the passage of the Alaska Current near to S16 because it broke up the density gradient that was still present from the cold water anomaly (Chapter 2), thereby allowing the MLD to deepen (Chapter 3).

In the year 2004-05, there were several periods of strong advection (Chapter 2), the MLD was shallow except for a period in April when it deepened past 90m and the outgoing heat fluxes and wind speeds were strong (Chapter 3). The MLD was the most sensitive to doubling the wind speeds suggesting that no oceanographic process prevented it from deepening (Chapter 3). As was seen at OSP, there was a period of a heat gain caused by horizontal advection in the fall of 2004 that may have been caused by a Rossby wave and I attribute that strong advection coupled with a heat loss in the spring to the Alaska Current (Chapter 2).

At CAG during the winter of 2001-02 there was minimal advection (Chapter 2), a shallow MLD and strong outgoing heat fluxes and wind speeds (Chapter 3). The MLD was the most sensitive to zeroing the outgoing heat fluxes, as it was during all winters of the period studied, suggesting that these caused most of the MLD deepening (Charter 3). In addition, the MLD shoaled in February, which is 1-2 months earlier than other years and could be caused by the decreased outgoing heat fluxes observed at that time, suggesting that the early meteorological phase of the 2002-03 ENSO also affected CAG (Chapter 3). The MLD during all summers was the most sensitive to both changes to the wind speeds and the SW indicating that they were the processes that had the greatest impact on the MLD (Chapter 3).

87

The winter of 2002-03 was characterized by significant advection in September (Chapter 2), a shallow MLD until March when it deepened suddenly, and weak outgoing heat fluxes and wind speeds (Chapter 2). I explain the strong heat gain due to advection in September by the passage of the Haida 2000a Eddy (Crawford, 2005) to within the same vicinity as CAG. I suggest that since 2002-03 ENSO brought decreased atmospheric forcing and the eddy transported heat and freshwater into the Gulf of Alaska (Crawford, 2005), the MLD at CAG was prevented from deepening until March when the effects of the eddy had dispersed (Chapter 3).

During the winter of 2003-04, there were a few months with significant advection (Chapter 2), the observed MLD deepened to below 100m, the outgoing heat fluxes were strong and the wind speeds were moderate (Chapter 3). Although there were no observed eddies near to CAG during this time (Crawford and Whitney, 2005), some anomalous water mass may have passed through this region to have caused the significant advective heat gain followed by a heat loss in the fall of 2003 (Chapter 2).

In the winter of 2004-05, CAG underwent 2 months with significant advection (Chapter 2), the MLD was anomalously shallow and the outgoing heat fluxes and wind speeds were relatively strong (Chapter 3). In addition, the MLD was much more sensitive to zeroing the SW than any other winter, indicating that SW was causing up to 30m of stratification (Chapter 3). The period of significant advection in November was accompanied by a heat gain and had a similar timing to the warming of the heat content caused by advection at OSP and S16, indicating that this phenomenon was region-wide (Chapter 2).

At NSG, the winter of 2002-03 was characterized by having strong advection (Chapter 2), a relatively deep MLD and very strong outgoing heat fluxes and wind speeds (Chapter 3). The MLD was the most sensitive to zeroing the SW, indicating that this caused almost 60m of stratification and may explain why, despite similar atmospheric forcing, the observed MLD was not as deep as in 2004-05 (Chapter 3).

During the winter of 2003-04, there was significant advection during 3 months (Chapter 2), the MLD was anomalously shallow and the outgoing heat fluxes and wind speeds were moderately strong (Chapter 3). The MLD was equally sensitive to zeroing the SW and doubling the wind speeds, indicating the observed winds were not strong enough to cause significant MLD deepening (Chapter 3). However, this reaction to the changing the atmospheric forcing does not explain why the MLD was so shallow during this year (Chapter 3).

Finally, during the winter of 2004-05, there was strong advection (Chapter 2), a very deep MLD, strong outgoing heat fluxes and moderate wind speeds (Chapter 3). The MLD was very sensitive to zeroing the SW (Chapter 3). Again, the strong advection seen in fall and spring was first accompanied by a heat gain then by a heat loss, implying that this phenomenon affected the whole northeast Pacific (Chapter 2).

In addition, I have shown that a 1-D ML model, GOTM (Burchard, et al., 2005), realistically reproduced the MLD at four stations in the northeast Pacific, however the computation of the MLD was more accurate at the southern stations than CAG and I suggest that this is because of how the model calculates density (Chapter 3). Previous studies have found that the density equation in oceans that are south (north) of the subarctic front is dominated by temperature (salinity) (Freeland, et al., 1997; Carmack,

2000) but GOTM calculates the turbulence diffusivity based solely on temperature fluxes (Umlauf, et al., 2004), a method that I have found is inaccurate in regions such as CAG where turbulence diffusivity is dominated by salinity fluxes (Chapter 3).

Through this study, I have shown that there are periods when advection at OSP is greater than was previously reported (Tabata, 1965) and can affect the calculation of the MLD as was seen during the winter of 2004-05. Thus, researchers using a 1-D ML model in the Gulf of Alaska may wish to investigate the advection first to determine how it may impact their results. In addition, I have that found both atmospheric and oceanographic processes have a significant impact on the MLD in the northeast Pacific. These processes may be small-scale and short-lived such as a winter storm or region-wide and long-lived such as ENSO events and PDO. Future studies of advection and the sensitivity of the MLD to different atmospheric forcing in both different regions and during different time periods would give a greater understanding of how these processes vary in time and space. Once we have a greater understanding of these mechanisms, we can begin to predict how climate change will affect the MLD and in turn how that will impact biological productivity in the oceans.

Bibliography

Bograd, S.J. and R.J. Lynn. 2003. Anomalous subarctic influence in the southern California Current during 2002. *Geophysical Research Letters,* 30(15), 8020, doi:10.1029/2003GL017446.

Brown, R.G. and L.L. Fu. 2000. An Examination of the Spring 1997 Mid-Latitude East Pacific Sea Surface Temperature Anomaly. *Atmosphere-Ocean*, 38(4), 577-599.

Burchard, H., K. Bolding and L. Umlauf. 2005. GOTM – The General Ocean Turbulence

Model. http://www.gotm.net

Carmack, E.C. 2000. The Arctic Ocean's Freshwater Budget: Sources, Storage and

Export. In *The Freshwater Budget of the Arctic Ocean*, Kluwer Academic Publishers,

The Netherlands, 91-126.

Crawford, W.R. 2005. Heat and fresh water transport by eddies into the Gulf of Alaska.

Deep-Sea Research II, 52, 893-908.

Crawford, W., P. Sutherland and P. van Hardenberg. 2005. Cold water intrusion in the

Eastern Gulf of Alaska in 2002. *Atmosphere-Ocean*, 43(2), 119-128.

Crawford, W. and F. Whitney. 2005. *Graphic Images of the Haida Eddy.*

http://www.sci.pac.dfo-mpo.gc.ca/osap/projects/HaidaEddy

Freeland, H.J. and P.F. Cummins. 2005. Argo: A new tool for environmental monitoring

and assessment of the world's oceans, and example from the N.E. Pacific. *Progress in*

Oceanography, 64, 31-44.

Freeland, H., K. Denman, C.S. Wong. F. Whitney and R. Jacques. 1997. Evidence of

change in the winter mixed layer in the Northeast Pacific Ocean. *Deep-Sea Research I,*

44(12), 2117-2129.

Freeland, H.J., G. Gatien, A. Huyer and R.L. Smith. 2003. Cold halocline in the northern

California Current: An invasion of subarctic water. *Geophysical Research Letters,*

30(3), 1141, doi:10.1029/2002GL016663.

McPhaden, M.J. 2004. Evolution of the 2002/03 El Nino. *Bulletin of the American*

Meteorological Society, 85, 677 – 695.

Tabata, S. 1965. Variability of oceanographic conditions at Ocean Station "P" in the

northeast Pacific Ocean. *Transactions of the Royal Society of Canada*, Series 4, 3,

Section 3, 367-418.

Umlauf, L., H. Burchard and K. Bolding. 2004. *GOTM: Sourcecode and Test Case*

Documentation, version 3.0, http://www.gotm.net

Appendix 1: Input Files Used for GOTM

```
!$Id: airsea.proto,v 1.1.1.1 2003/03/11 13:38:58 kbk Exp $
!-------------------------------------------------------------------------
! Air-sea interaction (heat and momentum fluxes)
!
! heat_method=2,
! heatflux_file='heatflux.dat',
! momentum_method=2,
! const_tx=0.0,
! const_ty=0.0,
! momentumflux_file='momentumflux.dat',
! p_e_method=0,
! p_e_flux_file='p_e.dat',
! sst_method=2,
! sst_file='sst.dat',
! sss_method=0,
! sss_file='sss.dat',
! airt_method=0,
! airt_file='airt.dat',
!-------------------------------------------------------------------------
&airsea
  calc_fluxes=       .false.,
  meteo_file =       'meteo.dat',
  heat_method=       2,
  const_qin=         0.0,
  const_qout=        0.0,
  heatflux_file=     'heatflux.dat',
  momentum_method=    2,
  const_tx=          0.0,
  const_ty=          0.0,
  momentumflux_file=  'momentumflux.dat',
  p_e_method=        0,
  p_e_flux_file=     'p_e.dat',
  sst_method=        2,
  sst_file=          'sst.dat',
  sss_method=        0,
  sss_file=          'sss.dat',
  airt_method=       0,
  airt_file=         'airt.dat',
  /
```

!$Id: gotmmean.proto,v 1.1.1.1 2003/03/11 13:38:58 kbk Exp $
!---
! The namelists 'meanflow' is read in meanflow.F90.
!---

!---
! Specify variables related to the 1D meanflow model.
!
! h0b=   bottom roughness - Note: z0b=0.03*h0b+0.1*nu/ustar [m]
! z0s_min=   minimum value of z0s, default value if charnok=.false. [m]
! charnok=   .true.: adaptation of Charnok 1955 formula used
!   .false.: constant surface roughness length z0s_min used
! charnok_val= emp. constant in Charnok 1955 formula (default = 1400.)
! ddu=   grid zooming (surface), 0: no zooming; > 3 strong zooming
! ddl=   grid zooming (bottom), 0: no zooming; > 3 strong zooming
! grid_method= 0: zooming of grid with ddl, ddu >= 0
!   1: sigma grid (relative depth fractions) read from file
!   2: cartesian grid (fixed layer height in m) read from file
!   3: adaptive grid (see Burchard and Beckers, 2003), set
!   c1ad - dtgrid accordingly, see adaptivegrid.F90
! c1ad=   weighting factor for adaptation to buoyancy frequency
! c2ad=   weighting factor for adaptation to shear frequency
! c3ad=   weighting factor for adaptation to surface distance
! c4ad=   weighting factor for adaptation to background
! Tgrid=   grid adaptation time scale
! NNnorm=   normalisation factor for adaptation to buoyancy frequency
! SSnorm=   normalisation factor for adaptation to shear frequency
! dsurf=   normalisation factor for adaptation to surface distance
! dtgrid=   time step for grid adaptation (must be fraction of dt)
!
! grid_file= file for sigma or cartesian grid. the first line gives the
!   number of layers, the following lines give fractions or
!   layer heights in m from the surface down to the bottom.
! gravity=   gravitational acceleration [m/s^2]
! rho_0=   Reference density [kg/m^3].
! cp=   Specific heat of sea water [J/kg/K].
! avmolu=   molecular viscosity for momentum   [m^2/s].
! avmolt=   molecular diffusity for temperature [m^2/s].
! avmols=   molecular diffusity for salinity   [m^2/s].
! MaxItz0b=   max # of iterations for z0b as function of u_taub.
! no_shear=   .true.: shear production term P is set to zero
!---
&meanflow
 h0b=   0.05,
 z0s_min=   0.02,
 charnok=   .false.,

94

```
charnok_val= 1400.,
ddu=       0,
ddl=       0.,
grid_method= 0,
c1ad=      0.4,
c2ad=      0.4,
c3ad=      0.1,
c4ad=      0.1,
Tgrid=     604800.,
NNnorm=      0.5,
SSnorm=      0.05,
dsurf=      10.0,
dtgrid=     5.,
grid_file=   'grid.dat',
gravity=     9.81,
rho_0=      1027.,
cp=         3985.,
avmolu=      1.3e-6,
avmolt=      1.4e-7,
avmols=      1.1e-9,
MaxItz0b=    1,
no_shear=    .false.,
```

95

!$Id: gotmrun.proto,v 1.1.1.1 2003/03/11 13:38:58 kbk Exp $
!---
! The namelists 'model_setup', 'station', 'time', 'output' and 'eqstate'
! are all read from init_gotm() in gotm.F90
! They have to come in this order.
!---

!---
! General model setup is here.
!
! title=   Title of Simulation
! nlev=   number of levels
! dt=   time step in seconds
! cnpar=   Cranck-Nicholson Parameter
! buoy_method= 1: equation of state, 2: dynamic equation
!---
&model_setup
  title=   "GOTM Simulation",
  nlev=   250,
  dt=   100.,
  cnpar=   1.0,
  buoy_method= 1,
/

!---
!Information of the station/site is specified here
!
! name=   Name of the station
! latitude=   Latitude in degree (north is positive)
! longitude=   Longitude in degree (east is positive)
! depth=   Water depth in meters
!---
&station
  name=   "Ocean Weather Station Papa"
  latitude=   50.
  longitude= -145.
  depth=   250.
/

!---
!Specify time related formats and variables here.
!
! timefmt=   1,2,3 - implicitly uses timestep=dt
!   1- MaxN only - fake start time used.
!   2- start and stop - MaxN calculated.
!   3- start and MaxN - stop calculated.

96

```
! MaxN=      do loop from n=1,MaxN
! start=     Initial time: YYYY/MM/DD HH:MM:SS
! stop=      Final  time: YYYY/MM/DD HH:MM:SS
!----------------------------------------------------------------
&time
 timefmt=    2,
 MaxN=       800,
 start=      "2001-07-10 00:00:00",
 stop=       "2001-07-20 00:00:00",
 /


!----------------------------------------------------------------
!Format for output and filename(s).
!
! out_fmt=    1=ascii, 2=NetCDF, 3=GrADS
! out_dir=    Path from here to output directory (set permissions)
! out_fn=     output name, will be appended an extension
! nsave=      save every 'nsave' timesteps
! variances=   .true.: Variances are written to output
! diagnostics=  .true.: Diagnostics are written to output
! mld_method=  1: Mixed layer depth from TKE>Diffk criterium
!             2: Mixed layer depth from Ri<RiCrit criterium
! diff_k=     critical TKE in m^2/s^2 for mixed layer depth
! ri_crit=    critical Ri number for Mixed layer depth
! rad_corr=   .true.: Correct surface buoyancy flux for solar radiation
!----------------------------------------------------------------
&output
 out_fmt=    2,
 out_dir=    ".",
 out_fn=     "ows_papa",
 nsave=      864,
 variances=  .true.,
 diagnostics= .false.,
 mld_method= 1,
 diff_k=     1.e-5,
 Ri_crit=    0.5,
 rad_corr=   .true.,
 /


!----------------------------------------------------------------
! Specify variables related to the equation of state.
!
! eq_state_method =
!         1: full UNESCO equation of State
!         2: UNESCO equation of state related to surface pressure
!         3: Linearisation of UNESCO equation at T0,S0,p0
```

97

```
!          4: Linearisation of equation of state with T0,S0,dtr0,dsr0
! T0=      Reference temperature (deg C) for linear equation of state
! S0=      Reference salinity (psu) for linear equation of state
! p0=      Reference pressure (bar) for linear equation of state
! dtr0=    thermal expansion coefficient for linear equation of state
! dsr0=    saline expansion coefficient for linear equation of state
!-------------------------------------------------------------------------
&eqstate
eq_state_method= 1,
T0=       10.,
S0=       35.,
p0=       0.,
dtr0=     -0.17,
dsr0=     0.78,
/
```

```
!$Id: gotmturb.proto,v 1.1.1.1 2003/03/11 13:38:58 kbk Exp $
!-------------------------------------------------------------------------
! the namelists 'turbulence',.....
! They have to come in this order.
!-------------------------------------------------------------------------


!-------------------------------------------------------------------------
! What type of equations are solved in the turbulence model?
!
! turb_method=  0: Convective Adjustment
!           1: Analytical eddy visc. and diff. profiles, not coded yet
!           2: Turbulence Model calculating TKE, length scale, stab. func.
! tke_method=   How to calculate TKE.
!           1= Algebraic equation.
!           2= Dynamic equation for k-epsilon and generic model.
!           3= Dynamic equation for Mellor-Yamada model.
! len_scale_method=  How to calculate the lenght scale.
!           1= Parabolic shape
!           2= Triangle shape
!           3= Xing and Davies [1995]
!           4= Robert and Ouellet [1987]
!           5= Blackadar (two boundaries) [1962]
!           6= Bougeault and Andre [1986]
!           7= Eifler and Schrimpf (ISPRAMIX) [1992]
!           8= Dynamic dissipation rate equation
!           9= Dynamic Mellor-Yamada q^2l-equation
!           10= Generic length scale equation
!
! stab_method=  How to calculate stability functions.
!      1, Mellor and Yamada [1982],      full version
!      2, Kantha and Clayson [1994],     full version
!      3, Burchard and Baumert [1995],    full version
!      4, Canuto et al. [2000] version A,  full version
!      5, Canuto et al. [2000] version B,  full version
!      6, Galperin et al. [1988],       quasi-eq. version
!      7, Kantha and Clayson [1994],      quasi-eq. version
!      8, Burchard and Baumert [1995],    quasi-eq. version
!      9, Canuto et al. [2000] version A,  quasi-eq. version
!      10, Canuto et al. [2000] version B, quasi-eq. version
!      11, Constant stability functions
!      12, Munk and Anderson [1954]
!      13, Schumann and Gerz [1995]
!      14, Eifler and Schrimpf [1992]
!
!-------------------------------------------------------------------------
&turbulence
```

99

```
turb_method=      2,
tke_method=       2,
len_scale_method=    10,
stab_method=      11,
/


!---------------------------------------------------------------
! What boundary conditions are used?
!
! k_ubc, k_lbc:      upper and lower boundary conditions
!                for the k-equation
!
! psi_ubc, psi_lbc:   upper and lower boundary conditions
!                for the length-scale equation (e.g.
!                epsilon, kl, omega, generic)
!
! In each case:      prescribed boundary condition,
!                Dirichlet-type            : 0
!                flux boundary condition,
!                Neumann-type              : 1
!
! ubc_type, lbc_type:  boundary layer type
!
! In each case:      viscous sublayer (not yet impl.)  : 0
!                log-law                   : 1
!                tke-injection (breaking waves)   : 2
!                (this of course only for ubc_type)
!
!---------------------------------------------------------------
&bc
 k_ubc=          1,
 k_lbc=          1,
 psi_ubc=        1,
 psi_lbc=        1,
 ubc_type=       1,
 lbc_type=       1,
/


!---------------------------------------------------------------
! What turbulence parameters have been described?
!
! cm0_fix=     value of cm0, if stab_method=11-14
! Prandtl0_fix= value of the turbulent Prandtl-number, if stab_method=11-14
! cw=         constant of the wave-breaking model,
!             Craig & Banner (1994) use cw=100
! compute_kappa compute kappa from model parameters
```

100

```
! kappa       the desired von Karman constant (if compute_kappa=.true.)
! compute_c3   compute c3 (E3 for Mellor-Yamada) for given Ri_st
! Ri_st       the desired steady-state Richardson number (if compute_c3=.true.)
! length_lim=  apply length scale limitation (see Galperin et al. 1988)
! galp=        coef. for length scale limitation
! const_num    minimum eddy diffusivity (only with turb_method=0)
! const_nuh    minimum heat diffusivity (only with turb_method=0)
! k_min=       minimun TKE
! eps_min=     minimum dissipation
!
!-----------------------------------------------------------------------
&turb_param
cm0_fix=         0.5477,
Prandtl0_fix=    0.74,
cw=              100.,
compute_kappa=   .false.,
kappa=           0.4,
compute_c3=      .true.,
ri_st=           0.25,
length_lim=      .true.,
galp=            0.53,
const_num=       5.e-4,
const_nuh=       5.e-4,
k_min=           1.e-10,
eps_min=         1.e-12,
/


!-----------------------------------------------------------------------
! The generic model (Umlauf & Burchard, J. Mar. Res., 2003)
!
! This part is active only, when len_scale_method=10 has been set.
!
! compute_param=       compute the model parameters:
!                      if this is .false., you have to set all
!                      model parameters (m,n,cpsi1,...) explicitly
!                      if this is .true., all model parameters
!                      set by you (except m) will be ignored and
!                      re-computed from kappa, d, alpha, etc.
!                      (see Umlauf&Burchard 2002)
!
! m=                   exponent for k
! n=                   exponent for l
! p=                   exponent for cm0
!
! Examples:
!
```

```
! k-epsilon (Rodi 1987)       :     m=3/2, n=-1, p=3
! k-omega (Umlauf et al. 2003)  :     m=1/2, n=-1, p=-1
! (see Umlauf & Burchard 2003)
!
! cpsi1=      emp. coef. in psi equation
! cpsi2=      emp. coef. in psi equation
! cpsi3minus=    cpsi3 for stable stratification
! cpsi3plus=    cpsi3 for unstable stratification
! sig_kpsi=    Schmidt number for TKE diffusivity
! sig_psi=     Schmidt number for psi diffusivity
!
!----------------------------------------------------------------------
&generic
compute_param=         .false.,
gen_m=              1.0,
gen_n=              -0.67,
gen_p=              3.0,
cpsi1=              1.,
cpsi2=              1.22,
cpsi3minus=            0.05,
cpsi3plus =            1.0,
sig_kpsi=             0.8,
sig_psi=             1.07,
gen_d=              -1.2,
gen_alpha=             -2.0,
gen_l=              0.2,
/


!----------------------------------------------------------------------
! The k-epsilon model (Rodi 1987)
!
! this part is active only, when len_scale_method=8 has been set!
!
! Empirical parameters used in the k-epsilon model.
!
! ce1=      emp. coef. in diss. eq.
! ce2=      emp. coef. in diss. eq.
! ce3minus=    ce3 for stable stratification, overwritten if compute_c3=.true.
! ce3plus=     ce3 for unstable stratification (Rodi 1987: ce3plus=1.0)
! sig_k=      Schmidt number for TKE diffusivity
! sig_e=      Schmidt number for diss. diffusivity
! sig_peps = .true.: The wave breaking parameterisation suggested
!              by Burchard (JPO 31, 2001, 3133-3145) will be used.
!----------------------------------------------------------------------
&keps
ce1=        1.44,
```

```
ce2=        1.92,
ce3minus=   -0.4,
ce3plus=    1.0,
sig_k=      1.,
sig_e=      1.3,
sig_peps=   .false.,
/


!-------------------------------------------------------------------------------
! The Mellor-Yamada model (Mellor & Yamada 1982)
!
! this part is active only, when len_scale_method=9 has been set!
!
! Empirical parameters used in the Mellor-Yamada model.
!
! e1=        coef. in MY q**2 l equation
! e2=        coef. in MY q**2 l equation
! e3=        coef. in MY q**2 l equation, overwritten if compute_c3=.true.
! sq=        turbulent diffusivities of q**2 (= 2k)
! sl=        turbulent diffusivities of q**2 l
! my_length= prescribed barotropic lengthscale in q**2 l equation of MY
!            1=parabolic
!            2=triangular
!            3=lin. from surface
! new_constr= .true.: stabilisation of Mellor-Yamada stability functions
!                     according to Burchard & Deleersnijder [2001]
!-------------------------------------------------------------------------------
&my
 e1=        1.8,
 e2=        1.33,
 e3=        1.8,
 sq=        0.2,
 sl=        0.2,
 my_length= 3,
 new_constr= .false.,
/


!-------------------------------------------------------------------------------
! The internal wave model
!
! iw_model=   IW specification
!             0=no IW, 2=Large et al. 1994
! alpha=      coeff. for Mellor IWmodel (0: no IW, 0.7 Mellor 1989)
!
! The following six empirical parameters are used for the
! Large et al. 1994 shear instability and internal wave breaking
```

103

```
! parameterisations (iw_model = 2, all viscosities are in m**2/s):
!
! klimiw=      critcal value of TKE
! rich_cr=     critical Richardson number for shear instability
! numshear=    background diffusivity for shear instability
! numiw=       background viscosity for internal wave breaking
! nuhiw=       background diffusivity for internal wave breaking
!---------------------------------------------------------------------------
 &iw
 iw_model=    2,
 alpha=       0.0,
 klimiw=      1e-6,
 rich_cr=     0.7,
 numshear=    5.e-3,
 numiw=       1.e-4,
 nuhiw=       1.e-5,
 /
```

104

!$Id: obs.proto,v 1.1.1.1 2003/03/11 13:38:58 kbk Exp $
!---
! General info on reading variables from file:
! Relaxation times:
! All relaxation times have to be positive (non-zero)
! Relaxation time > 1.e10 ==> no relaxation
!---

!---
! Salinity profiles
!
! s_prof_method=0:S not calculated, 1:analytical, 2:from file
! z_s1=   Upper layer thickness, if s_prof_method=1
! s_1=   Upper layer salinity, if s_prof_method=1
! z_s2=   Depth below surface of start of lower layer, if s_prof_method=1
! s_2=   Lower layer salinity, if s_prof_method=1
! s_prof_file= file with salinity profiles
! SRelaxTauM= relaxation time for bulk of the flow [s]
! SRelaxTauB= relaxation time for bottom layer of thickness SRelaxBott [s]
! SRelaxTauS= relaxation time for surface layer of thickness SRelaxSurf [s]
! SRelaxBott= height of bottom relaxation layer, set to 0. if not used
! SRelaxSurf= height of bottom relaxation layer, set to 0. if not used
!---
&sprofile
 s_prof_method=2,
 z_s1=   30.,
 s_1=   20.,
 z_s2=   40.,
 s_2=   15.,
 s_prof_file= 'argo_sprof.dat',
 SRelaxTauM= 7776000,
 SRelaxTauB= 1.e15,
 SRelaxTauS= 1.e15,
 SRelaxBott= 0.,
 SRelaxSurf= 0.,
 /

!---
! Potential temperature profiles
!
! t_prof_method=0: T not calculated, 1=analytical, 2=from file
! For the following 4 lines, see analytical_profile.F90
! z_t1=   Upper layer thickness, if t_prof_method=1
! t_1=   Upper layer temperature, if t_prof_method=1
! z_t2=   Depth below surface of start of lower layer, if t_prof_method=1
! t_2=   Lower layer temperature, if t_prof_method=1

105

! t_prof_file= file with temperature profiles
! TRelaxTauM= relaxation time for bulk of the flow [s]
! TRelaxTauB= relaxation time for bottom layer of thickness TRelaxBott [s]
! TRelaxTauS= relaxation time for surface layer of thickness TRelaxSurf [s]
! TRelaxBott= height of bottom relaxation layer, set to 0. if not used
! TRelaxSurf= height of bottom relaxation layer, set to 0. if not used
!---
&tprofile
t_prof_method=2,
z_t1=   30.,
t_1=   20.,
z_t2=   40.,
t_2=   15.,
t_prof_file= 'argo_tprof.dat',
TRelaxTauM= 7776000,
TRelaxTauB= 1.e15,
TRelaxTauS= 1.e15,
TRelaxBott= 0.,
TRelaxSurf= 0.,
/

!---
! External Pressure Forcing
!
! ext_press_method=0=const,1=tidal,2=from file
! PressMethod= 0,1,2 - external pressure method
!   0= sea surface elevation gradients
!   1= current meter obs.
!   2= vertical mean velocities
! ext_press_file= used if PressType=2
! The following two variables are used only for ext_press_method=0
! PressConstU=   const. pressure gradient - x direction
! PressConstV=   const. pressure gradient - y direction
! The following variable is used only if ext_press_method=0 or =1
! PressHeight=   height above bottom of current obs.
! The following 10 variables are used only if ext_press_method=1
! PeriodM=   period of 1. harmonic (eg. M2-tide)
! AmpMu=   u amp. of 1. harmonic - [m/s]
! AmpMv=   v amp. of 1. harmonic - [m/s]
! PhaseMu=   u phase of 1. harmonic - [s]
! PhaseMv=   v phase of 1. harmonic - [s]
! PeriodS=   period of 2. harmonic (eg. S2-tide)
! AmpSu=   v amp. of 2. harmonic - [m/s]
! AmpSv=   v amp. of 2. harmonic - [m/s]
! PhaseSu=   v phase of 2. harmonic - [s]
! PhaseSv=   v phase of 2. harmonic - [s]

106

```
!---------------------------------------------------------------------------
&ext_pressure
 ext_press_method=0,
 PressMethod=  0,
 ext_press_file='pressure.dat',
 PressConstU=  0.0,
 PressConstV=  0.0,
 PressHeight=  0.0,
 PeriodM=      44714.0,
 AmpMu=        0.0,
 AmpMv=        0.0,
 PhaseMu=      0.0,
 PhaseMv=      0.0,
 PeriodS=      43200.0,
 AmpSu=        0.0,
 AmpSv=        0.0,
 PhaseSu=      0.0,
 PhaseSv=      0.0,
 /


!---------------------------------------------------------------------------
! Internal Pressure Forcing
!
! int_press_method=   0=const,1=const,2=from file
! int_press_file=file with profiles of dsdx,dsdy,dtdx,dtdy
! const_dsdx=  x-gradient of S [psu/m]
! const_dsdy=  y-gradient of S [psu/m]
! const_dtdx=  x-gradient of T [K/m]
! const_dtdy=  y-gradient of T [K/m]
! const_idpdx= x-gradient of p [m/s^2]
! const_idpdy= y-gradient of p [m/s^2]
! s_adv=       advection of salinity (.true./.false.)
! t_adv=       advection of temperature (.true./.false.)
!---------------------------------------------------------------------------
&int_pressure
 int_press_method=0,
 int_press_file='intern_press.dat',
 const_dsdx=  0.0,
 const_dsdy=  0.0,
 const_dtdx=  0.0,
 const_dtdy=  0.0,
 const_idpdx= 0.0,
 const_idpdy= 0.0,
 s_adv=       .false.,
 t_adv=       .false.,
 /
```

107

```
!----------------------------------------------------------------------
! Light extinction - Jerlov type or from file
!
! extinct_method= 0: from file, 1-6=Jerlov type
!          1= Jerlov type I
!          2= Jerlov type 1 (upper 50 m)
!          3= Jerlov type IA
!          4= Jerlov type IB
!          5= Jerlov type II
!          6= Jerlov type III
!          7= Adolf Stips, Lago Maggiore
! extinct_file= used if extinct_method=0
!----------------------------------------------------------------------
 &extinct
  extinct_method=5,
  extinct_file= 'extinction.dat',
 /


!----------------------------------------------------------------------
! Vertical advection - none, constant or from file, see get_w_adv.F90.
!
! w_adv_method= 0=const, 1=constant, 2=from file
! w_adv0=      const. vertical advection velocity
! w_adv_file=  used if w_adv_method=2
! w_adv_discr= 0: no vertical advection
!          1: not used, program will abort
!          2: first order upstream
!          3: third-order polynomial
!          4: TVD with Superbee limiter
!          5: TVD with MUSCL limiter
!          6: TVD with ULTIMATE QUICKEST
!----------------------------------------------------------------------
 &w_advspec
  w_adv_method= 0,
  w_adv0=      0.,
  w_adv_file=  'w_adv.dat',
  w_adv_discr= 6,
 /


!----------------------------------------------------------------------
! Sea surface elevations - none, from file or 2 tidal constituents.
!
! zeta_method= 0=const,1=tidal,2=from file
! zeta_file=   used if zeta_method=2
! The following variables is used only if zeta_method=0
```

108

! zeta0=   const. sea surface elevation
! The following 6 variables are used only if zeta_method=1
! period1=   period of 1. harmonic (eg. M2-tide) - [s]
! amp1=   amp. of 1. harmonic - [m]
! phase1=   phase of 1. harmonic - [s]
! period2=   period of 2. harmonic (eg. S2-tide) - [s]
! amp2=   amp. of 2. harmonic - [m]
! phase2=   phase of 2. harmonic - [s]
!---
&zetaspec
 zeta_method= 0,
 zeta_file=   'zeta.dat',
 zeta_0=   0.00000,
 period_1=   44714.0,
 amp_1=   1.00000,
 phase_1=   0.00000,
 period_2=   43200.0,
 amp_2=   0.50000,
 phase_2=   0.00000,
/

!---
! Observed velocity profiles
!
! vel_prof_method=   0=no,1=not impl. yet,2=from file
! vel_prof_file=   file with velocity profiles
! vel_relax_tau=   relaxation time constant for velocity in [s]
! vel_relax_ramp=   duration of initial relaxation in [s]
! set vel_relax_tau=vel_relax_ramp=1.e15 for no relaxation
! set vel_relax_ramp=1.e15 for constant relaxation
!---
&velprofile
 vel_prof_method=0,
 vel_prof_file='velprof.dat',
 vel_relax_tau=1.e15,
 vel_relax_ramp=1.e15,
/

!---
! Turbulent dissipation rate profiles
!
! e_prof_method= 0=no,1=not impl. yet,2=from file
! e_obs_const=   a constant filling value - [W/kg]
! e_prof_file=   file with dissipation profiles
!---
&eprofile

109

```
e_prof_method=0,
e_obs_const= 1.e-12,
e_prof_file= 'eprof.dat',
/


!--------------------------------------------------------------------------------
! Buoyancy - only used if buoy_method .ne. 1 (see buoyancy.f90)
!
! b_obs_surf=   prescribed initial buoyancy at the surface - [m/s^2]
! b_obs_NN=     prescribed initial const. NN (Brunt-Vaisalla squared) - [1/s^2]
! b_obs_sbf=   prescribed constant surface buoyancy flux
!--------------------------------------------------------------------------------
&bprofile
 b_obs_surf=  0.0,
 b_obs_NN=    1.e-4,
 b_obs_sbf=   0.0,
/
```

110